The Assessment of Practical Per-Cooling Targeting Peripheral Limbs During Exercise in Hot and Humid Environments

by

Alexander G. Stothart

A thesis

presented to the University of Waterloo

in fulfillment of the

thesis requirement for the degree of

Master of Applied Science

in

Mechanical and Mechatronics Engineering

Waterloo, Ontario, Canada, 2022

Author’s Declaration

This thesis consists of material all of which I authored or co-authored: see Statement of Contributions included in the thesis. This is a true copy of the thesis, including any required final revisions, as accepted by my examiners.

I understand that my thesis may be made electronically available to the public.

Statement of Contributions

This thesis contains content paraphrased from the following manuscript published in The Journal of Sports Sciences [1]:

- Eric T. Hedge , Kathryn A. Zuj , Alexander G. Stothart , Erica H. Gavel , Len S. Goodman , Andrew J.M. Buckrell & Sean D. Peterson (2020): Continuous forearm cooling attenuates gastrointestinal temperature increase during cycling, Journal of Sports Sciences, DOI: 10.1080/02640414.2020.1835222

This publication was co-authored by Eric T. Hedge, Kathryn A. Zuj, Alexander G. Stothart, Erica Gavel, Sean D. Peterson, Len S. Goodman, and Andrew J. M. Buckrell. Kathryn A. Zuj. Len S. Goodman, Andrew J.M. Buckrell, and Sean D. Peterson contributed to the study conception and design. Material preparation and data collection were performed by Eric T. Hedge, Kathryn A. Zuj, Alexander G. Stothart, and Erica H. Gavel. Data analysis was performed by Eric T. Hedge, Kathryn A. Zuj, and Alexander G. Stothart. The first draft of the manuscript was written by Eric T. Hedge, and all authors commented on versions of the manuscript. All authors read and approved the final manuscript. Alexander G. Stothart specifically was responsible for the construction and operation of the cooling system apparatus, and collection and analysis of data related to heat energy absorbed by the cooling system. Alex assisted in experimental trial operation, and authored the first draft of publication sections relating to the employed forearm cooling system. Paraphrased content appears only within Chapter 3 of this document, with all other chapters authored by Alexander G. Stothart.

Abstract

When excess body heat generation owing to the performance of exercise coincides with the heat dissipation limitations presented by hot and humid environments, the body's ability to maintain thermal balance is compromised, and internal temperatures can rise to dangerous levels. Individuals who exercise in hot environments commonly look to acute cooling strategies to provide thermoregulatory assistance in order to avoid the health risks and performance decrements brought about by elevated thermal stress. Many cooling techniques aim to apply cold surfaces to large areas of skin on the torso, head, or neck to extract heat directly from core regions of the body. These locations, however, are often difficult to access without disrupting movement. In many exercise modalities including cycling, paddle sports, or wheelchair sports, however, peripheral regions such as the upper or lower limbs remain almost stationary, and may present a convenient location to apply cooling garments/equipment without disrupting required movements. The research studying the impact of practically applicable cooling techniques at these locations, however, is limited and inconclusive, prompting the present work.

This document first outlines the quantifiable heat transfer principles that determine human thermal behaviour, and discusses the effects of thermal stress and acute cooling interventions. It then outlines practical considerations regarding the applications of cooling techniques, motivating the proposal of a novel technique that does not interfere with exercise performance by targeting the volar forearm skin of cyclists during exercise. The impacts of forearm cooling are then assessed experimentally during cycling ergometry exercise in a hot and humid environment. The cooling was observed to reduce the rate of core temperature rise by 0.43 ± 0.34°C/hr ($p=0.002$), while also eliciting significant reductions in heart rate drift and rating of thermal comfort. Computational modelling of the human thermal system was then employed to extend the experimental investigation and assess what impact the cooling may have during true cycling applications outside of the laboratory setting. Model outcomes suggest that the effects of the outdoor environment may reduce the effectiveness of the applied cooling slightly, but that the cooling will still be capable of providing quantifiable benefits. The impact of the cooling was also simulated across a range of ambient conditions, and the cooling was generally observed to be more impactful in hotter air temperatures and at higher ambient humidity levels.

Acknowledgements

I would like to thank my supervisor, Dr. Sean Peterson, for the ongoing guidance and encouragement throughout the conducted research, and for his patience and understanding as my research timeline was disrupted. His enthusiastic support was essential in allowing me to manage unforeseen circumstances and navigate the evolving research project.

I would also like to thank all researchers, graduate students, and others who I have collaborated with and looked to for support throughout my studies, including Kathryn Zuj, Eric Hedge, Erica Gavel, Supun Pieris, Winston Hu, Jon Deng, Jon Kurelek, Julian Howarth, Ramin Manouchehri, Kaycee Okoye, Iara Santelices, Andrew Robertson, Chekema Prince, Len Goodman, Robert Limmer, and others.

I would additionally like to thank University of Waterloo personnel I worked with throughout my graduate studies. Jason Benninger and Rob Kraemer provided essential fabrication and machining support. Countless other course instructors, administrative staff, and support personnel provided valuable help in navigating the various tasks and requirements of my master's studies.

Finally, I would like to thank my mother, sisters, and all other friends and family for their support through the rigours of the past several years. I would simply not be in the position I am without it, and would not have had the opportunity to see this thesis through to completion.

Table of Contents

List of Figures

List of Tables

Nomenclature

Symbol	Description
ΔBF	Total elevation of blood flow in the body above basal level
ΔH_{fus}	Latent heat of fusion of melting substance
ΔH_{vap}	Latent heat of vapourization of water
A_c	Area of the body in contact with an external surface
A_s	Body surface area being studied
BC_N	Heat conductance between perfusing blood and N^{th} node
$BF_{skin_{max}}$	Maximal total skin blood flow rate
$\dot{C}$	Heat exchanged from human body surface to surroundings via convective transfer
c_{p_a}	Specific heat capacity of air
$c_{p_{ave}}$	Average specific heat capacity of the human body represented as a lumped thermal mass
c_{p_b}	Specific heat capacity of blood
c_{p_w}	Specific heat capacity of water
C_N	Heat capacity of the N^{th} thermal model node
D	Diffusion coefficient
D_P	Diffusion coefficient based on vapour pressure gradient
DT	Size of timestep
$\dot{E}$	Heat exchanged from human body surface to surroundings via the evaporation of sweat on the skin
E_{MAX_N}	Maximal sweat evaporation rate at N^{th} node surface
E_N	Evaporative heat loss from N^{th} node
F_{s-e}	View factor between the body surface and the surrounding long-wave radiating enclosure
F_{s-i}	View factor between the body surface and the i^{th} sub-region of an inhomogeneous surrounding long-wave radiating enclosure
F_s	Area factor of body surface with respect to incoming solar irradiation
$h_{evap_{mass}}$	Evaporative mass transfer coefficient
h_{cont}	Contact conductance between body surface and external contacting surface
h_{conv}	Convective heat transfer coefficient between body surface and surroundings
h_{evap}	Evaporative heat transfer coefficient

H_{met}	Total metabolic rate
H_N	Metabolic heat generation within Nth node
h_{rad}	Linearized long-wave radiation heat transfer coefficient
HC_N	Convective heat transfer from Nth node
HR_N	Radiative heat transfer from Nth node
I	Incident flux of solar irradiation
J	Diffusive flux of a substance in a mixture
J_v	Diffusive mass transfer flux of water vapour
k	Thermal conductivity
$\dot{K}$	Heat exchanged from human body surface and contacting solid surface via conduction transfer
$\dot{L}$	Heat exchanged from human body to surroundings via respiratory exchange
$\dot{L}_{dry}$	Dry respiratory heat loss rate
$\dot{L}_{evap}$	Evaporative respiratory heat loss rate
$\dot{M}$	Total energy released in the body from metabolic reactions
$\dot{m}$	Mass flow rate of coolant water through cooling system apparatus
$\dot{m}_e$	Rate of sweat mass evaporation
$\dot{m}_s$	Rare of sweat mass secretion
m_b	mass of the human body
m_{melt}	Mass of melting substance used to store extracted heat
m_w	Mass of warming water
P	Partial pressure of water vapour
P_{skin_N}	Maximum vapour pressure at Nth node skin surface
P_∞	Vapour pressure in ambient air
P_{insp}	Vapour pressure of inspired air
P_{skin}	Vapour pressure at skin surface
$\dot{Q}$	Heat introduced into the human body via metabolic generation
$\vec{q}$	Conduction heat flux through a medium
$\dot{Q}_{cool}$	Rate of heat energy absorption by experimental cooling system apparatus
Q_b	Heat extracted from a human body as it is being cooled
Q_{cool}	Total heat energy absorption by cooling system apparatus

q_m	Metabolic heat generation density
Q_{melt}	Heat stored by a melting mass
Q_w	Heat stored by a warming thermal mass of water
$\dot{R}$	Heat exchanged from human body surface to surroundings via radiative transfer
$\dot{R}_{LW}$	Long-wave radiative heat exchange between body surface and surroundings
$\dot{R}_{SW}$	Heat gain from solar short-wave radiation
R_{cont}	Contact resistance between body surface and external contacting surface
S_b	Heat exchanged from perfusing blood to surrounding tissue
S_N	Skin surface area of N^{th} node
T	Local tissue temperature
t	Time variable
T_{b_f}	Final temperature of human body being cooled
T_{b_i}	Initial temperature of human body being cooled
$T_{N_{t+1}}$	Temperature at thermal model N^{th} node one timestep into the future
T_{N_t}	Temperature at thermal model N^{th} node at present timestep
T_{N+1}	Temperature of the $N+1^{th}$ thermal model node
T_{N-1}	Temperature of the $N-1^{th}$ thermal model node
T_{w_f}	Final temperature of a warming mass of water
T_{w_i}	Initial temperature of a warming mass of water
T_A	Ambient air temperature surrounding the body
T_{ave}	Average temperature of the human body represented as a lumped thermal mass
T_b	Blood temperature
T_B	Temperature of thermal model blood node
T_c	Temperature of external contacting surface
T_e	Temperature of the surrounding long-wave radiating enclosure surface
t_{end}	End of cooling period
T_{exp}	Temperature of expired air
T_i	Temperature of the i^{th} sub-region of an inhomogeneous surrounding long-wave radiating enclosure
T_{in}	Temperature of coolant water entering heat exchanger block
T_{insp}	Temperature of inspire air

T_{mrt}	Effective mean radiating temperature of an inhomogeneous surrounding long-wave radiating enclosure
T_N	Temperature of the Nth thermal model node
T_{op}	Operative temperature accounting for impact of solar irradiation
T_{out}	Temperature of coolant water exiting heat exchanger block
T_s	Temperature of the body surface
t_{start}	Beginning of cooling period
$TC_{N\rightarrow N+1}$	Thermal conductance between Nth node and N+1th node
$TC_{N-1\rightarrow N}$	Thermal conductance between N-1th node and Nth node
$\dot{V}$	Volumetric respiration rate
w	Blood perfusion rate density
$\dot{W}$	Work performed by the body on the surroundings
W_{exp}	Moisture concentration of expired air
W_{insp}	Moisture concentration of inspired air
x	Length dimension variable
α_{sw}	Short-wave solar absorptivity of body surface
ε_b	Long-wave emissivity of the body surface
ρ_a	Air density
ρ_b	Blood density
σ	Stefan-Boltzmann constant
φ	Concentration of a diffuse substance in a mixture

Chapter 1
Introduction

1.1 Motivation and Objectives

The thermal state of the human body is determined by the continuous balance of heat gain and heat loss, primarily through avenues of convection, radiation, and evaporation [2]. Hot and humid ambient conditions severely limit the quantity of heat that can be lost through such pathways, often rendering them insufficient to balance internal heat production, causing body temperature to rise. Additionally, physical activity elevates internal heat production well above resting levels, which may also render heat loss pathways insufficient to dissipate the generated heat [3]. During exercise in the heat, these effects conspire to produce rapidly rising body temperatures. Elevated temperatures, especially in core body regions, expose an individual to a variety of heat related illnesses, ranging in severity from mild to life threatening. In addition, even when heat illness is avoided, elevated core body temperatures will hinder athletic performance [4] and elicit discomfort in the body [5]. For many athletes, especially those competing in scheduled events, exercise in the heat is unavoidable, and strategies to fight the rise of body temperature and limit exposure to the identified risks are therefore often desired.

One strategy employed is the application of acute per-cooling interventions, which commonly involve positioning cold surfaces or substances against the body to extract heat directly during exercise. A variety of research exists investigating the impacts of these cooling interventions on physiological markers and exercise performance, as outlined in reviews by Bongers *et al.* [6] [7]. One limitation of much of the research conducted, is that many of the cooling modalities employed are impractical to use during actual exercise. Because the cooling interventions studied ultimately aim to reduce core temperature, they are often applied directly to large skin surface areas on the torso, head or neck. While this provides the most direct access to core body regions for cooling, it requires the application of often bulky equipment or garments to these locations. This is feasible during laboratory studies where exercise is conducted on stationary ergometer setups, but would be likely to interfere with movement in true mobile exercise, and therefore cannot be practically employed during activity. In some forms of exercise, especially when activity is confined to the upper or lower body, the inactive limbs remain almost stationary, and may provide a more convenient location to apply acute cooling interventions. An example of such an arrangement that will be investigated in detail in this

thesis is the performance of cycling exercise in the “aero” position. While the head and large portions of the torso do not move considerable during this cycling, the application of bulky garments to these body segments would not only be heavy and uncomfortable, but would contribute significant unwanted aerodynamic drag. Accordingly, the arms represent a body location that may be more convenient to target, as they rest against the aerobar supports and remain almost stationary throughout the performed activity.

While peripheral locations like this may be convenient to target, they only represent practical locations to apply cooling if the effects can be distributed to reduce whole-body heat stress. Research investigating the impact of cooling applied at peripheral locations on whole-body heat stress is much more limited, has produced conflicting outcomes, and often still employs modalities that are impractical to recreate in true exercise applications. The present thesis aims to investigate the potential impact of cooling applied to peripheral body regions that are practical to target during exercise, focusing on cooling applied to the forearms during cycling exercise in the heat. Specifically, this document aims to:

- Provide a quantitative understanding of the physical processes that govern the body’s thermal behaviour to contextualize investigation of the applied cooling.
- Assess experimentally whether peripheral cooling applied to the arms is capable delivering quantifiable whole-body benefits during cycling exercise in hot and humid environments.
- Formulate a whole-body model that can be used to further study the thermal behaviour in the body resulting from the application of cooling, and apply the model to further investigate the impact of forearm cooling during cycling.

1.2 Document Structure

To recount the approach employed to address the identified goals, this document features four additional upcoming chapters.

Chapter 2 outlines relevant background information to contextualize the subsequent chapters. It aims to combine both engineering and physiological principles to provide an understanding of the body’s thermal behaviour. The quantifiable heat transfer principles governing the body’s thermal state

are presented, and the impacts on health and performance that result when these governing principles produce high body temperatures are described. The effectiveness and practical considerations of acute cooling approaches are then outlined. Finally, models described in literature combining the identified heat transfer principles to predict thermal outcomes and assess levels of thermal stress in various applications are discussed.

Chapter 3 describes an experimental investigation studying the impact of localized acute cooling applied at the forearms during cycling exercise. A cooling system apparatus was constructed to simulate the practical application of cooling at the forearms during cycling ergometry in hot and humid environments. Core temperature and other markers of physiological stress are compared during exercise bouts conducted both with and without applied cooling to assess whether the cooling modality can offer quantifiable whole-body benefits.

Subsequently, Chapter 4 outlines computational modelling work performed to build on the experimental observations presented in Chapter 3. Practical limitations of the experimental study prevented it from capturing several relevant considerations impacting thermal behaviour in the body, such a relative air motion, solar irradiation, and elevated work rates. A whole-body thermal model was therefore constructed and populated to account for these considerations, and assess whether the applied cooling is expected to be beneficial in true outdoor cycling applications. The model also allows the effects of cooling to be assessed over a range of ambient inputs, providing insight on their dependence on the ambient conditions under which exercise is conducted.

Finally, the document is concluded with a summary of the performed investigations and a discussion of future extensions of interest inspired by the present work.

Chapter 2
Background & Literature Review

The systems comprising the human body function and interact with such complexity that it can be challenging to capture their behaviour theoretically. Accordingly, much of our understanding of human physiology is developed and reinforced through experimental observation. Despite this, human physiology is still bound by the physical laws of nature that govern the universe. Concepts such as the conservation of energy, and the principles of heat transfer in matter will still apply within human tissue, which has led to attempts to describe human thermal behaviour mathematically.

Experimental observations often lack the generalized applicability of mathematical descriptions and models, while mathematical descriptions can underappreciate the complexity and variability of human physiology. The background presented in the following sections aim to connect the physical principles of heat transfer with the physiological knowledge and observation of human thermoregulation, allowing the perspectives of both physiology and engineering to combine for a more balanced understanding of the behaviour. A brief general overview of human thermal behaviour will first be presented to contextualize further discussion, at which point the specific physical processes involved in human temperature control will be outlined quantitatively in further detail. A discussion will then follow of the outcomes arising when the physical principles governing body heat balance combine with hot ambient conditions to produce elevated body temperatures. These outcomes include heat related illness, and reductions in the ability to perform physical work. The discussion will then shift to interventions that can be employed to mitigate these adverse outcomes by cooling the body. The background discussion will finally conclude with an overview of modelling efforts employed attempting to capture all of the previously discussed elements to predict human thermal behaviour and avoid adverse thermal outcomes.

2.1 Overview of Thermal Behaviour

The systems within the human body tend to operate best when the core body temperature is roughly 37°C, with deviations of more than a few degrees from this point presenting life-threatening challenges. Accordingly, the body aims to maintain a core temperature close to this value regardless of its situation or surroundings. The body generates heat as a by-product of the metabolic reactions employed to meet its energy needs. This internally generated heat allows the body to warm itself

above the temperature of its surroundings. In order to safely limit this heating however, the body must also dissipate heat to its surroundings. It is able to do so through a combination of convective, conductive, radiative, and evaporative heat losses. The temperature of the body will therefore be determined by the balance of heat generation and heat loss – if generation exceeds loss, the body will warm, if losses exceed generation, the body will cool. [2]

Assuming the body is warmer than its surroundings, the physical principles of heat transfer dictate that higher body temperatures will naturally promote further heat loss, with cooler body temperatures inhibiting it. This provides a natural regulating mechanism discouraging the variation of body temperature, though it is insufficient on its own to maintain temperatures within the narrow desired ranged. Accordingly, the body must employ further interventions to maintain safe temperatures when it senses deviation from its desired state. When body temperatures fall too low, the body will shiver in order to produce additional metabolic heat. Furthermore, it will inhibit blood flow to the skin, dramatically lowering skin temperature and reducing heat loss to the surroundings. When the body is too warm, it will promote blood flow to the skin in order to further raise its surface temperature and enhance heat loss. Additionally, it will secrete sweat to the skin surface, which will absorb and remove heat as it evaporates. In addition to these subconscious physiological processes, the sensation of excess warmth or cold will also encourage conscious behavioural changes, such as changing location or adding or removing clothing. The body's ability to sense its state and employ these regulatory interventions to fight excessive temperature variation from its desired value is referred to as thermoregulation. [2]

The principles behind heat gain and loss in the body that contribute to its overall thermal state will be described in more detail in the following sections.

2.2 Quantifiable Physical Principles Governing Human Thermal Behaviour

2.2.1 Whole Body Heat Balance

If the entire body is treated as a single isolated system with a total mass of m_b, an average heat capacitance of $c_{p_{ave}}$, the average temperature, T_{ave}, will change based on the net balance of heat flow into and out of the system [8]. This can be described mathematically using equation 2.1:

$$m_b c_{p_{ave}} \frac{dT_{ave}}{dt} = \dot{Q} - \dot{C} - \dot{R} - \dot{K} - \dot{E} - \dot{L}$$

(2.1)

where, $\dot{Q}$ denotes the rate at which waste heat is being generated metabolically, $\dot{C}$ represents the rate of heat loss through convection, $\dot{R}$ represents the rate of heat loss through radiation, $\dot{K}$ represents the rate of heat loss through conduction, $\dot{E}$ represents the rate of heat lost to evaporation of sweat, and $\dot{L}$ represents the rate of heat loss through respiration.

The summation of total body heat in Equation 2.1 neglects the fact that energy can be gained or lost through the consumption or elimination of fluids and food substances with their own internal stored heat energy. To account for these considerations, one would need to additionally include the inflow or outflow of heat energy contained within the substance in the body's overall heat balance, while concurrently accounting for the change in body heat capacity introduced by the ingested or eliminated thermal mass. For example, an individual ingesting cold water would be introducing additional thermal mass into the system that contains less heat energy per unit of heat capacity than the rest of body. Therefore, once the temperatures of the ingested water and internal body tissue equilibrate, the average body temperature would be reduced. The energy balance in Equation 2.1 is simplified to neglect these considerations because the current analysis of the body's heat balance will be limited to periods where no food or drink are consumed, and where urination and defecation do not occur, meaning relatively little mass, and consequently, stored heat energy, will be consumed or eliminated. Furthermore, substances are often consumed or eliminated at temperatures close to average body temperature, meaning that the internal heat energy gained or lost will be offset by the heat capacity gained or lost from the substances' mass, and body temperature will not be changed substantially. [8]

The above formulation of the heat balance allows for an understanding of how the body's various thermal behaviours can change its temperature in real time. The following sections will discuss the meaning of each of the terms in Equation 2.1 and outline how their values can be described quantitatively.

2.2.3 Metabolic Heat Generation

The metabolism of fuels like carbohydrates, fats, and sometimes proteins is the process that allows humans to derive the energy they require to perform basic, life-sustaining functions such as breathing, eating, and circulating blood. This energy also fuels all other human behaviour, such as the performance of external work. However, the body performs work inefficiently – much of the energy generated metabolically will not contribute to the performance of work, and will become waste heat introduced into the body [3]. The rate at which waste heat is generated, $\dot{Q}$, will be given by the difference between total energy released through metabolic reactions, $\dot{M}$, and the rate at which the body is performing work on its surroundings, $\dot{W}$ [9]:

$$\dot{Q} = (\dot{M} - \dot{W}) \quad \textbf{(2.2)}$$

This heat production is essential to allow warm-blooded animals to maintain body temperatures above the temperature of their surroundings [3]. It is therefore a core component of the total thermal balance in the human body, making the quantification of metabolically generated heat an important, yet challenging, task. It is generally accomplished via a combination of ergometry and either direct or indirect calorimetry.

Ergometry

Ergometry is the measurement of work performed during exercise [10]. Devices used to measure work rate during various exercise modalities are referred to as ergometers, or commonly, ergs. Perhaps the most common form of ergometer is a cycle ergometer, which allows work rate to be measured during cycling exercise. The principles behind ergometers vary, though they generally involve measuring the speed at which an individual is propelling a mass, as well as the resistance they are propelling it against. While ergometry does provide a measure of work rate, it is insufficient on its own to quantify metabolically generated heat, and must be complemented by calorimetry.

Calorimetry

Calorimetry is the process of measuring the heat energy transferred to or from a system [8]. Calorimetry can be applied to animals and human beings to assess the amount of heat being released

by metabolic processes. Two primary approaches exist for this purpose, namely, indirect calorimetry and direct calorimetry [11].

Indirect calorimetry utilizes knowledge of the chemistry of metabolic reactions taking place within the body to estimate the total energy being produced. An enthalpy balance of the metabolic oxidation of glucose, the most common metabolic fuel, indicates that roughly 2800 kJ of energy are released per mole of glucose reacted at 25°C, or 470 kJ per mole of oxygen consumed. Because the glucose oxidized is taken from stores in the body, it can be difficult to measure the quantity reacted. Conversely, very little oxygen is stored within the body, and is extracted from inhaled air continuously to support metabolic reactions. Accordingly, analysis of respiratory gases can be performed to determine the difference of between oxygen content of air being inhaled and exhaled, revealing the amount of oxygen consumed by metabolic activity, often denoted VO_2. This knowledge, coupled with the knowledge of energy released per mole of oxygen consumed, allows the total energy produced through metabolism to be known. [8]

This approach, however, is complicated by the fact that glucose is not the only metabolic fuel; fats are also commonly used to produce energy. A similar calculation of the enthalpy of oxidation of tripalmitin, a common fat, yields an energy release of 32 MJ per mole of tripalmitin, or 430 kJ per mole of oxygen consumed, slightly less than the 470 kJ/mol of oxygen consumed when metabolizing glucose. Accordingly, in addition to knowledge of the amount of oxygen consumed, knowledge of what fuels are being metabolized is necessary to know how much energy is being released. This can be determined by analyzing inspired and expired air not only for oxygen content, but for carbon dioxide content as well. Because the metabolism of glucose produces a different quantity of carbon dioxide than fats for a given quantity of oxygen consumed, knowledge of the ratio of oxygen consumed to carbon dioxide produced reveals the balance of fuels being metabolized. The ratio of oxygen consumed to carbon dioxide produced is known as the respiratory exchange ratio, or respiratory quotient (RQ). Continuous measurement of the RQ is combined with measurement of the volume of oxygen consumed to quantify the energy released via metabolism. [8]

Metabolic energy may contribute to the performance of external work, or may be released as heat in the body. If the rate at which external work is being performed is measured via ergometry, it can be subtracted from the total rate at which energy is produced, measured by simultaneous indirect calorimetry, to reveal the rate of metabolic heat release, $\dot{Q}$ [9].

While indirect calorimetry is generally the most convenient way to measure metabolic heat generation, a limitation of the technique is its inability to measure energy produced by anaerobic metabolism. Anaerobic metabolism refers to metabolic processes that do not require oxygen consumption to convert fuels into usable energy for the body. This is in contrast to aerobic metabolism, which refers to metabolic processes that do require oxygen to occur. Under most circumstances, the body favours aerobic metabolism to fuel activity, since anaerobic metabolism produces by-products that interfere with muscle contraction and contribute to fatigue. For this reason, the vast majority of human energy production results from aerobic metabolic processes. However, in cases where exercise demand cannot be met by the body's ability to deliver oxygen to working muscles, anaerobic metabolism is employed to meet the excess demand. While this occurs mainly at high work rates that are not sustained for long durations, it will produce energy and heat that will not be accounted for by measuring the volume of oxygen consumed. To quantify heat produced both aerobically and anaerobically, direct calorimetry must be employed. [12]

Direct calorimetry refers to the direct measurement of produced heat. This is generally accomplished by allowing produced heat to flow only into an enclosed isolated system of known heat capacity. The change in temperature of the thermal mass of the system then reveals the heat gained. In the context of human calorimetry (or calorimetry involving other living creatures), the body can be completely enclosed in a fully insulated chamber. If a steady state temperature is achieved throughout the body, the heat produced metabolically will be equal to the heat transferred from the body into its surroundings in the chamber. If the rate of temperature change of the chamber contents is measured, and their heat capacity known, the total heat transfer rate from the body into the chamber (also equal to the total heat production rate in the body) can be determined. [11]

The techniques employed to measure heat transferred from the body into the calorimetry chamber vary, and have evolved with time, though a typical modern technique, outlined in [13], involves slowly circulating air through the chamber. If a steady temperature distribution is achieved in the body and chamber, the rate of airflow can be measured, along with the temperature difference between influent and effluent air to determine the heat lost by the body to the surroundings by conduction, convection, and radiation. Measurement of the difference in moisture content between influent and effluent air allow the evaporative heat loss from the body into the calorimeter to be determined as well. Discussions of the wider array of approaches to whole-body human calorimetry can be found in [8] and [11].

Simultaneous direct calorimetry, indirect calorimetry, and ergometry are often performed to compare and/or validate the various approaches to quantifying metabolic activity. Such measurements can also be used to establish approximate efficiencies of various exercise modalities relating external work rate to total rate of metabolic energy production. Typical efficiencies for humans performing external work reach a maximum of 25-30% [3], though efficiency can vary depending on exercise modality. A detailed discussion of the efficiency of cycling ergometry, an exercise modality commonly employed in research, can be found in [14]. Knowledge of typical mechanical efficiency for a given exercise modality can be quite useful, as it allows total metabolic energy production and heat production to be estimated from only ergometer measurements of work rate, which are much simpler to perform than either direct or indirect calorimetry.

2.2.4 Heat Exchange with Surroundings

Metabolic heat production allows the body to maintain a temperature that is typically greater than the surrounding environment. In order to balance the internally generated heat and avoid uncontrolled temperature rise, the body must transfer heat to its surroundings. Heat is typically lost through convection into the surrounding fluid, conduction into contacting surfaces, radiation exchange with surrounding surfaces, evaporation of sweat, and the warming and moistening of respired air [15].

Heat lost to radiation, convection, conduction, and the warming of respired air is referred to as sensible heat loss, or dry heat loss [16]. It results from heat flow from warm to cold substances. Under typical circumstances, heat lost through conduction into contacting surface and heat lost to warming of respired air contribute very minimally to total heat loss, and dry heat loss can often be assumed to be the sum of radiative and convective losses [8]. Heat lost to the evaporation of sweat and moistening of respired air are referred to as evaporative, or latent losses.

Radiation Heat Exchange

All objects, including the human body and its surroundings, emit energy constantly via electromagnetic radiation. The exchange of such radiative emissions allows heat to be transferred between surfaces, even when they are not contacting one another. A detailed discussion of radiative heat exchange can be found in common heat transfer textbooks, such as [17], while the information that follows presents a simplified summary of the key aspects of radiative heat transfer that apply to human thermal behaviour. The radiating bodies surrounding a human can generally be classified as

either short wave radiation sources, which will have very high surface temperatures, or long-wave radiation sources, which will have surface temperatures in common ambient ranges.

Long-Wave Radiation

The majority of objects and surfaces on earth will have temperatures close to ambient values, and will therefore emit what is referred to as long-wave radiation. If an individual is surrounded entirely by a long wave radiating enclosure, such as a room, it can be shown that the long wave radiative heat exchange, $\dot{R}_{LW}$ between the individual's body with area A_s and absolute surface temperature T_s, and the enclosure surface with an absolute temperature T_e, is given by:

$$\dot{R}_{LW} = \varepsilon_b A_s F_{s-e} \sigma (T_s^4 - T_e^4) \quad \textbf{(2.3)}$$

Where σ is the Stefan Boltzman constant, and F_{s-e} denotes the view factor from the body to the enclosure surface. This will be a number between 0 and 1 that describes the proportion of the radiation emitted by the body that strikes the surface of the enclosure. Radiation is assumed to be emitted from the body equally across its surface in all directions, so the value of F_{b-e} will depend purely on the geometry of the body within the enclosure. A fully concave body surrounded completely would have a view factor equal to 1, since all emitted radiation will leave the body and strike the surface of the surrounding enclosure. Mitchell *et al.* [18] reported a whole-body view factor value of 0.8 for a human body, reflecting the existence of concavity in the body shielding some skin surface from radiation exchange with the surroundings. ε_b is a property of the body surface, known as the emissivity, that describes the radiating efficiency of the body. Ideal radiating surfaces, referred to as "black" surfaces, have an emissivity value of 1 by definition, and emit the highest possible amount of radiation for an object at their temperature. All other non-ideal surfaces will have emissivity values between 0 and 1, with the value indicating the ratio of energy radiated from the surface to the amount that would be radiated by a black surface of the same temperature. The surfaces of many everyday objects possess values close to 1, including human skin, which is often reported to have an emissivity of roughly 0.95 [8].

It is often convenient to represent radiative heat exchange from a human body to the surface of its surrounding enclosure in the following form [8]:

$$\dot{R}_{LW} = h_{rad} A_s (T_s - T_e)$$

(2.4)

Where h_{rad} is a radiative heat exchange proportionality coefficient. Comparing equations 2.3 and 2.4, we note that the use of a linear relationship between the net heat exchange and the temperature difference from skin to surrounding surfaces is an approximation. In reality, h_{rad} must depend on the temperatures of the skin and enclosure themselves. Equation 2.3 is in fact regained if h_{rad} is given by [8]:

$$h_{rad} = \varepsilon_s F_{s-e} \sigma (T_s^3 + T_s^2 T_e + T_s T_e^2 + T_e^3)$$

(2.5)

Assuming a constant value of h_{rad} is an acceptable simplification if the range of $(T_s - T_e)$ studied is small compared to the absolute temperatures T_s and T_e themselves. For example, for a skin temperature of 30°C (~303K), computing values of h_{rad} with Equation 2.6 reveals that such a linear approximation will result in inaccuracies less than 5% over a range of $(T_s - T_e)$ from 10°C to 30°C. The simplified linear relationship between heat flux and temperature difference displayed in Equation 2.4 is often employed accordingly in the study of human thermoregulation.

The actual environments humans reside within will generally be made up of a combination of many different long-wave radiating surfaces, which can have different temperatures. To account for this while still allowing radiative exchange to be represented by equation 2.3 or 2.4, the array of surrounding temperatures is represented by a single equivalent temperature, known as the mean radiative temperature (MRT). The MRT is the surface temperature of an imaginary enclosure with a uniform temperature that would result in the same radiative heat exchange with the body as the true, inhomogeneous environment. The mean radiative temperature can be given by [19]:

$$T_{mrt}^4 = \sum_{i=1}^{N} F_{b-i} T_i^4$$

(2.6)

where T_{mrt} is the mean radiative temperature representing the *N* different surfaces in the actual environment, F_{b-i} is the view factor between the body and the i^{th} surface, and T_i is the temperature of

the i^{th} surface. A similar linear simplification to that employed in equation 2.4 can be used to produce the following approximation of the mean radiant temperature [19]:

$$T_{mrt} = \sum_{i=1}^{N} F_{b-i} T_i \qquad \textbf{(2.7)}$$

The obtained value can then be used in place of T_e in Equation 2.4.

If the temperatures of the body and surroundings are known, the remaining task of quantifying h_{rad} then becomes a key challenge in the study of human thermal behaviour. It can be measured experimentally or estimated theoretically using equation 2.5 with assumed surface temperatures and view factors [20] [21] [22]. Many experimental approaches employ direct calorimetry with human subjects to estimate total heat loss, which can then be combined with measurements of skin and surrounding temperatures to infer heat loss coefficients. Mannequins simulating the human figure are also often employed, as they allow skin temperature distribution and heat fluxes to be more precisely controlled and measured [8]. In either case, the challenge remains of distinguishing the heat loss owing to radiation from the heat loss resulting from other pathways. Approaches aiming to measure only radiative losses include the use of an array of photometric detectors around a subject [18], as well as the use of environmental chambers where air temperatures and wall temperatures are separately controllable, allowing air temperature to be maintained at an equal value to skin temperature to ensure that measured heat loss results solely from radiation [23]. Another approach involves performing calorimetric measurements while covering the surface of a mannequin with a known low-emissivity foil to eliminate radiative heat losses to the greatest extent possible [16] [24]. Further measurements can then be made once the foil is removed, and the difference in detected sensible heat loss is used to determine the radiation transfer. In general, it is also common for the body surface to be broken down into sub-regions covering different body parts, and for radiative transfer coefficients to be measured locally within these sub-regions for a more detailed breakdown of the heat transfer behaviour. Table 2.1 reports both whole-body and local radiative heat transfer coefficients.

Table 2.1: Several values of the radiative heat transfer coefficient reported in literature for various locations on the body.

Study Author	**de Dear *et al.* [24]**		**Sorensen & Voigt [20]**	**Ichihara *et al.* [23]**	**Stolwijk & Hardy [21]**	**Quintela *et al.* [16]**		**Manabe *et al.* [22]**	
Approach	Thermal mannequin with and without low emissivity coating		Theoretical computation based on mannequin geometry	Thermal mannequin calorimetry with separately controllable T_{air} and T_{wall}	Theoretical estimation based on simplified representation of body with geometric shapes	Thermal mannequin with and without low-emissivity coating		Theoretical computation based on mannequin	
Posture	Seated	Standing	Seated	Standing	Standing	Seated	Standing	Seated	Standing
h_{rad} **[W/(m²K)]**: **Whole body**	4.5	4.5	4.83		4.97	4.4	4.6	4.3	4.6
- **head**	3.9	4.1	5.22	4.3	6.4	5.7	5.7	5.5	5.5
- **Chest**	3.4	4.5	4.73	3.8	5.24	3.5	4.5	4.3	4.7
- **Back**	4.6	4.4	5.07	3.6	5.24	3.9	4.2	4.8	4.7
- **Pelvis**	4.8	4.2	5.01	3.9	5.24	4.4	4.5		
- **Upper arms**	4.8	5.2	4.63	4.0	5.00	4.6	4.6	3.2	3.2
- **Lower arms**	5.2	4.9	4.30	3.9	5.00	4.2	4.5	3.2	3.2
- **Hands**	3.9	4.1	4.12	3.7	3.49	4.3	4.2		
- **Thighs**	4.6	4.3	4.61	4.2	4.65	4.4	4.6	4.3	4.8
- **Calves**	5.4	5.3	5.12	4.8	4.65	4.7	5.1	4.3	4.8
- **Feet**	4.2	3.9	5.36	7.3	4.65	4.8	5.0		

It can be seen from Table 2.1 that whole-body values of the radiation coefficient are reasonably consistent across studies, with an average value of 4.6 W/m^{2}K and a standard deviation of 0.2 W/m^{2}K, Local values (e.g., arms, hands, etc.), however, show larger variance. The lower arms for example, have an average radiative transfer coefficient of 4.3 W/m^{2}K and a standard deviation of 0.7 W/m^{2}K. The fact that this variation is observed in local measured values, but is recovered over the whole body to produce more consistent values across studies, suggests that the local measurements

may be sensitive to factors that could differ from study-to-study, such as measurement techniques, the division of body segments, or specific mannequin features, proportions, and positioning. Such factors may not impact whole-body measurements as substantially, so long as appropriately sized mannequins are employed in reasonably similar positions.

Short-Wave Radiation

Short wave radiation sources have very high surface temperatures, often thousands of degrees Kelvin hotter than Earth's ambient temperatures, which emit radiation with shorter wavelengths than objects at ambient temperatures. The primary short wave radiation source encountered by humans is the sun, possessing an effective surface temperature of roughly 5800K [25]. Because the temperature of the sun is so much greater than the temperature of an individual's skin, the radiative heat exchange from the sun to a human body will have virtually no dependence on the temperature of the body surface. The level of radiative energy from the sun incident upon the earth's atmosphere is roughly 1367 W/m^2 [26]. Some of this solar irradiation will be reflected or scattered, while some will be transmitted through to the earth's surface. In clear conditions, solar irradiation can strike the earth's surface at levels of roughly 1000 W/m^2 [27]. The level of heat energy absorbed by the body from solar irradiation can generally be described by [28]:

$$\dot{R}_{SW} = I\alpha_{sw}F_s \tag{2.8}$$

Where $\dot{R}_{SW}$ is the heat energy absorbed from solar irradiation per unit area, I is the incident solar irradiation flux, α_{sw} is the short-wave absorptivity of the body surface, a dimensionless quantity often assumed to be 0.7 [29], and F_s is the solar area factor, which can generally be thought of as the ratio of the projected body area normal to the incident solar irradiation to the total body surface area. The value of this property will vary based on the angle at which sunlight is incident upon the body, with whole-body values reported in [30] and [31] ranging from roughly 0.1 for sunlight incident directly overhead, up to almost 0.4 for sunlight incident directly upon the front or back of the body.

Convection Heat Exchange

Convection heat transfer refers to the transfer of heat between the skin and the surrounding fluid medium, typically air. Heat will flow from warm to cold, meaning the body loses heat via convection when the surrounding air is cooler than the skin. While it is possible for heat to *conduct* from skin,

into and through a stationary fluid, the term convection implies that the heat transfer is assisted by advective transport of thermal energy via the motion of fluid particles [17].

The term “forced convection” is used to describe situations where the flow of fluid particles transporting heat from the skin into the bulk of the fluid results from externally driven relative fluid motion. Examples of this in the context of human thermoregulation include wind blowing over a body, a fan circulating air within a room, or a person moving through surrounding air. Conversely, the term “free convection” or “natural convection” is used to describe situations where there is no externally driven relative motion between the solid body and surrounding fluid. Spontaneous fluid motion still arises in these cases, however, as heat conducted into the initially stationary fluid leads to density inhomogeneities and consequent imbalanced buoyant forces acting within the fluid field. This results in motion of the fluid over the surface of the body, allowing heat to be carried by the moving fluid [17].

The heat flow between the human body and surrounding fluid is typically described quantitatively as [8]:

$$\dot{C} = h_{conv} A_s (T_s - T_A) \qquad \textbf{(2.9)}$$

where T_A is the bulk temperature of the surrounding fluid, and h_{conv} is a convective heat transfer proportionality coefficient. Similar to the representation of radiative heat exchange in equation 2.4, this representation of convective heat exchange once again assumes a linear relationship between the heat flow and the temperature difference between the skin and surroundings. In cases of forced convection, this is generally an appropriate representation of convective heat exchange, with the proportionality constant h_{conv} depending on the bulk fluid flow speed. However, in the case of free convection with no bulk air velocity, heat flow is actually reported to vary with $(T_s - T_A)^{1.2}$ to $(T_s - T_A)^{1.25}$ [8]. Comparing heat flows computed using equation 2.9 to similar computations based on $(T_s - T_A)^{1.25}$ reveals that the assumed linear representation would result in inaccuracies in the estimation of convective exchange of less than roughly 15% over a range of $(T_s - T_A)$ from 10-30°C. Furthermore, because relatively little total heat is exchanged with the surroundings through convection when no bulk air flow is present, the contribution of this inaccuracy to the whole-body heat balance will be even less impactful.

The determination of an appropriate value for the heat transfer coefficient is essential to the description of convective exchange. Computational fluid dynamics simulations can be used to make estimations [20], though the inclusion of fluid density variation with temperature adds to the computational challenge. Additionally, experimental measurements can be obtained by combining knowledge of skin and fluid temperatures with direct calorimetry employing human subjects or thermal mannequins. Radiative losses can be estimated using the previously discussed techniques and subtracted from the total heat loss. The remaining measured heat loss can then be assumed to result only from the convective transfer contribution [24] [32]. Values for free convection coefficients reported in literature for bodies in still air are outlined in Table 2.2. Note that it is once again common for the body surface to be broken down into sub-regions covering different body parts, and for convective transfer coefficients to be measured locally within these sub-regions. Table 2.2 reports both whole-body and local radiative heat transfer coefficients.

Table 2.2: Several values of the natural convective heat transfer coefficient reported in literature for various locations on the body.

Study Author	**de Dear *et al.* [24]**		**Sorensen & Voigt [20]**	**Nishi & Gagge [33]**	**Oliviera *et al.* [32]**
Approach	Thermal mannequin with and without low emissivity coating		CFD Simulation based virtual mannequin geometry	Mannequin experiment employing naphthalene mass transfer	Calorimetry with known radiative losses (from Quintela [16]) subtracted
Posture	Seated	Standing	Seated	Standing	Standing
Whole body average coefficient [W/(m²K)]	3.3	3.4	3.1	3.2	3.5
Local coefficients [W/(m²K)]					
- **Head**	3.7	3.6	3.6	3.2	4.3
- **Chest**	3.0	3.0	2.4	2.5	2.3
- **Back**	2.6	2.9	2.2	2.5	2.8
- **Pelvic region**	2.8	3.4	2.8	2.5	2.8
- **Upper arms**	3.4	2.9	2.7	3.5	3.3
- **Forearms**	3.8	3.7	3.8	3.5	3.7
- **Hands**	4.5	4.1	4.5	3.9	4.7
- **Thighs**	3.7	4.1	3.2	3.2	3.9
- **Lower legs**	4.0	4.1	3.0	3.2	3.7
- **feet**	4.2	5.1	4.7	3.5	4.4

The whole-body free convection heat transfer coefficients can be seen to be relatively consistent, with an average value of 3.3 W/m^{2}K and a standard deviation of 0.1 W/m^{2}K. Once again, variation across studies is often greater for local values, especially at peripheral locations, such as the lower legs, with an average value of 3.6 W/m^{2}K and standard deviation of 0.4 W/m^{2}K. The local variation is likely a result of differences in mannequin features, proportions, and positioning, as well as body segments divisions, or measurement techniques.

When either the body or surrounding air are moving, the convective heat transfer coefficient will rise significantly. In these cases, its value is generally reported as a function of the relative bulk velocity between the fluid and body, v, typically in the form $h_{conv} = cv^a$, where c and a are determined constants. Reported relationships giving convective heat transfer coefficient as a function of airspeed found in literature are outlined in Table 2.3.

Table 2.3: Several relationships reported in literature giving of the values of the forced convection heat transfer coefficients for various locations on the body.

Study Author	**de Dear *et al.* [24]**		**Oliviera *et al.* [32]**	**Stolwijk [21]**	**Ichihara *et al.* [23]**
Approach	Mannequin experiment		Calorimetry with known radiative losses (from Quintela [16]) subtracted	Mannequin experiment employing naphthalene mass transfer	Thermal mannequin calorimetry with separately controllable T_{air} and T_{wall}
Posture	Seated	Standing	Standing	Standing	Standing
Whole body average coefficient [W/(m^{2}K)]	$10.1v^{0.61}$	$10.4v^{0.56}$	$7.34v^{0.49}$	$10.2v^{0.5}$	
Local coefficients [W/(m^{2}K)]					
- **Head**	$4.9v^{0.73}$	$3.2v^{0.97}$	$7.72v^{0.5}$	$10.08v^{0.5}$	
- **Chest**	$9.1v^{0.59}$	$9.1v^{0.59}$	$5.90v^{0.55}$	$7.91v^{0.5}$	$11.0v^{0.67}$
- **Back**	$8.9v^{0.63}$	$8.9v^{0.63}$	$5.33v^{0.59}$	$7.91v^{0.5}$	$17.0v^{0.5}$
- **Pelvic region**	$8.2v^{0.65}$	$8.8v^{0.59}$	$5.43v^{0.54}$	$7.91v^{0.5}$	
- **Upper arms**	$11.6v^{0.66}$	$11.2v^{0.62}$	$8.04v^{0.55}$	$11.03v^{0.5}$	$17.0v^{0.59}$
- **Forearms**	$11.9v^{0.63}$	$12.7v^{0.53}$	$8.01v^{0.46}$	$11.03v^{0.5}$	$17.0v^{0.61}$
- **Hands**	$12.6v^{0.60}$	$12.6v^{0.60}$	$13.78v^{0.52}$	$12.33v^{0.5}$	
- **Thighs**	$8.9v^{0.60}$	$10.0v^{0.52}$	$7.30v^{0.43}$	$10.8v^{0.5}$	$14.0v^{0.61}$
- **Lower legs**	$13.4v^{0.56}$	$13.0v^{0.51}$	$8.38v^{0.48}$	$10.8v^{0.5}$	$16.0v^{0.75}$
- **feet**	$12.8v^{0.55}$	$12.1v^{0.49}$	$9.61v^{0.51}$	$11.03v^{0.5}$	$13.0v^{0.78}$

If an airspeed of 5 m/s is assumed, as an example, the average resulting whole-body coefficient from the listed publications reporting a whole-body relationship is 22.9 W/m^{2}K, with a standard deviation of 4.2 W/m^{2}K. Slightly more variation across studies is observed in measurements of forced convection coefficients than free convection or radiation coefficients, which is likely due to additional experimental considerations introduced by the relative air motion. Despite this, the standard deviation of the coefficients produced by the reported relationships still do maintain reasonable consistency. Greater variation across studies can once again be found in the local measurements, however, especially at peripheral body regions such as arms and legs. For the same airspeed of 5 m/s, the reported relationships produce an average value for the convective coefficient at the lower legs of 26.2 W/m^{2}K with a standard deviation of 5.6 W/m^{2}K. This variation is again likely attributable to different divisions between body parts between studies, as well as differences in the size, shape, position and other features of the mannequins. The bulk fluid motion could interact with slight changes in geometry to produce different resulting flows, and exaggerate the impact of slight changes in mannequin postures and proportions in comparison to the case of free convection and radiation.

Conduction Heat Transfer

An additional pathway through which heat can transfer between a human body and its surroundings is conduction into solid surfaces contacting the skin. In general, heat flowing from the body to a contacting surface can be quantified using Equation 2.10 [17]:

$$\dot{K} = A_c h_{cont}(T_s - T_c)$$

(2.10)

where A_c is the contact patch area, T_c is the temperature of the contacting surface, and h_{cont} is the contact conductance coefficient. An equivalent formulation to equation 2.10 is shown below:

$$\dot{K} = \frac{A(T_{s1} - T_{s2})}{R_{cont}}$$

(2.11)

In this case, the contact coefficient is reframed as a contact resistance: $R_{cont} = \frac{1}{h_{cont}}$. Attempts at quantifying the contact resistance for human skin against objects is outlined by Ho & Jones [34]

employing the methodology of Yovanovich [35] for general contacting surfaces. In general, the resistance will depend on the surface characteristics and physical properties of the skin and contacting objects, as well as the contact pressure. Calculations will provide only a rough estimation however, and heat lost to conduction will vary dramatically depending on the specific nature of the solid contact. Fortunately, conduction losses typically represent a very small portion of heat lost from the human body, and can often be neglected [32]. When standing, the only conductive losses will occur through the soles of the feet, which will generally be well insulated with rubber shoe soles. Under certain circumstances, such as when lying on a cold or hot surface, conduction heat transfer can be substantial, though the quantification of the transfer should be undertaken on a case-by-case basis. Experimental measurements are likely more reliable than theoretical estimations.

Heat Loss through the Evaporation of Sweat

An additional important pathway by which the body is able to eliminate heat is the evaporation of sweat. The body secretes sweat from the skin in response to the sensation of elevated body temperatures, allowing it to evaporate to the ambient air. In order to evaporate, it absorbs heat from the skin, allowing it to overcome the intermolecular bonds holding it in liquid form. Sweat is primarily composed of water, meaning the energy extraction rate relates to the sweat evaporation rate according to equation 2.12 [8].

$$\dot{E} = \dot{m}_e \, \Delta H_{vap} \qquad \textbf{(2.12)}$$

Where $\dot{E}$ is the rate of evaporative heat loss, $\dot{m}_e$ is the rate of sweat evaporation, and ΔH_{vap} is the latent heat of vaporization of water at the local skin temperature.

Typically, at low and moderate sweat rates, almost all sweat is able to evaporate as it is secreted, meaning the rate of evaporation will be roughly equal to the rate of sweat secretion [8]. For high sweat rates, or in very humid conditions, the rate at which sweat can evaporate will eventually be limited by mass transfer considerations governing the rate of diffusion of water vapour from sweat on the skin into the surrounding bulk air. Diffusion of water vapour in air, or any diffuse substance in a mixture, is driven by the concentration gradient of the substance and described by Fick's first law of diffusion. This can be represented in one dimension using equation 2.13 [8].

$$J = -D\frac{d\varphi}{dx}$$

(2.13)

Where J is the diffusive flux of the substance, φ is the concentration of the substance, x is length dimension in the direction of diffusion, and D is a proportionality coefficient known as the diffusion coefficient. If air is treated as an ideal mixture, the moisture concentration relates directly to the partial pressure of water vapour, P. Accordingly, for water vapour in air, the diffusive mass transfer flux of water vapour, J_v, can be expressed as [8]

$$J_v = -D_p\frac{dP}{dx}$$

(2.14)

where D_p is the diffusion coefficient that additionally accounts for the conversion from vapour concentration to partial vapour pressure. It can be observed that equation 2.14 is analogous to the mathematical description of heat conduction through a medium, only the mass transfer rate is driven by a pressure gradient, as opposed to a temperature gradient. Furthermore, the flow of fluid around the body will bring fluid with bulk field properties close to the skin, allowing for accelerated mass transfer. This is once again analogous to the phenomenon of convective heat transfer from the skin into the surrounding fluid. It can therefore be reasoned that the mass transfer rate of water vapour from the skin into the surrounding fluid (*i.e.*, the rate of evaporation) can be described analogously to convective heat transfer as [8]

$$\dot{m}_e = A_s\, h_{evap_{mass}}(P_{skin} - P_\infty)$$

(2.15)

where P_{skin} is the vapour pressure at the skin, P_∞ is the ambient vapour pressure, which will be the product of the relative humidity and saturation vapour pressure at ambient air temperature, and $h_{evap_{mass}}$ is the evaporative mass transfer coefficient. Inserting equation 2.15 into equation 2.12:

$$\dot{E} = \Delta H_{vap}\, A\, h_{evap_{mass}}\,(P_{skin} - P_\infty) = A\, h_{evap}(P_{skin} - P_\infty)$$

(2.16)

where h_{evap} is the evaporative heat loss coefficient, equal to the product of $h_{evap_{mass}}$ and ΔH_{vap}. Because the fluid flow over the body assisting both convective heat transfer and evaporative mass transfer is in fact that same flow, the values of the transfer coefficients will be proportional to each other. Dimensional analysis arguments can be used to show that $h_{evap} = 2.2h_{conv}$ when vapour pressures are expressed in mmHg, and h_{conv} is expressed W/(m^{2}K), and Q_{evap} is desired in W [8].

The vapour pressure at the skin can never exceed the saturation pressure of water at local skin temperature, and sweat evaporation can therefore never exceed the rate determined by equation 2.15 when P_{skin} is assumed to be equal to saturation pressure. If sweat secretion exceeds this maximal evaporation rate, the excess secreted sweat simply accumulates on the skin or drips off, and evaporative cooling is equal to the amount allowed by the maximal evaporative rate given by equation 2.16 [21]. For sweat rates that fall below the maximal supported rate, it is often assumed that all sweat evaporates as it is secreted, and the rate of heat loss is given by [8]:

$$\dot{E} = \dot{m}_s \, \Delta H_{vap}$$

(2.17)

where $\dot{m}_s$ is the rate of sweat secretion. $\dot{m}_s$ will be determined by the body's thermoregulatory system in response to it's sensed thermal state, with maximal values in typical adults reaching 1 to 2L/hr under severe thermal stress [36].

Respiration Heat Loss

Respiratory heat loss refers to heat lost by the body in the warming and wetting of respired air. Air is inhaled at the ambient temperature, while it passes through the respiratory tract, it will be heated by the warm interior of the body. Furthermore, water within the body will evaporate into the inspired air, absorbing heat in the process. The warmed and wetted air will then be exhaled, carrying away the absorbed heat and moisture. The heat lost through respiration will result from the sum of heat exchanged through warming the air, $\dot{L}_{dry}$, and moistening it, $\dot{L}_{evap}$, and can be described as follows [8]:

$$\dot{L} = \dot{L}_{dry} + \dot{L}_{evap} = \dot{V}\left(\rho_a c_{p_a}\left(T_{exp} - T_{insp}\right) + \Delta H_{vap}\left(W_{exp} - W_{insp}\right)\right)$$

(2.18)

where $\dot{V}$ is the volumetric respiration rate, ρ_a and c_{p_a} are the density and specific heat capacity of air respectively, T_{exp} and T_{insp} are the temperatures of exhaled and inhaled air respectively, ΔH_{vap} is the latent heat of vaporization of water, and W_{exp} and W_{insp} are the expired and inspired moisture content of the air respectively. [8]

Investigations into the quantification of the parameters in equation 2.18 by McCutchan and Taylor [37] observed that both the temperature and humidity of expired air did not depend strongly on the properties of inspired air. Fanger [38] later combined the results of McCutchen and Taylor with other results of Astrand and Rodahl [39] to arrive at the following relationship for respiratory heat losses:

$$\dot{L}_{dry} = 0.0014 H_{met}\left(34 - T_{insp}\right) \quad \textbf{(2.19)}$$

$$\dot{L}_{evap} = 0.0023 H_{met}(44 - P_{H_2O,insp}) \quad \textbf{(2.20)}$$

Where the dependence on respiratory rate has been replaced with a dependence on total metabolic rate, H_{met}, which is more likely to be known in any thermoregulatory investigation than ventilation rate, making it a more convenient parameter in practice. Furthermore, the ventilation rate will largely be determined by the metabolic rate. The dependence on moisture content has also been replaced with dependence on vapour pressure of inspired air, P_{insp}. Under the assumption that air is an ideal mixture, moisture content and vapour pressure will be directly proportional. Many of the properties in Equation 2.18 have been combined into a single leading coefficient in each of Equations 2.19 and 2.20. Any necessary conversion factors between respiration rate and metabolic rate, as well as moisture content and partial pressure, have been implicitly absorbed into the leading coefficients as well. The coefficients included in equations 2.19 and 2.20 relate temperatures in °C and pressure in mmHg to heat loss in W. Respiratory losses will generally constitute a small portion of total heat loss from the body, and are often either neglected or combined with losses from convection and evaporation of sweat during calorimetric investigations [8].

2.2.5 Heat Transport and Distribution within the Body

Metabolic activity occurs throughout the body, though the majority takes places within the muscles, brain, and visceral organs [8]. These metabolically active sites will therefore be the source of most of the heat production in the body, and are also generally located deeper below the skin surface, buried under insulating tissue such as skin and fat. Accordingly, they will warm up to temperatures above ambient conditions. In order to avoid warming continuously towards dangerous levels, heat must flow from these locations through the surrounding tissue until it can be lost through the skin surface via the previously discussed heat loss mechanisms. The skin typically remains at temperatures closer to ambient than the core, allowing heat generated in warm, metabolically active tissue to flow down the gradient to the periphery of the body, where it can be lost. The body possesses two primary methods to transport heat along the core-to-skin gradient: heat conduction through body tissue and advection via flowing blood.

Heat Conduction Through Tissue

Heat conduction through any matter, including human tissue can be described by Fourier's law [17], given by

$$\vec{q} = -k\nabla T \qquad \textbf{(2.21)}$$

Equation 2.21 states that the conductive heat flux, $\vec{q}$, will be given by the product of the local temperature gradient, ∇T, and a proportionality constant, k, referred to as the thermal conductivity. This will be a property of the substance through which heat is conducting, with values of k in human tissue often measured around 0.5 W/mK [40].

Blood Flow and Advective Heat Transport

The flow of blood within the body complements heat conduction, aiding in the transport of heat from the muscles and core to the periphery. As blood flows through vessels, it exchanges heat with the surrounding tissue. This allows blood to be warmed by deep body tissues before it flows towards the skin. It then loses its heat to the cooler skin tissue before returning to the core to be re-warmed and continue the cyclical exchange. [3]

The body is able to modulate blood flow to given regions through vasomotor action, either dilating or constricting blood vessels to promote or inhibit flow, respectively. Greater amounts of blood flow to the skin allow greater amounts of heat to be transported from the core to the periphery. This elevates skin temperature while ensuring the heat exchange between deep tissue and skin can be sustained, promoting further heat loss to the surroundings. Accordingly, the body elicits cutaneous vasodilation when it is warm, directing more blood to the skin, allowing more heat to be lost from the body. Conversely, when cold, the body elicits cutaneous vasoconstriction, limiting blood flow to the skin. While this does cause skin temperatures to drop to sometimes uncomfortable levels, it preserves heat within the core, where it is needed to maintain vital organ function. [3]

As blood flows through the body, it diverges into progressively smaller, and more numerous vessels. Capillaries are the smallest of which, measuring only 5-10 microns in diameter, with the average person having roughly 10 billion within their body [41]. While this overwhelmingly large number of small diameter vessels promotes efficient heat transfer [42], it also makes the modelling of the exchange taking place in all individual vessels impractical. Accordingly, in the context of thermoregulation, heat exchange between tissue and perfusing blood is often described on a macroscopic level according to [43]

$$S_b = w\rho_b c_{p_b}(T_b - T) \tag{2.22}$$

where S_b is the heat exchanged from blood to surrounding tissue, w is the local tissue perfusion rate, ρ_b is the blood density, and c_{p_b} is the specific heat capacity of the blood, T_b is the temperature of the perfusing blood, and T is the temperature of the local tissue being perfused. Note that this assumes that all possible heat is transferred between blood and tissue, with the blood temperature reaching an equilibrium with the surrounding tissue temperature by the time it leaves the tissue. Some representations of Equation 2.22 include an additional equilibration coefficient to represent the possibility that the blood may not fully equilibrate to the surrounding tissue temperature, though the large number of microscopic capillaries through which the blood passes while perfusing allows for effective heat exchange [42].

Combined Thermo-physiological Balance

Considering both pathways discussed above, the balance of heat at any point within the human body with local tissue temperature T, density ρ_t, and specific heat capacity c_{p_t}, will then result from conduction exchange with neighbouring tissue, exchange with perfusing blood, and metabolic generation. This is represented by a governing second-order partial differential equation [43]:

$$\nabla(k\nabla T) + w\rho_b c_{p_b}(T_b - T) + q_m = \rho c_p \frac{\partial T}{\partial t} \quad \textbf{(2.23)}$$

The first term on the left-hand-side describes conduction heat exchange with surrounding tissue based on the local temperature gradients, the second term describes the heat exchange with blood perfusing the region, and the third term contains only the local metabolic heat generation density, q_m. At the skin surface, heat can also be lost through the mechanisms discussed previously. Such losses through the surface represent boundary conditions that can be imposed on equation 2.23 to determine the temperature distribution within body tissue.

In order to validate the developed thermo-physiological energy balance above, Pennes [43] measured steady state temperatures throughout the human forearm by inserting very fine thermocouple probes into forearm tissue in 8 subjects, and compared the results to those predicted when equation 2.23 is solved in its steady state with appropriate forearm properties assumed, and a combined convection and radiation boundary condition imposed at the arm surface [43]. The results were then re-visualized by Wissler [44] employing appropriate similarity scaling based on diameter of the subjects' arms, as shown in Figure 2.1, and the predicted distribution resembled the measured results closely.

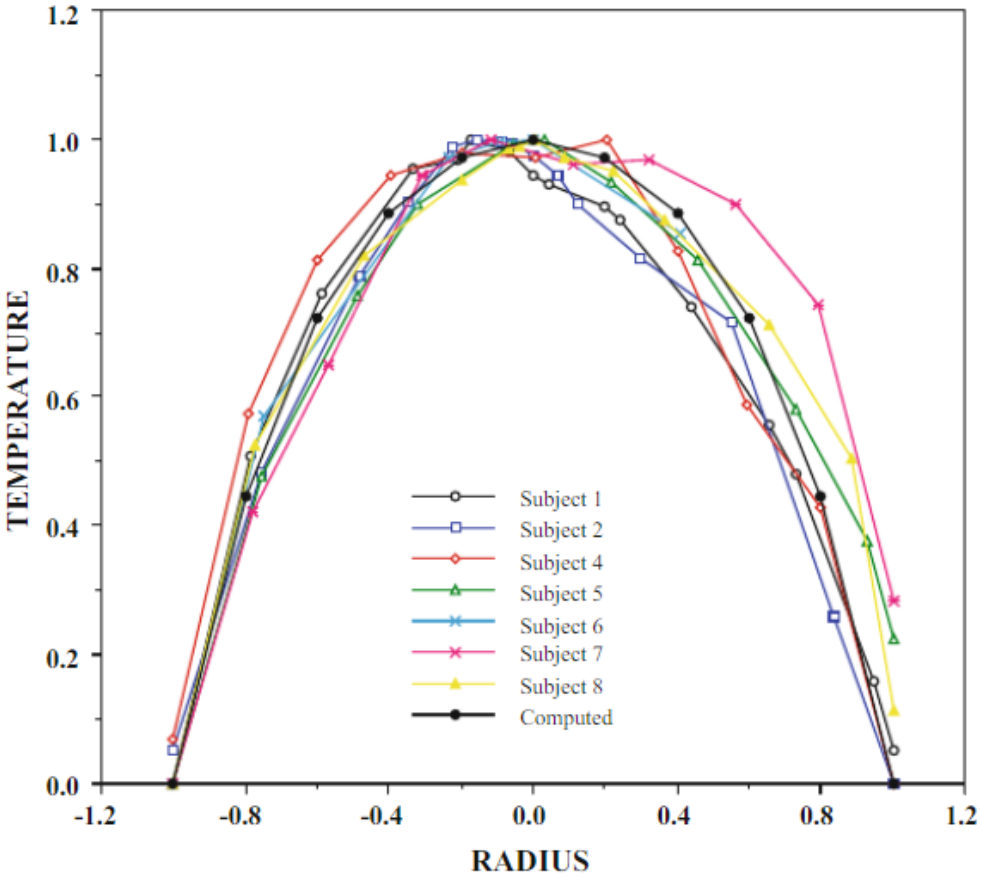

Figure 2.1: Distribution of tissue temperature throughout the forearm of 8 subjects compared with the theoretical distribution predicted by Pennes [43] and later scaled and visualized by Wissler [44].

While the heat production, flow, and losses previously described can be applied to isolated segments of the body such as the forearm, the principles will equally apply to the body as a whole. While the quantified heat balance generally results in safe and comfortable internal temperatures, these temperatures can move to concerning levels if generation and losses diverge. The previous sections described the dependence of the heat loss mechanisms on ambient conditions; high ambient temperatures, for example, will provide very little thermal gradient to drive dry heat loss, and the combination of high ambient temperatures and relative humidity levels will similarly provide very little gradient in vapour pressure to drive evaporative losses. Accordingly, such conditions often prevent the loss mechanisms from eliminating sufficient heat to achieve thermal balance in the body,

and core temperatures elevate. This is especially common during the performance of exercise in hot, humid conditions, since internal heat generations levels will rise as a by-product of the enhanced metabolic activity, further challenging the body's loss mechanisms. These undesired elevations in temperature are concerning, as they will put the body at risk of heat-related illnesses and injury, and will additionally impact its ability to perform external work. The following sections will therefore discuss these observed impacts of elevated temperatures on the body in further detail.

2.2 Exercise-induced Hyperthermia

When exercising, metabolic rates can rise to levels up to 15 times greater than resting rates to provide energy for skeletal muscle contraction, the majority of which is released as heat (between 70 to 100% depending on the type of exercise) [45]. This inevitably elevates temperatures throughout the body above their resting levels, eliciting thermoregulatory interventions of sweating and vasodilation. An elevated sweat rate increases evaporative heat losses, and cutaneous vasodilation elevates skin temperatures, thereby increasing convective, radiative, and conductive heat losses as well. During most exercise in cool and temperate conditions, these heat dissipation pathways are sufficient to restore thermal balance, and body core temperature settles at a slightly elevated, but stable and safe level. However, with a combination of sufficient exercise intensity and hot, humid ambient conditions, heat loss remains insufficient to achieve thermal balance even as sweat rate and the thermal gradient between skin and surroundings grow. Temperatures within the body then continue to rise, resulting in discomfort [5], hindered athletic performance [4] [46], or even severe adverse health outcomes [47] [46]. The elevated sweat rate brought about by high body temperatures also leads to an increased risk of dehydration, which can exacerbate the health risks and performance reductions associated with exercise in the heat [4] [46]. The following sections first discuss the spectrum of heat-related health risks resulting from elevated body temperatures, then discuss the observed reductions in measured athletic performance, and review the mechanisms bringing about such reductions.

2.2.1 Pathophysiological Impact of Heat Stress

Deviations exceeding several degrees above the body's desired core temperature of roughly 37°C can result in heat-related illnesses, which range in severity from mild to life-threatening. The spectrum of heat-related illnesses includes heat edema, heat rash, heat cramps, heat syncope, heat exhaustion, and the most life-threatening condition, heat stroke [46] [47].

Among the less severe forms of heat-related illness are heat edema and heat rash. Heat edema is a consequence of enhanced peripheral vasodilation, which leads to increased fluid buildup and swelling of the interstitial compartments in the skin. Symptoms can typically be improved through elevation of the limbs, combined with compression garments and proper rehydration with electrolytes [46]. Heat rash results from excessive sweating, and leakage from the sweat gland into the dermis layer, often occurring when sweat glands are blocked by clothing or athletic equipment. It is typically treated through immediate cooling of the affected area and removal of clothing around the rash [46]. In thermally stressful conditions, skin temperature typically rises rapidly before dramatic changes in core temperature are observed. Elevated skin temperatures can elicit increased sweating and peripheral vasodilation, meaning heat edema and heat rash can occur even in the presence of moderate core temperatures [46].

Heat induced peripheral vasodilation decreases the body's vascular resistance, and when accompanied by sudden exertion or postural changes can drop blood pressure sufficiently to cause dizziness or fainting, referred to as heat syncope. This condition can also occur in the absence of extremely high core temperatures, as vasodilation will begin with even mild heat stress. Treatment for this condition involves immediate transition to a supine position and elevation of the limbs to promote venous return. While individuals can recover rapidly from heat syncope itself when effectively treated, a brief loss of balance or consciousness during physical exertion can result in a falling injury, which presents further risk [46].

Heat cramps are sudden, involuntary contractions/spasms of muscles during activity in the heat. The exact cause is not known, though it is suspected to result from electrolyte and fluid imbalances arising from sweating without sufficient replacement of fluids and salts. Salt depletion may result in spontaneous discharge of muscle nerve axon terminals. Heat cramps are generally distinguished from exertional cramps by their effect on more widespread musculature, often impacting several adjacent muscles [46]. Unexpected muscle contractions could also lead to a risk of falling injury in some forms of exercise.

Heat exhaustion is characterized by feelings of intense fatigue, weakness, headache, nausea, and dizziness resulting from rising core temperatures [46]. It occurs when the body is no longer able to meet both exercise demands and thermoregulatory demands required to keep body temperature at tolerable levels, and can result in a rapid onset of symptoms. Immediate removal from the heat and

activity is advised for an individual experiencing heat exhaustion, and rapid cooling should be applied, along with the oral ingestion of cool fluids, if symptoms permit. Individuals can recover from heat exhaustion reasonably quickly if addressed effectively, however, proper treatment is critical to prevent heat exhaustion from escalating to heat stroke [46].

Heat stroke is the most dangerous heat-related illness, and can lead to long-term brain and vital organ damage, and even death. It is characterized by temperatures rising above 40°C, accompanied by strong central nervous system complications, such as dizziness or confusion [47]. Heat stroke represents the point where the body can no longer fulfill the simultaneous needs of thermoregulation, exercise, and general bodily function. As the body succumbs to the overwhelming demand for blood and fluids, proper thermoregulatory function is interrupted, sometimes resulting in a cessation of sweating and cutaneous vasodilation despite significant heat stress in the body [47]. Accordingly, body temperatures have been observed to quickly and unexpectedly rise to 41°C or greater during heat stroke, potentially leading to irreversible damage or death [46]. The specific pathologies resulting from heat stroke include heat-related tissue injury, rhabdomyolysis, and heart or other organ failure resulting from the challenge of simultaneously supplying blood to vital organs, exercising muscles, and thermoregulatory functions [46] [47].

2.2.2 Impact on Athletic Performance

Even in the absence of health complications, exercise in the heat results in well-documented reductions in athletic performance. This has been observed for many different forms of activity and exertional intensities. It has been studied extensively in the laboratory setting using stationary exercise equipment, as well as via analysis of recorded competition performances in a variety of ambient conditions.

Research in the Laboratory Setting

Athletic performance reduction owing to heat stress is frequently studied in the laboratory setting, where thorough monitoring of many physiological markers is possible. Ambient conditions can be finely controlled using environmental chambers or predictable environments, and stationary exercise equipment allows exercise bouts to be repeated precisely. Though it is not directly applicable to all forms of exercise and athletic competition, perhaps the most straightforward measure of athletic ability is the observation of maximal work capacity. This is typically determined by having study

participants perform maximal intensity exercise and measuring the work rate in watts through some form of ergometry, or by measuring maximal oxygen volume uptake (VO2max), which corresponds directly to the amount of aerobic metabolic work being done. Table 2.4 below highlights studies investigating the effect of heat stress on VO2max, and ergometry measures of maximal work rate.

Table 2.4 - Impact of thermally stressful conditions on measures of maximal athletic performance. Table adapted from [4].

Study	Number of participants	Control Condition	Heat Condition	VO_{2max} reduction	Maximum Work Capacity reduction
Arngrimsson *et al.* [48]	22	25°C	35°C 40°C 45°C	4% 9% 17%	8% 14% 32%
Gonzalez-Alonso *et al.* [49]	8	14-16°C	44°C water-perfused suit	8%	28%
Klausen *et al.* [50]	6	25°C	40°C	4%	
Lafrenz *et al.* [51]	10	22°C	35°C	9%	52%
Lorenzo *et al.* [52]	12 (acclimation test group)	13°C	38°C	16%	
Lorenzo *et al.* [52]	8 (unacclimated test group)	13°C	38°C	18%	
Nybo *et al.* [53]	6	14°C	44°C water-perfused suit		
Pirnay *et al.* [54]	18 (short heat exposure duration) 8 (long heat exposure duration)	23°C 23°C	46°C 46°C	7% 27%	
Rowell *et al.* [55]	27	26°C	49°C	3%	
Sawka *et al.* [56]	13	21°C	49°C	8%	
Williams *et al.* [57]	3	21°C	35°C	0%	
Wingo *et al.* [58]	7	22°C	35°C	7%	9%

As can be seen in Table 2.4, heat stress consistently reduces participant's maximal work capacity. Of the listed studies, the work of Williams *et al.* [57] was the only one that did not observe a reduction in performance; however, the very limited sample size of this study should be noted. While it is generally challenging to compare across studies with varying protocols, it appears that maximum capacity is reduced further in progressively more thermally stressful conditions. This can be seen directly in the results of Arngrimsson *et al.* [48] which reports the reduction in three separate environmental temperatures. Additionally, the results of Pirnay *et al.* [54] show a greater reduction capacity following longer duration of exposure to thermally stressful conditions. This suggests that the impact of heat stress can vary in severity and is not simply a binary phenomenon that either occurs absolutely or not at all. Such features are of interest in the discussion of performance reduction mechanisms in the coming sections.

In addition to reductions in maximal work capacity, there is a widely documented reduction in submaximal and endurance exercise performance in thermally stressful conditions as well. Table 2.5 documents laboratory studies investigating the impact of thermally stressful conditions on prolonged submaximal exercise performance.

Table 2.5 - Impact of thermally stressful conditions on submaximal athletic performance. Table from [4] with modifications. The test format TT represents a time trial, where either distance or time is fixed, and power output is measured throughout. Test format TTE represents a time-to-exhaustion test, where work rate is fixed, and the time until volitional exhaustion is recorded.

Study	Number of participants	Test Format	Control	Heat	Performance Reduction
Alteraki *et al.* [59]	9	Cycling TT	13°C	35°C	2%
Bannister & Cotes [60]	3	Running TTE	17°C	25°C	12%
Dill *et al.* [61]	5	Cycling TTE	12°C	34°C	25%
Ely *et al.* [62]	8	Cycling TT	21°C	40°C	17%
Galloway & Maughan [63]	8	Cycling TTE	21°C	31°C	36%
Gonzalez-Alonso *et al.* [64]	7	Cycling TTE	36°C (water immersion)	40°C (water immersion)	39%
Lorenzo *et al.* [52]	12 (acclimation test group)	Cycling TT	13°C	38°C	17%
Lorenzo *et al.* [52]	12 (unacclimated test group)	Cycling TT	13°C	38°C	18%
MacDougall at al. [65]	6	Running TTE	23°C	39°C	36%
Périard *et al.* [66]	8	Cycling TT	20°C	35°C	7%
Roelands *et al.* [67]	8	Cycling TT	18°C	30°C	25%
Tatterson *et al.* [68]	11	Cycling TT	23°C	32°C	7%
Tucker *et al.* [69]	10	Cycling TT	15°C	35°C	6%
Tyler & Sunderland [70]	9	Running TT	14°C	30°C	7%
Watson et al [71]	9	Cycling TT	18°C	30°C	30%

Once again, it can be observed that thermally stressful conditions consistently reduce exercise performance, this time in a submaximal endurance context. While the different nature of time-to-exhaustion and time-trial performance metrics mean that performance reductions cannot simply be compared directly, it is of note that performance is reduced across both forms of study. Time-trial tests allow for a self-selected exercise intensity, potentially allowing conscious perceptual impacts of heat stress on the participants to impact their pacing and effort. In contrast, time-to-exhaustion tests enforce a set work rate and measure the duration for which it can be sustained. While time-trial tests may be a more representative simulation of many forms of competition, time-to-exhaustion tests can be useful to directly observe the effects of heat stress on the body's ability to perform a given, set exercise task. The fact that performance is consistently reduced across both forms of exercise test suggests that the reductions cannot simply be explained by conscious sensation impacting self-selected pacing, and that other underlying physiological mechanisms likely contribute as well. Such mechanisms will be discussed in upcoming sections.

Additionally, the work of Lorenzo *et al.* [52] and Sawka *et al.* [56] listed in the above tables, as well as many other studies, observe that heat acclimation can improve exercise performance in the heat. This can serve to counteract some of the performance reduction owing to thermal stress, though not to the point of eliminating it. Meta-analyses by Benjamin *et al.* [72] and Waldron *et al.* [73] summarize many of the studies investigating the impact of heat acclimation on exercise performance in the heat, though a full discussion of this topic falls beyond the present scope.

Exercise Performance in the Field

While laboratory studies allow for monitoring and measurement of an extensive array of physiological markers, as well as precise control of exercise protocols and ambient conditions, they will always produce environments that do not fully reflect the conditions of live events in true competition venues. Racinais *et al.* [74] aimed to observe the impact of hot ambient conditions on cycling time trial performance in true outdoor cycling circuits, citing that laboratory tests do not adequately capture the effects of convective cooling changes resulting from cycling motion, and air resistance changes owing to the variation of air density with temperature. They observed that even in true outdoor conditions, time trial performance was diminished in hot conditions compared to cool conditions, also noting that performance in the heat improved with acclimation. While this experiment revealed that performance reductions are in fact observed while accounting for effects of

an outdoor environment and true cycling motion, it still fails to recreate the competitive environment of actual races, and participants were acutely aware that they were participating in a research study. While it can be more challenging to measure, it is the impact of heat stress on true competition results that is ultimately of most interest.

Some sports, such as endurance racing or track and field events, result in precisely quantifiable outcomes, such as recorded race times. These indicators allow performance to be documented from past events, enabling comparison of results between events in hot conditions to events in temperate and cool conditions. Ely *et al.* [75] related running times across marathon events to environmental heat stress based on Wet Bulb Globe Temperature (WBGT). The times relative to the course record of the 1^{st}, 2^{nd}, 3^{rd}, 25^{th}, 50^{th}, 100^{th}, and 300^{th} place finishers in each race were compared, and it was observed that performance progressively diminished as WBGT rose. Top male finishers were 1.7 ± 1.5% slower than the course record in the coldest quartile of races investigated, and were 4.5 ± 2.3% slower than the course record in the warmest quartile. The top women finishers were 3.2 ± 4.9% slower than the course records in the coldest quartile, and 5.4 ± 4.1% slower in the warmest quartile. The 25^{th}, 50^{th}, 100^{th}, and 300^{th} place finishers were slowed even more than top runners for increasingly hot conditions. Similar work by Guy *et al.* [76] compared performance in International Association of Athletics Federation (IAAF) World Championships spanning from 1999-2011 in environmental temperatures greater than 25°C to those in temperatures below 25°C. They similarly observed that the average times of the top 10 finishers in endurance events were reduced by roughly 3% (Cohens $d > 0.8$) in the hotter condition group.

In contrast, sports that involve head-to-head competition between individuals or teams, such as soccer/football, do not allow for as straightforward of a comparison between performance in hot and temperate conditions. While racing sports provide objective and absolute performance metrics, head-to-head sports result only in scores relative to an opponent, who would be subject to the same ambient conditions. Nonetheless, certain measures can be recorded and compared to gain insight into the performance reductions owing to environmental heat stress. Several studies have tracked player movement in soccer/football games using camera or GPS-based systems, including work by Ozgunen *et al.* [77], Mohr *et al.* [78], and Nassis *et al.* [79]. While top sprint speed was generally not reduced in hot conditions, and only Mohr *et al.*observed a reduction in total distance covered by players, all studies observed a reduction in distance covered at high speeds. Conversely, work by Aughey *et al.* [80] performing similar analysis on Australian rules football matches observed that players covered

less total distance in the heat, while the quantity of high intensity running was not significantly reduced. While the above investigations mostly aim to quantify sport performance based on movement tracking, Sunderland *et al.*aimed to observe the impact of exertion in the heat on skill test performance among trained field hockey players. They found that when participants completed a protocol involving the Loughborough Intermittent Shuttle Test (LIST) interspersed with field hockey skill tests involving running, dribbling, passing, and shooting, the skill test performance was reduced when the protocol was completed in hot environmental conditions.

While the ways that the performance reductions manifest themselves may vary, the above research, when combined with the results obtained for studies in the laboratory setting clearly indicate that athletic performance is reduced by heat stress. The physiological mechanisms behind the performance reductions will be discussed in the following sections.

2.2.3 Performance Reduction Mechanisms

The reduced athletic performance observed in hot conditions is likely the product of several conspiring mechanisms. The most straightforward among them may be the exacerbated challenge of supplying blood to the working muscles resulting from the additional demand for blood flow of the skin for thermoregulatory purposes. Another likely mechanism is the suppression of the motor driving signals initiating muscle contraction from the central nervous system as a defensive response to limit further heat production. Furthermore, heat stress can lead to enhanced feelings of exertion, discomfort, or pain impacting motivation and pacing. The following sections will discuss these mechanisms in further detail.

Aerobic Capacity Limitations

The rates at which an individual's muscles can perform and sustain work will be a direct contributor to athletic performance in virtually all forms of competition. As discussed, muscular work is powered by the aerobic and anaerobic metabolism of fuels to release usable energy. Aerobic metabolism is favoured by the body to support the performance of work, as it is able to sustain consistent energy delivery to working muscles for long periods of time (up to hours or days) since the by-products of the processes can be continually removed from the body. However, the rate at which aerobic metabolism can supply energy, and therefore the rate of muscular work that it can support, is limited by the amount of oxygen that can be delivered to the muscle site. If the body is performing work at

such a rate that energy demand exceeds the amount that can be supported by the body's oxygen delivery capabilities, excess required energy is produced via anaerobic metabolism. However, the anaerobic chemical processes produce by-products that can accumulate and interfere with muscle contraction and force production, resulting in muscle fatigue. This means that anaerobic metabolism cannot be relied upon to produce energy sustainably for long periods of time. [81]

Accordingly, the body's ability to deliver oxygen to working muscles is a key contributor to an individual's athletic performance, as it directly relates to the work rate the individual can sustain throughout athletic competitions. VO2max is therefore often used as an indicator of athletic ability. During high intensity exercise, elevated stroke volume and heart rate combine to increase cardiac output, and direct additional blood to working muscles for oxygen delivery. Sufficiently high intensity exercise will elicit a maximal heart rate and cardiac output, at which point no further blood (and therefore oxygen) can be delivered to muscles for aerobic work, and VO2max is reached.

While in heat stress, cutaneous vasodilation directs blood flow towards the skin as a thermoregulatory response to carry heat from the body core to the periphery. Not only does this present an additional demand for blood delivery, but the increased blood volume in the cutaneous venous bed depletes the central blood volume, which reduces cardiac filling, and consequently, stroke volume [82] [83]. Heart rate must therefore rise even further during exercise in the heat to compensate for the impacted stroke volume and meet the combined demand for blood from both the muscles and skin. Exercise of sufficient intensity will cause heart rate to approach its maximal value, at which point it cannot compensate for the limited stroke volume any further, leading to a reduction in cardiac output [82] [55] [83] [84] [85]. Accordingly, less oxygen can be delivered to working muscle when compared to thermoneutral conditions, leading to reduced VO2max, and reduced aerobic work capacity [49] [84]. The reduced aerobic capacity limits the body's total maximal work rate, and also necessitates a greater reliance on anaerobic metabolism at higher work rates, which elicits fatigue as previously discussed. Additionally, dehydration caused by heat-induced sweat rate elevations is associated with lower blood volume overall [86]. This further reduces central blood reserve volume and cardiac filling, exacerbating the above effects [87] [88]. For this reason, it is generally accepted that dehydration and hyperthermia have conspiring effects on athletic performance reductions.

Limited oxygen delivery to working muscles is undeniably a dominant contributor to performance reductions, especially for higher intensity exercise [4]. However, it has been observed that muscle oxygen delivery can be sustained during lower intensity exercise in the heat in which heart rate can compensate for reduced stroke volume [89] [90], or in exercise of smaller muscle groups that do not require high cardiac output to meet blood demand [91]. Accordingly, other mechanisms must contribute to the performance reductions present in such exercise bouts.

Suppression of Central Motor Driving Signals

Since the earliest studies of exercise in the heat, researchers have suspected that the central nervous system (CNS) plays a role in limiting performance [92]. It was not until the work Nybo and Neilsen [93] in 2001, however, that strong supporting evidence was uncovered. In this work, participants were made to perform cycling exercise in hot conditions until volitional exhaustion, at which point core temperatures rose to roughly 40°C. Following the cessation of cycling exercise, maximal voluntary contraction (MVC) knee extensions were performed, and the participants' force production was measured. It was observed that the force that could be sustained by participants during MVC knee extension was significantly reduced following exercise in the heat when compared to knee extensions performed after cycling exercise of the same intensity in thermoneutral conditions. However, when electrical stimulation of the muscles was superimposed with maximal voluntary contraction, force generation was not reduced by the hot conditions, suggesting the force generating capability of the muscles themselves was preserved, and the reductions in force production resulted from less activation of the muscles by the CNS motor driving signals. This is supported by electromyography measurements made on the *m. vastus lateralis* muscle during the knee extension MVCs, which showed significantly less muscular activation activity following exercise in the heat. To further ensure that local muscular fatigue resulting from the exercise bout did not contribute the reduced force generation ability, maximal voluntary contractions were also performed measuring handgrip strength following bouts of cycling exercise in the heat. The muscles contributing to handgrip strength would be relatively inactive during the cycling bout and would not fatigue locally; however, a reduction in sustained hand grip force generating capability was still observed following cycling exercise in the heat in comparison to thermoneutral exercise. This once again indicates that reduced contractile ability did not result from muscle fatigue caused by the exercise bout, but instead from a limitation to motor drive coming from the central nervous system. This central drive inhibition limiting exercise performance is often referred to as central fatigue

Similar studies have since been carried out supporting the results of Nybo and Neilsen, and further investigating the effects of heat stress on maximal muscle activation [94] [95] [96]. Work by Thomas *et al.* [96] and Morrison *et al.* [95] employed passive heating using water-perfused garments to manipulate temperatures in specific body parts, allowing the impact on contractile ability of elevated temperatures in the core, working muscles, and skin to be observed separately. They noted that leg force production was reduced even when core temperature was raised passively, allowing leg muscle temperature to remain at moderate levels. This further supports the conclusion that motor drive signal from the CNS is reduced, and the contractile ability reduction is not brought about by local muscle conditions.

While it may also relate to cerebral changes brought about by heat stress such as brain temperature, oxygenation, or neurotransmitter levels [4], the observed central fatigue is likely a defensive response triggered by afferent sensation to limit the body temperature rise and other physiological strains imposed by excessive exercise intensity in the heat. Several different sources of afferent information likely contribute to the sensation of physiological strain that prompts the suppression of muscle contraction, including perception of temperature throughout the body core and periphery, as well as feedback from the muscles and respiratory and cardiovascular systems [97] [98]. The works of Thomas *et al.* [96] and Morrison *et al.* [95] however, indicate that core temperature has a strong independent effect on the behaviour. Sustained MVC knee extension force generation is limited for elevated core temperatures even in the presence of moderate muscle and skin temperatures, and conversely, contractile ability was not observed to be limited for core temperatures below 38.5°C, even in the presence of elevated temperatures in the skin and muscle. For higher core temperatures (above 38.5°C) however, it is likely that several afferent signals contribute to motor drive inhibition. It is generally observed in all work mentioned above, that initial, brief maximal contractile ability of the muscles is maintained, and it is the ability of the muscles to sustain contraction that is limited. This suggest that a combination of both elevated body temperatures and muscle feedback indicating sustained contraction may be necessary to elicit the suppressed central motor drive [4].

The concept of a “critical core temperature” governing central fatigue has been proposed, suggesting that the ability to sustain exercise will suddenly cease when the body core exceeds a temperature threshold, typically around 40°C, in order to prevent the damaging effects of tissue temperatures exceeding this value. While study participants are often observed to cease exercise at

this threshold even for differing core temperatures at the beginning of exercise, and differing rates of heat storage throughout an exercise bout [64], it has been observed that motivation can enable athletes to achieve higher core temperatures in competition than in training, suggesting that the mechanism may not be as simple as a critical core temperature [99] [100], and it is likely that a progressive inhibition of muscle driving signals based on core temperature contributes the reductions in sustained contractile ability [101] [95] [93] [96].

Comfort, Motivation, and Pacing

In addition to the challenges imposed on muscle oxygen delivery and the subconscious inhibition of central motor driving signals, it is also suspected that performance reductions may stem from an athlete's conscious responses to the sensation of thermal stress during exercise. It is well established that exercise in the heat leads to elevated heart rate as described previously, which itself is strongly associated with rating of perceived exertion during exercise. Ventilation rates are also observed to increase during exercise in the heat [102] which may result in feelings of dyspnea, further elevating the perception of exercise difficulty. Such responses, combined with the direct sensation of high body temperatures, likely contribute to discomfort and increased perception of exercise difficulty. This is supported by the observations of Maw *et al.* who did in fact observe an increase in feelings of discomfort and ratings of perceived exertion during exercise in the heat [5]. Such feelings may impact athlete motivation and pacing, and could lead to voluntary cessation of exercise due to intolerance of discomfort, all of which could elicit performance reductions. Work of Van Cutsem *et al.* [103] further indicates that perception alone is sufficient to elicit performance reductions. They observed that the sensation of thermal stress alone, brought about by a heating pack held against athletes' backs, was sufficient to decrease time to exhaustion in cycling bouts in temperate environments, even in the absence of any changes to indicators of actual thermal stress, such as core temperatures or heart rate.

Additional Proposed Mechanisms

Potential mechanisms beyond those discussed above that may also lead to exercise performance reductions in the heat. These include the suggestion that higher temperatures may result in diminished muscular efficiency in generating energy from a given quantity of oxygen and fuel [104] [105], or that warmer muscle temperatures may alter neuromuscular recruitment to favour muscle fibre types employing anaerobic metabolism more than aerobic [106]. There is limited evidence at this point, however, indicating that these would be prominent contributors to performance reductions [4].

Ultimately, it is likely that performance limitations result from a combination of muscle oxygen delivery challenges, especially in higher intensity exercise, as well as inhibited motor driving ability from the CNS, and impacts on pacing and self-selected exercise intensity owing to discomfort and increased perception of exertion.

2.3 Cooling Interventions

The described health risks and performance reductions motivate both recreational and competitive athletes to seek methods to avoid or limit heat stress during activity. In many cases, risk of heat stress can be reduced through organizational changes to the activity itself, including performing the activity in a cooler location or venue, or scheduling strenuous activities at times of the day where thermal load is minimized. The extent to which this can be done, however, is limited by scheduling considerations such as venue availability, and convenience for spectators, especially at elite levels of competition. Accordingly, athletes are often forced to develop their own strategies to combat the effects of hot and humid ambient conditions on health and performance. Heat acclimation programs are frequently employed and are generally effective at combating performance reductions brought about by heat stress, but do not completely eliminate them [107] [56]. Furthermore, the duration and training volume required for heat acclimation programs can interfere with regular training programs of athletes [108]. Acute cooling interventions before or during competition therefore represent another potential method to assist athletes as they compete in thermally stressful conditions. These interventions can vary, but generally involve some form of direct cooling applied to the body of the athletes aiming to extract heat and reduce body temperatures.

2.3.1 Pre-cooling and Per-cooling

In general, cooling interventions aim to reduce body temperatures in order to avoid the unwanted effects brought about by heat stress. There are two main approaches to accomplish this goal, referred to as pre-cooling and per-cooling [7] [6]. Pre-cooling refers to the application of cooling prior to the start of activity, reducing the body temperature at the beginning of competition, allowing it to store more heat before reaching concerning temperatures during competition [6]. Per-cooling on the other hand, refers to the application of cooling during activity, allowing additional heat to be removed from the body, and resulting in less heat accumulation for a given metabolic activity level and ambient environment [6].

Pre-cooling offers advantages in practicality, as equipment and garments can be employed that would be impractical or not permitted during competition. Because athletes can remain stationary during pre-cooling, aggressive cooling techniques can be applied to large surface areas of skin, such as cold-water submersion. Pre-cooling only allows the beginning body temperatures to be lowered however, and the impacts can eventually be lost in prolonged bouts of exercise [109]. The extent to which body temperatures can be reduced before exercise will also be limited, as it will eventually result in discomfort or limitations to muscular performance [110]. A meta-analysis of the impact of pre-cooling on athletic performance found a 5.7 ± 1.0 % increase (effect size 0.44) in recorded performance metrics when compared to control conditions [6]. While the finding that performance is frequently improved is of value, the meaning of the quantified improvement may be limited, as the studies included in the meta-analysis featured widely varying exercise protocols, performance metrics, cooling methods, and ambient conditions.

Per-cooling on the other hand, is capable of delivering prolonged benefits by extracting additional heat from the body throughout exercise, leading to slower temperature rises, and making it easier for the body to achieve thermal equilibrium in stressful conditions. The application of per-cooling can be more challenging in practice, however, as it must be applied in ways that comply with competition rules and do not interfere with athlete performance by restricting movement or adding excessive weight/bulk [7]. A meta-analysis of the impact of per-cooling on athletic performance found a 9.9 ± 1.9 % increase (effects size 0.40) in recorded performance metrics when compared to control conditions [6]. As with the pre-cooling meta-analysis, the meaning of the quantified improvement may once again be limited due to widely varying exercise protocols, performance metrics, cooling methods, and ambient conditions.

2.3.2 Heat Removal Pathways for Acute Cooling Interventions

Regardless of whether cooling is applied before or during competition, it aims to extract heat from the body. As previously discussed, heat is eliminated naturally from the human body via a combination of conduction into contacting surfaces, convection into surrounding fluid, radiation exchange with surrounding surfaces, and the evaporation of sweat from the skin surface [3] [111]. Cooling interventions employ similar pathways to extract additional heat from the body. Common heat removal methods/pathways employed in acute cooling techniques are discussed in this section.

Perhaps the most common heat extraction pathway employed by acute cooling interventions is conduction heat transfer. Cold surfaces are held against the skin, allowing heat to flow from the body into the contacting surface. Examples of such cooling interventions include the use of ice packs, vests, and cooling collars/hoods, which can be employed in both pre-cooling and per-cooling. Generally, the colder the surface held against the skin, the larger the thermal gradient between the body and the cooling surface, and the more heat that can be extracted; however, colder surfaces elicit more vasoconstriction in the skin and result in colder skin temperatures, thus limiting the gradient and the amount of heat the can be extracted [112]. Eventually, the added effectiveness of further reducing the cooling surface temperature progressively diminishes [113] [114]. Intuitively, applying cooling to large surface areas of skin in regions with high amounts of superficial blood perfusion will be most effective.

Another heat extraction pathway commonly employed to provide cooling is convection to a surrounding fluid. It should be noted that heat will be continuously lost via convection to the surrounding air in almost all circumstances, however, acute interventions can alter the conditions of convective loss to provide additional cooling. Examples of this include the use of air conditioning systems to cool ambient air in an enclosed environment, or the use of fans to increase relative velocity of air moving over the skin. Cooling ambient fluid results in a larger temperature gradient between the skin and surrounding fluid, driving further heat loss, while increasing fluid velocity leads to greater heat loss for a given temperature gradient between skin and environment [115]. Another example of the use of convective heat loss in an acute cooling strategy is the submersion of body parts in a cool water bath. Not only will water below the ambient temperature increase the gradient driving heat loss, but the thermal properties of water result in more convective heat loss than in air for a given gradient [116]. Some forms of stationary exercise may allow parts of the body to be submerged in cooled water during activity, but it is generally challenging to employ this technique as per-cooling, especially in the field setting. Cold water submersion is therefore more commonly employed in pre-cooling, where baths can be setup to allow for submersion of as much body surface area as is desired. A similar approach that can be employed more practically during activity is the spraying or pouring of cold water onto the body. Similar to conductive cooling, colder fluid temperatures generally allow more heat to be extracted, though added effectiveness diminishes for progressively cooler temperatures, as vasoconstriction effectively increases the insulating effect of the skin [113] [114].

Another pathway employed to cool athletes during activity is evaporative cooling. This could involve water spray onto the skin, or the use of an evaporative cooling vest or hood that stores large quantities of water for evaporation near the skin. In reality, the heat lost to evaporation must flow from the body into the water via convection or conduction before it can be used to evaporate the liquid, however, evaporation is typically considered its own heat loss pathway in the context of human thermoregulation. It should be noted however, that while the water added by these methods will enable additional evaporative cooling for low sweat rates, it is common for evaporation to reach a maximal level due to ambient humidity when the skin is sufficiently wetted from sweat, at which point further moisture added to the skin simply accumulates or drips, and will not result in greater evaporative heat losses [111]. Even in these cases, however, the external wetting of the skin may still offer benefits, as higher skin wettedness will suppress the secretion of further sweat [111]. This would allow the body to achieve the same benefits of maximal evaporative cooling while experiencing less fluid loss. Furthermore, the limitation of maximal evaporation rates can be addressed through the use of a fan combined with the water spray, as increased air velocity over moist skin will promote additional evaporation [117]. It should be noted, however, that the fan would similarly contribute to additional evaporation of sweat even in the absence of a water spray.

A final common heat extraction pathway, referred to as internal cooling, involves the ingestion of cold water, or ice-water slurry. An advantage of such methods is that they are often among the more practical to employ during activity [7], since athletes will be consuming water during activity anyways, though the amount that can be ingested may be limited before it results in gastro-intestinal discomfort [118]. It is worth noting, that while the heat does not immediately leave the body in this case, the added fluid contributes additional mass with thermal capacity to the body at a lower temperature, reducing average body temperature.

2.3.3 Literature Review of the Impact of Pre-cooling

Table 2.6 below documents prominent publications investigating the effects of pre-cooling on body core temperature and athletic performance, as gathered in a meta-analysis review by Bongers *et al.* [6]. As can be seen, the cooling techniques generally employ the heat removal pathways outlined above. As indicated in these publications, pre-cooling is very capable of combatting the impacts of high core temperatures to improve measured performance metrics. Performance metrics employed include time trial times, time to exhaustion measurements at a fixed exercise intensity, or intermittent

sprint times. It should be noted that pre-cooling does not consistently reduce maximum core temperature in the above studies, however, this should not be taken as a sign that the cooling is ineffective. In order to achieve the observed performance improvements, more total metabolic work would have been completed by the study participants, thus generating more metabolic heat that would counteract the impacts of the applied cooling. Allowing participants to achieve similar core temperatures after completing more total work is in fact the intended effect of pre-cooling.

Table 2.6: Assembled results from various publications studying the impact of pre-cooling on subsequent core temperature and exercise performance. Table adapted from [6]. Performances changes marked with a * were found to be statistically significant.

Study	Cooling Description	Max T_{core} in control	Max T_{core} in cooling	Performance change
Castle *et al.* [119]	Cooling packs (-16.0 ±5.8°C at start) covering quadriceps and hamstrings	39.1	38.8	4.3%
Castle *et al.* [119]	Cooling vest (10.7 ± 2.5°C at start) on torso	39.1	38.9	1.5%
Castle *et al.* [119]	Whole body water immersion (17.8 ± 2.1°C at start)	39.1	38.4	-0.5%
Minett *et al.* [120]	Iced towel on head (5.0±0.5°C)	39.1	39.1	4.3%
Minett *et al.* [120]	Iced towel on head (5.0±0.5°C), hand submersion in cold water (9.0±0.5°C)	39.1	39.0	5.2% *
Minett *et al.* [120]	Iced towel on head (5.0±0.5°C), hand submersion in cold water (9.0±0.5°C), Ice vest and ice packs on quadriceps (both stored at -20°C)	39.1	38.7	9.5% *
Arngrimsson *et al.* [121]	Ice-filled vest	39.8	39.6	1.3%
Duffield *et al.* [122]	Ice cooling jacket	38.8	38.7	2.4%
Duffield *et al.* [123]	Ice-vest	39.6	39.2	1.3%
Duffield *et al.* [123]	Cold water bath at 14±1°C followed by ice-vest	39.6	39.2	1.3%
Quod *et al.* [124]	Cooling Jacket	39.6	39.7	1.5%
Quod *et al.* [124]	Cold water immersion followed by cooling Jacket	39.6	39.5	4.0%
Uckert *et al.* [125]	Cooling vest at 0-5°C	38.8	38.4	7.3%

Burdon *et al.* [126]	Ice slushy ingestion	38.7	38.7	10.5%
Byrne *et al.* [127]	Cold water (2°C) ingestion	38.6	38.1	2.9%
Ihsan *et al.* [128]	Crushed ice ingestion	38.8	39.1	6.9% *
Siegel *et al.* [129]	Ice slurry ingestion	39.5	39.8	12.8% *
Stanley *et al.* [130]	Ice slush beverage	39.1	39.0	1.9%
Stevens *et al.* [131]	Ice slurry ingestion	39.0	38.2	2.8% *
Cotter *et al.* [132]	Ice vest, cold air (3°C) exposure, and cooling pads on thighs	38.9	38.5	15.2% *
Duffield *et al.* [133]	Cooling vest, towel soaked in 3°C water, ice bags in thighs	39.3	38.8	7.7% *
Duffield *et al.* [134]	Ice vest, towels soaked in 5°C water on head and neck, ice-slushie ingestion	39.0	38.9	3.0%
Minnett *et al.* [135]	Ice vest and ice packs on thighs stored at -20°C prior to start, towel soaked in 5°C water, hands immersed in 9°C water	39.1	38.7	4.7% *
Duffield *et al.* [136]	Immersion of lower body in 14 ± 0.3°C water	39.0	38.9	7.2% *
Kay *et al.* [137]	Whole body water immersion	38.8	38.5	6.0% *
Siegel *et al.* [129]	Immersion in 24°C water	39.5	39.5	21.6% *
Skein *et al.* [138]	Whole body submersion in 10°C water bath	38.9	38.7	2.4% *

It is also noted in the review by Bongers *et al.* [6] that the most effective pre-cooling techniques were those that employed multiple forms of cooling, such as a combination of ice vests and cooling packs on other body parts. It was also suggested that techniques targeting as much of the body surface as possible would be most effective.

2.3.4 Literature Review of the Impact of Per-cooling

Table 2.7 below documents prominent publications investigation the effects of per-cooling on body core temperature and athletic performance, as gathered in meta-analysis reviews by Bongers *et al.* [7] [6]. The publications in Table 2.7 indicate that per-cooling can be quite effective in augmenting athletic performance in the heat. Only one of the included studies reduced performance, and this could possibly be attributed to poor design of the cooling technique. In this study, participants performed running exercise while wearing a cooling garment on one hand. The garment featured a

cooling pack held against the palm, and was otherwise insulated on all other sides to prevent heat from escaping the cooling pack away from the body. Not only would this add weight to one hand while running, which would make the task more difficult and awkward, but as the cooling pack warms towards the temperature of the skin it would not only be unable to remove heat from the body, but the insulation around the garment on all sides may result in less total heat being lost from the hand. This case should emphasize the importance of effective cooling design, and of considering the unintended effects added weight and bulk can have on athletic performance. Beyond this, all studies observed increases in performance metric values, with the majority observing statistically significant improvements.

Table 2.7: Assembled results from various publications studying the impact of per-cooling on subsequent core temperature and exercise performance. Table adapted from [7]. Performances changes marked with a * were found to be statistically significant.

Study	Cooling Description	Max T_{core} in control	Max T_{core} in cooling	Performance change
Hsu *et al.* [139]	Cooled metal surface on palms in negative pressure chamber	38.4	38.1	6.6% *
Minitti *et al.* [140]	Cold neck collar stored in industrial freezer before use	Not reported	Not reported	6.6% *
Sheadler *et al.* [141]	Cold pack strapped to palms	39.2	39.4	-11.6% *
Tyler *et al.* [142]	Cold neck collar stored in industrial freezer before use	39.3	39.1	5.1% *
Tyler *et al.* [142]	Cold neck collar stored in industrial freezer before use	38.3	38.4	1.9%
Tyler & Sunderland [143]	Cold neck collar stored in industrial freezer before use	38.9	38.9	13.0% *
Tyler & Sunderland [144]	Cold neck collar stored in industrial freezer before use	39.2	39.7	7.0% *
Luomala *et al.* [145]	Ice vest	38.9	39.1	20.4% *
Mundel *et al.* [146]	4°C drink consumption	38.7	38.4	12.7% *
Ansley *et al.* [147]	Facial water spray cooling every 30s with fans directed at head	39.0	38.9	51% *
De Carvalho *et al.* [148]	10°C water ingestion	39.3	38.9	2.8%
Cuttell *et al.* [149]	Vest soaked in water and frozen at -24°C	38.4	38.1	16.7% *
Cuttell *et al.* [149]	Cooling pack neck collar frozen at -24°C	38.4	38.2	8.7%
Eijsvogels *et al.*	Cooling vest soaked in water and stored at 6.0°C±0.5°C	39.1	39.0	0.6%
Schlader *et al.* [150]	Forced convection of 20°C air at 0.74 m/s	38.0	38.0	17.8% *
Stevens *et al.* [151]	Three 22°C water sprays every km with fan blowing air at 4m/s	38.9	38.9	2.4% *
Teunissen *et al.* [152]	4 m/s wind	39.0	38.8	4.4% *

One form of cooling sometimes used during activity that was not included in the current discussion is menthol cooling. Menthol cooling is often employed as a per-cooling technique due to the practicality of applying it without adding weight or interfering with motion. Such techniques fell beyond the scope of the present discussion however, since menthol does not actually remove heat

from the body, it simply triggers the sensation of cooling [7]. As discussed previously, performance reductions can result simply from the sensation of heat, so menthol techniques do have the potential to elicit performance improvements, but users should exercise caution, as overriding the body's protective throttling of activity levels could result in unwanted further elevations in body temperatures [7].

2.3.5 Engineering & Design Considerations for Acute Cooling Interventions

In general, powerful cooling interventions are much easier to implement in the laboratory setting than in the field. Many laboratory studies feature exercise performed on stationary equipment, such as a cycle ergometer, which allows a broader range of cooling techniques to be employed than could be used in the field. Examples of such techniques are the submersion of participants' arms in cooled water during stationary cycling exercise [153] [154], or the use of perfused cooling suits/vests [155], or other techniques that make use of heavy/bulky equipment. While practical challenges exist that can limit the range of pre-cooling techniques that can be used, such as a lack of space at competition venues, or difficulties transporting equipment, it is generally easier to use large equipment for pre-cooling purposes than for per-cooling, as the equipment can be set up for the athlete to use before competition. When attempting to employ per-cooling, however, the variety of practical techniques is far more limited [7], and the following discussion will therefore focus on the challenges and design considerations associated with mobile cooling applied during exercise. Bulkier equipment and garments can sometimes be used during breaks in competition, but many endurance sports do not provide this opportunity. In these cases, even techniques as straightforward as placing cooling packs against the athlete's body are challenging to implement, as it is difficult to hold the packs in place while the athlete competes. Garments such as cooling vests or collars can hold the cold surfaces against the body, but can be bulky and heavy, and depending on the nature of the activity can severely restrict movement and hinder performance in other ways. Avoiding adding excessive weight and bulk to the load that athletes must carry during competition is therefore a central challenge to the development of any per-cooling strategy.

All cooling techniques aim to lower body temperatures by drawing heat out of the body, however, there must be a way to eliminate or store this extracted heat energy in order to continually provide sustained cooling. The requirement that cooling techniques not contribute excessive weight or bulk renders the use of any powered cooling cycles impractical, meaning other methods to eliminate or

store the heat must be relied upon. Physical principles that can be employed for this purpose include storing the extracted heat as sensible thermal energy in an external storage substance thus raising its temperature, storing the extracted heat as latent thermal energy in a substance causing it to change state, or having the extracted heat be absorbed by an endothermic chemical reaction [156]. These heat elimination mechanisms will be discussed in the following sections.

Warming of an external storage substance

Heat extracted from the body can be stored via the warming of an external substance. What was once sensible heat energy in the body will now become sensible heat energy in the storage substance, thereby raising its temperature. The substance used to store the heat extracted from the body should therefore be cooled before use to lower it's starting temperature, and should have a high specific heat capacity in order to prevent its own temperature from rising quickly as it absorbs heat energy [156]. Examples of existing cooling techniques that employ this energy storage method are cooling packs/garments that must be stored in cold locations prior to use [140] [141] [143] [144] [142] [145] [149] [157], as well as the ingestion of cold fluid [146] [148].

Water is likely the most common substance used to store heat energy due to its availability and high heat capacity [156]. Most commercially available ice packs contain water mixed with other substances to lower the freezing point and produce a more a gel-like consistency that can conform to the shape of the body more conveniently [158]. This helps it achieve more favourable physical properties, though does not typically increase the specific heat capacity considerably. Accordingly, most cold packs will possess a specific heat capacity similar to that of water of 4.19 J/(g*K) at typical temperatures of use [156].

To quantify the impact of the heat that can be stored by water as its temperature rises, consider a simplified example where the human body is treated as a lumped thermal mass of $m_b = 80kg$ with a specific heat capacity of $c_{p_{ave}} = 3.47\ \mathrm{KJ/(kg * K)}$ [159]. In this example, it will be assumed that the heat generation and dissipation through traditional pathways remain in perfect balance in the body, ensuring that its lumped temperature can be changed only by the acute cooling applied using cold water. If $m_w = 1kg$ of cold water beginning at $T_{w_i} = 2°\mathrm{C}$ is ingested or confined in a cold pack and held against the body, beginning at an initial lumped body temperature $T_{b_i} = 37°\mathrm{C}$, heat will transfer from the body into the water until the two have reached the same temperature, $T_{b_f} = T_{w_f} = T_f$. The

heat gained by the water, Q_w, will be related to its temperature rise according to equation 1, as shown below [160]:

$$Q_w = m_w c_{p_w}(T_{w_i} - T_{w_f})$$

(2.24)

This value will be equal and opposite to the heat lost by the body, Q_b, which in turn will be related to the temperature change of the body as follows:

$$Q_b = m_b c_{p_{ave}}(T_{b_i} - T_{b_f})$$

(2.25)

Equating $|Q_w| = |Q_b|$, and solving for T_{b_f} yields a final body temperature of 36.5°C. The 1kg of water therefore had the heat capacity to absorb 144KJ of heat energy and can cool the average temperature in the body by roughly 0.5°C. It should be noted that in the case where cooling is applied externally, this is likely an overestimate of the true potential for water to store extracted heat since temperature will not remain equal throughout the body. Skin temperature will lower in response to the applied cooling, and the highest temperature the water will reach will be roughly that of the skin, not of the body core. Furthermore, the above example considers only the total storage capacity of the water, ignoring the rate at which heat will transfer from the body into the water, which will progressively diminish as the water warms. When truly evaluating the practicality of a heat storage method, the ability to maintain a sufficient temperature gradient to drive cooling at an impactful rate must also be considered.

Phase Change: Melting

Melting of a solid into a liquid represents another source of heat storage that can be employed during per-cooling. Once again, the storage substance employed must be at a lower temperature than the tissue it rests against for heat to flow into it from the body. Substances with a melting point (at atmospheric pressure) below skin temperature can be packaged and held in their solid form against the body at their melting temperature. Heat flowing into the substance can then be absorbed as the material changes state from solid to liquid [156]. Examples of cooling techniques that employ this energy storage method are cooling packs/garments employing ice or other phase change materials

[149] [145] [140] [143] [144] [142], as well as the ingestion of frozen substances such as ice slurry [126] [128] [129] [130] [131].

The amount of heat that can be stored, Q_{melt}, by a melting substance of mass m_{melt} is given by equation 38 [160]:

$$Q_{melt} = m_{melt}\Delta H_{fus}$$

(2.26)

where ΔH_{fus} is the latent heat of fusion of the substance. An advantage of this heat elimination mechanism over the warming of a substance with heat capacity is that heat can be absorbed by the storage substance without changing its temperature and reducing the thermal gradient driving the cooling [156]. Additionally, the latent heat capacities of substances are often much greater than their sensible heat capacities when warming over ranges realistic for athletic cooling, allowing phase change materials to absorb far more energy per unit volume or mass than sensible storage materials [156]. For example, water has a latent heat of fusion of 335 J/g [161]. When comparing to the previous example calculation, we can see that the same 1 kg of water could store 334 KJ as it melts, enough to lower the temperature of the 80kg body by 1.2°C, all while maintaining a constant temperature. Furthermore, this heat removal mechanism can be applied in conjunction with the warming of the cooling substance to absorb even more heat per unit of mass. For example, a 1kg ice pack could be cooled to below 0°C, at which point it could first absorb heat to warm to 0°C, then absorb more as it melts, and finally absorb additional heat to warm the now liquid water mass [156].

Phase change materials are employed to store thermal energy in many applications, and water is likely the most widely used material [162], though others exist. These other materials include water mixed with additives, waxes, oils, and other organic substances, salt hydrates, or low-melting metals [156]. Water does feature a very high latent heat of fusion compared to many of these other materials, is widely available, is economical, and does not present major safety concerns, making it a good choice for athletic cooling applications, however, other materials do offer certain advantages as well. A primary advantage is that some materials have a melting point slightly higher than water, often in the range of 10-30°C. These materials can be solidified and kept cool more easily as they do not require a freezer [163], and can be more comfortable for users, eliciting less cutaneous vasoconstriction [164]. That being said, other phase change materials generally have latent heat capacities lower than that of water [156], rendering them less efficient for heat storage by weight.

Phase change: Evaporation

State change from liquid to gas of a cooling substance is another technique often employed to store/eliminate heat extracted from an individual's body. In this case, the extracted heat is absorbed by the cooling substance, allowing it to evaporate. This technique is in fact already employed by the human body naturally, as secreted sweat removes heat from the body in order to vaporize into liquid water. One desirable feature of this heat removal mechanism is that the latent heat of vaporization of substances is typically much greater than the sensible heat capacity when warming over a realistic range, and than the latent heat capacity when transitioning from solid to liquid [156]. This allows far more heat to be removed by a given mass of a substance, such as water, through vaporization than through warming or melting. 1kg of liquid water at a typical body temperature of 37°C, for example, requires 2410 KJ of energy to evaporate [165], an amount more than 7 times greater than the energy required to melt ice into liquid water. An additional advantage is that vaporized water no longer contributes to the mass that an athlete must transport. For this reason, water evaporation can be a practical technique to apply as per-cooling, often applied as a water spray onto the skin of athletes [151] [147] [166]. However, as previously discussed, this technique will be limited by the same maximal evaporation rates achievable under given ambient conditions as sweating, suggesting other techniques may be necessary to augment the total amount of heat the body can dissipate under maximally thermally stressful conditions.

Endothermic chemical reactions

An additional method of eliminating heat extracted from the body is by allowing a spontaneous endothermic reaction to absorb it. As any chemical reaction occurs, energy is released and absorbed as bonds between particles are broken and reformed. If the total energy absorbed in the progression of the reaction exceeds the energy released, the reaction is endothermic, and will absorb heat from the surroundings as it occurs [160]. If such a reaction occurs spontaneously, it will begin once the reactants are introduced to each other and absorb heat as it progresses. An example of a cooling strategy employing this heat removal mechanism is the use of instant cold packs commonly found in first aid kits. In these packs, a chemical compound is contained within a sealed package, and the package rests in a bag of water. If the sealed package is broken open, the compound mixes with the water and an endothermic dissolution reaction begins. There are several compounds that spontaneously dissolve endothermically in water that can be used in such applications, with the most

common being ammonium nitrate (NH_4NO_3) [160]. The dissolution of ammonium nitrate absorbs 25.7KJ of heat per mole of solute. This corresponds to 321 KJ per kg dissolved. In addition to the mass of solute, the mass of solvent required to allow it to dissolve completely without saturating must be considered. The solubility of ammonium nitrate at 25°C is reported to be 213g/100g of water [167], meaning that at least 100g of water must be used to dissolve 213g of ammonium nitrate, or else the solution will saturate, and some solute will remain undissolved. This means that a total of 1kg of combined solvent and solute can absorb 218 KJ of heat. It should be noted that other factors should be considered when deciding on the amount of water necessary for a given quantity of solute, such as the rate of dissolution that can be maintained, and the amount of heat that can be absorbed from the surrounding water before it freezes. These requirements will generally necessitate the use of more water for a given quantity of solute than is required to simply avoid saturation, though the precise amount will depend on the specific context of a given application.

The heat absorbed per unit mass of this process is less than that of melting phase change materials such as water. Furthermore, it will not produce a constant temperature cooling mass, as the reaction will first cool the water rapidly, which will then slowly warm as it absorbs heat from the body. A distinct advantage of such a heat absorption mechanism, though, is the fact that it does require the use of any freezer or refrigerator to first cool a substance. This can make it very portable and easy to apply in remote settings.

Summary of Engineering Considerations

The discussion above outlines the physical principles that can be used to store extracted heat, allowing a cooling device or garment to maintain a cool enough temperature to continually extract heat from the body. All mobile cooling devices/garments will employ some mass of a cooling substance to absorb heat extracted from the body, and minimizing the mass and volume of this substance that must be packaged and transported is a primary challenge involved in the development of any per-cooling technique. Requiring an athlete to transport excessive bulk or weight for the purposed of storing extracted heat could in fact be detrimental when trying to improve comfort and performance during exercise in the heat. For this reason, higher energy storage density is desired; phase change materials are generally among the techniques that can store the most heat in a given mass or volume, making them an attractive option. Regardless of the mechanism employed to extract

and store heat, any cooling technique must feature careful design to maximize effectiveness, while ensuring they are not cumbersome or restrictive.

2.4 Thermo-physiological Modelling

The harmful impacts of elevated body temperatures on health and performance discussed in preceding sections, as well as the potential for acute cooling strategies to combat temperature rise motivates extensive investigation of the body's response to thermally stressful conditions and applied cooling. While the complexity and variability of human physiology ensure that experimentation with human subjects remains an invaluable tool in such investigations, the ability to model and predict temperature distribution and thermoregulatory behaviour within the human body without the need for experimentation is also quite useful. Predictive modelling of human thermoregulation would allow the body's response to given ambient conditions to be estimated in manner that is far less time consuming and resource intensive than human experimentation, and would allow predictions to be made for conditions that are impractical or dangerous to recreate experimentally.

Accordingly, various researchers have combined the quantitative descriptions of the previously discussed heat transfer processes to develop theoretical models aimed at predicting thermal behaviour in the human body. Burton [168] published what is likely the first thermal model of the human body in 1934, though it was quite rudimentary in comparison to modern modelling efforts. It represented the entire body as a single solid cylinder with uniform thermal conductivity and heat generation to obtain an internal temperature distribution. Though Burton recognized the role perfusing blood plays in transporting heat throughout the body, he did not include this explicitly in the model. He instead simply increased the effective thermal conductivity of all tissue, to reflect the enhanced heat flow from body core to surface brought about by circulating blood. As discussed in Section 2.2.5 Heat Transport and Distribution within the Body, Pennes [169] described the heat exchange between blood in capillary vessels and the surrounding tissue based on their respective temperatures in 1948. This allowed the total heat balance at a given location within the body to be described by Equation 2.25, a partial differential equation relating the rate of change of temperature within the tissue at any given time to local temperature gradients, heat generation, and blood perfusion. This provided a useful tool for modelling heat balance throughout the body. Wissler was among the first to employ this approach to model passive heat flow throughout a simplified geometry representing an entire body, in 1961 [170]. Such an approach has been adopted in a host of

contemporary models aiming to predict human thermal behaviour. The following sections will first contextualize the discussion of human thermal modelling by outlining the general approach common to most contemporary models, before discussing prominent examples in literature and their significance. Finally, a more detailed description of the model developed by Stolwijk [21] will be provided, as this model will be recreated and adapted in coming chapters.

2.4.1 General Approach to Human Thermal Modelling

The exact formulations of the different models existing in literature vary; however, most prominent models employ similar approaches. These models typically feature both a passive "controlled" system, as well as an active "controlling" system. The controlling system senses temperatures within the modelled body and adjusts controlling parameters in response, such as sweat rate, shivering rate, and skin blood perfusion rate, while the controlled system describes the passive heat flow in the body resulting from the current temperature distribution and the values of the controlling parameters. The controlled system typically describes heat transfer throughout the body using Equation 2.25. This equation is then solved numerically within a geometric domain representing the human body. To do this, the geometry of the body is discretized spatially by defining a network of nodes throughout body tissue. An additional node is typically defined representing the pool of central blood which will perfuse all body tissue, exchanging heat with other nodal regions. A first order approximation of Equation 2.25 can then be employed at every node within the body, allowing the temperature at each discretized location to be related to temperatures at neighbouring nodes, to the temperature of perfusing blood, and to its own temperature at successive time steps. Boundary nodes located at the skin surface feature additional terms describing heat exchange with surroundings. The discretized heat balance equations formulated at each node produce a system of equations relating all temperature values within the body across successive time steps. If an initial temperature distribution is provided, the system of equations can be solved explicitly or implicitly to determine the temperature distribution throughout the geometric representation of the body at all future time steps.

Many models simplify the human geometry, representing the body as a collection of discrete cylinders and spheres, each corresponding to different segments of the body. A representative example of the use of cylindrical and spherical components to recreate the human geometry is shown in Figure 2.2.

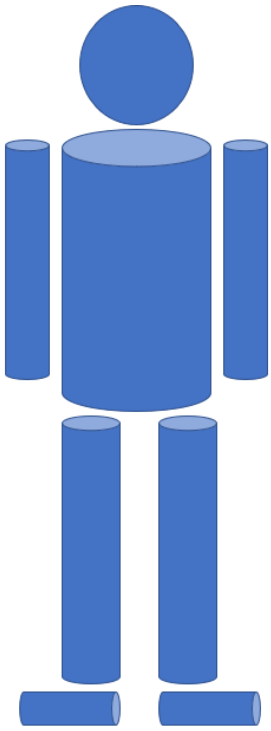

Figure 2.2: A representative recreation of the human body using spherical and cylindrical segments.

These segments are then typically subdivided into concentric layers, representing the different tissue types within the body (viscera, muscle, fat, skin etc.). Because most body regions resemble long, thin cylinders, and because temperature gradients are typically greatest in the radial direction, radial heat flow will dominate flow in other directions. It is therefore common to simplify the nodal heat balance equations by neglecting heat flow in the axial and azimuthal directions, implicitly assuming that the heat exchange between the different body segments occurs only through the central blood pool that perfuses all regions. Figure 2.3 shows a representative example of the layered construction of a cylindrical body segment.

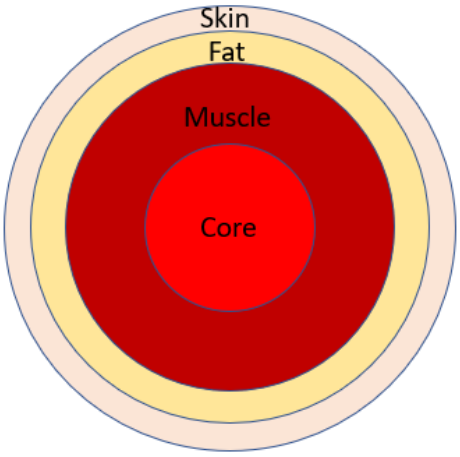

Figure 2.3: A simple representation of the tissue layers in a body segment.

The thermal state of the body at a given time step is fed into the controlling system, simulating the body's afferent sensation of heat in the body. The controlling system then adjusts model parameters, such as sweat rate, shivering rate, and blood perfusion rates, based on the sensed values. These updated parameters are then included in the heat balance equations at each node, allowing them to influence the system of equations relating current temperatures with temperatures at successive time steps. This simulates the body's ability to facilitate warming and cooling in response to the sensation of its current thermal state.

The relations used to determine controlling model parameters based on sensed temperatures can also vary between models, but tend to produce thermoregulatory responses based on deviations of temperatures in the skin and core from target setpoint values. They are often obtained through regression analysis relating measured rates of sweating, blood flow, etc. to recorded deviations from the setpoint values. They can also accept as inputs the rates of change of body temperatures, especially in the skin, as this is known to impact the body's thermoregulatory behaviour.

2.4.2 Contemporary Models in Literature

Iterative attempts to build on the early efforts to model human thermal behaviour have produced an array of contemporary models with varying aims and applications. One of the most influential models is that of Stolwijk [21], developed in 1971 at the request of NASA to predict the

thermal state expected in astronauts in outer space. The body geometry features six regions represented by cylinders and spheres, with each region consisting of 4 nodes representing the core tissue, muscle layer, fat layer, and skin layer respectively. A central blood node is also included, which exchanges heat with all body regions. The model includes a thorough feedback control methodology, allowing for vasoconstriction, vasodilation, shivering, and sweating to be initiated in response to core and skin temperatures. This model marked a noteworthy advance in the field by providing a complete representation of the body with a detailed methodology for capturing the thermoregulatory responses. Other models developed around the same time period, such as those of Fanger in 1970 [171], and Gagge *et al.* in 1971 [172], featured only a single cylindrical element used to represent the entire body, with only two concentric layers representing the "core" and the "shell". The model of Stolwijk is still used frequently in the present day, and the framework developed serves as the foundation upon which many other modern models are built. Advances in computational power in following years allowed models with more body segments and nodes to be solved, including that of Wissler in 1985 [173].

From the late 90's through the early 2010's, several prominent models were developed that are still frequently cited and widely used for modern applications. These include the model developed by Fiala *et al.* in 1999 [28] [174], the model of the UC Berkely team in 2001 [175] [176], the model of Tanabe *et al.* in 2002 [177], and the model developed by Kingma *et al.* in 2012 [178] [179], often referred to as the thermoSEM model.

The model developed by Fiala *et al.* [28] [174] included a highly detailed recreation of the average human male geometry with cylindrical and spherical elements, as well as a detailed representation of controlling thermoregulatory responses developed through analysis of collected and published data. Thorough quantification of local parameters governing heat exchange allows heat loss through the body boundary to be represented effectively. Countercurrent heat exchanger modeling is employed to capture the known effect of arterial and venous blood exchanging heat with each other while in transit between the central pool and extremities of the body. This counter-current heat exchange, and many other features employed in this model, are not novel concepts in bioheat modelling, having previously appeared in the work of Wissler [170]. However, the detailed recreation of relevant phenomena and quantification of key parameters allows the model to predict experimental results quite effectively in comparison to other models. This makes the Fiala *et al.* model one of the more widely used models in modern applications [180] [181] [182] [183].

The UC Berkely model [175] [176] developed a “body-builder” feature, aimed at allowing greater customization of parameters to better represent individual human bodies. As opposed to building the model geometry and properties based on population averages, the UC Berkely model accepts inputs such as skin colour, height, weight, and several other physiological measurements. Furthermore, the model includes additional features to capture the heat exchange with blood in the body. Instead of defining a single node to represent the central pool of blood that perfuses the body, it defines both an artery node and vein node in all body regions. These vessels both supply local perfusing blood, and also exchange heat with surrounding tissue directly, causing the temperature of arterial and venous blood to change throughout the body.

Tanabe *et al.* developed a series of models beginning in 2002 [177]. The models also featured artery and vein nodes in each body region, as well as representation of superficial veins and arteriovenous anastomoses to further depict blood blow in the body. Models of Tanabe *et al.* also allow physiological parameters such as height weight, sex, age, body fat percentage, cardiac index, and basal metabolic rate to be adjusted.

The thermoSEM model [178] [179] is similar to the model of Fiala *et al.* in its geometry and much of its passive controlled system. The primary differences are found in the function of the active controlling system. The thermoSEM model aims to recreate body’s neural sensation and effector pathways to better depict the engagement and control of thermoregulatory responses.

Numerous more recent models have aimed to build on the existing work in various ways. Roelofsen & Vink extend the influential Stolwijk model to include the effects of clothing on convective and evaporative losses, as well as to predict thermal sensation and perception based on temperature distribution in the body and regulatory responses [184]. A model by Salloum *et al.* [185], later extended by Al Othmani *et al.* [186], includes a similar depiction of heat exchange between circulating blood and tissue to the UC Berkeley model; however, these newer models employ theoretical prediction of the circulatory system to determine blood flow rates throughout the body, instead of relying on measured values. The circulatory system model used is that first developed by Avolio [187], which calculates the complex impedance of each major artery based on arterial properties, such as dimensions and tissue elasticity. With the impedance of each major artery known, the arterial tree can be represented as branching circuit diagram. A cardiac ejection waveform can then be used with the known impedances in each vessel to determine the flowrate. Differences in

flowrates between arteries entering and exiting a body region indicate how much flow has been lost to perfusion in the local body segment. While the inclusion of the Avolio circulation model provides interesting additional detail, it is not clear that it is more useful or practical than the methods of quantifying local blood flow rates through recorded measurements employed by other models. The information provided by the circulatory modeling is simply the basal flow rates in the various regions of the body, which could be measured by existing tools without fear of methodological modeling inaccuracies. Furthermore, the Avolio model requires known input values such as lengths, wall thicknesses and elasticity properties of all major arteries, which are likely more difficult to obtain than the measured flow rates themselves. Accordingly, the model relies on the values reported by Avolio, and would be challenging to adapt to specific individuals.

Mnemnieh *et al.* [188] would later build on the model of Salloum *et al.*, altering it for individuals with spinal cord injury. The employed adaptations include changes to both the active controlling system and passive controlled system. Changes to the controlled system include adjustments to arterial dimensions and wall tissue properties, local metabolic rates, and body tissue distribution based on published data. Changes to the controlling system include removing the body's ability to vasodilate, vasoconstrict, and sweat in affected regions.

Other efforts in recent decades have focused on adapting models to better represent individual subjects, rather than average humans. Individual variation of physiological parameters such as weight, skin colour and surface area, tissue distribution and thermal properties, blood flow rates, age, gender etc. will impact thermal behaviour in the body. Prominent examples of efforts to capture these variations include the previously mentioned UC Berkely model [175] [176], a model of Havenith in 2001 [189], and the individualization of the Fiala *et al.* model by Van Marken *et al.* in 2006 [190]. In 2009, Takada *et al.* [191] identified 6 coefficients for individuals impacting blood flow and sweat rates. In 2010, Yokota *et al.* [192] incorporated a Monte Carlo approach into a thermoregulatory model to address the effect of individual variability on simulated heat stress.

Additionally, many recent model developments have focused on improving the geometric representation of the human body and capturing three-dimensional heat flow within it. Fereirra & Yanagihara [193] represent the body using elliptic cylinders, as opposed to the traditional cylinders with circular cross-sectional shapes. Sun *et al.* [194] incorporate the curvature and changing cross sectional area of human body segments into their model. Li *et al.* [195] employ an even more faithful

recreation of the human geometry using 3-d meshing. Models have also been developed incorporating the location, shape, and physiological properties of internal organs into the representation of the domain. This work dates back to a passive model of Werner in 1988 [196], with recent work of Tang *et al.* [197], Mfolozi *et al.* [198], as well as Castelani *et al.* [199] building further on the principle. While the above models incorporate heat conduction through tissue in three dimensions, they employ the same Pennes bioheat equation to capture heat transfer with perfusing blood.

While models of Li *et al.* [195] and Castelani *et al.* [199] do show very good predictive abilities when validated, this is not necessarily the case for all modern models mentioned above. Because heat transfer through perfusing blood and conduction from body core to surface tend to dominate conduction in other directions, three-dimensional models that recreate the human geometry more faithfully do not necessarily offer improved capabilities of predicting core temperature responses to ambient conditions. The more faithful geometric recreations, especially ones incorporating internal organs, do offer value when attempting to understand spatial temperature variation within body segments. However, when simply attempting to predict the body's response to ambient conditions without regard for detailed spatial temperature distributions, models employing the more traditional cylindrical formulation that have performed well in validation studies are often still employed.

A look at selected applications for which thermo-physiological models have been used highlights the value of estimating the human body's reaction to given environmental conditions without the need for costly or impractical experimentation. As mentioned, the Stolwijk model was developed at the request of NASA to investigate the impacts that the environment of outer space has on astronauts during the Apollo program, as such conditions would be very challenging and dangerous to recreate experimentally. Similarly, the Fiala *et al.* model was used by researchers to model body temperatures in open heart surgery patients [180]. Appropriate adaptations to the model were made, such as the incorporation of the effects of anaesthetic drugs on vasomotion.

Many other applications of note involve the extension of models to assess thermal comfort and perception, bridging the gap between predicting temperatures in the body, and understanding how this makes and individual "feel". These tools have since been applied to the development and design of clothing [181], car cabins [181], sports stadiums [182], and other applications, allowing the designs to be tailored to result in pleasant thermal sensation for end users.

Furthermore, the ability to predict thermal state and sensation of individuals in given ambient conditions has been valuable in the development of climatic thermal indices. Factors such as humidity and wind will undoubtably impact an individual's thermal state and perception but are not captured when ambient conditions are described using only a dry bulb temperature value. Thermal indices have been developed to establish universal descriptions of ambient conditions that account for such confounding factors. A common example would be describing weather using a "windchill" adjusted temperature. This, and other indices, are primarily based on human experimental trials, measuring heat loss and collecting feedback on thermal comfort and perception from participants, allowing equivalent sets of conditions to be observed. Incorporation of human thermal modeling provides a valuable tool that allows researchers to cover a much broader range of ambient inputs when assessing what conditions will result in similar thermal state and sensation in the body. The most prominent example of a climatic index developed with thermal modeling is the UTCI-Fiala climate index [183]. This index makes use of the Fiala *et al.* model to combine the array of climatic inputs, allowing ambient conditions to be described by an equivalent temperature that would elicit the same thermal strain under reference conditions.

2.4.3 Stolwijk Model Formulation

The model of Stolwijk [21] is used as the foundation for the model development described in Chapter 4, with adaptations and extension employed as needed to simulate the thermal behaviour of interest. The present description will provide an overview of the construction and function of the seminal Stolwijk model to contextualize the upcoming discussion of model extensions, adaptations, and resulting outputs. For further detail on the model formulation, a full description is provided in [21].

The passive controlled system represents the geometry of the body as 6 separate segments: The head, trunk, arms, hands, legs, and feet. The head is represented as a sphere, while all other body regions are represented as cylinders. Each body segment contains 4 control-volume nodes in the radial direction, with each nodal volume representing a different concentric tissue layer, namely, the core, muscle, fat, and skin of each body segment. The length of the body segments and knowledge of the relative proportion of tissue types within them allow the size of all layers to be estimated. An additional node is defined to represent the central pool of blood in the body, yielding a total of 25 nodes in the system.

Metabolic heat generation occurs throughout the body, with the majority of metabolic activity taking place in muscle layers, and in the core of the trunk and head. Heat is exchanged between the central blood pool and all individual nodal regions in the body in proportion to the rate at which blood perfuses the region. Heat conduction within tissue is assumed to occur only in the radial direction between neighbouring nodal layers. Employing a first order approximation of the radial temperature gradients driving heat conduction in each body segment allows a discretized representation of the governing heat balance presented in Equation 2.25 to be established for each internal nodal region:

$$C_N \frac{dT_N}{dt} = TC_{N\to N+1}(T_N - T_{N+1}) + TC_{N-1\to N}(T_{N-1} - T_N) + BC_N(T_B - T_N) + H_N$$

(2.27)

where T_N denotes the temperature of the local node, T_{N+1} denotes the temperature of the neighbouring node to the outside, T_{N-1} denotes the temperature of the neighbouring node to the inside, and T_B denotes the temperature of the central blood pool. C_N denotes the heat capacity of the local nodal volume; the value of this parameter depends on the masses and the specific heat capacitances of the constitutive tissue within each nodal region. $TC_{N\to N+1}$ denotes the conductance between the local node and node neighbouring it to the outside, while $TC_{N-1\to N}$ denotes the thermal conductance between the local node and the node neighbouring it on the inside. The values of these parameters depend on the thicknesses and lengths of the tissue layers and thermal conductances of their constitutive tissue. BC_N represents the conductance proportionality constant for heat exchange between local tissue and perfusing blood, and its value depends on the distribution of blood flow rates. H_N denotes the metabolic heat generation in the local nodal volume, and its value will be given by the sum of the basal metabolic generation, metabolic heat generation resulting from the performance of work, and metabolic generation from shivering.

Skin layers at the surface of each body segment additionally feature heat exchange with the surroundings through convection, radiation, and evaporation. These additional heat flows produce a thermal balance in the discretized skin surface nodal volumes of:

$$C_N \frac{dT_N}{dt} = TC_{N-1\to N}(T_{N-1} - T_N) + BC_N(T_B - T_N) + H_N - E_N - (HC_N + HR_N)S_N(T_N - T_A)$$

(2.28)

where T_A denotes the temperature of the ambient air, HC_N denotes the local linear convective heat transfer proportionality coefficient, and HR_N denotes the local linear radiative heat transfer proportionality coefficient. The surrounding effective radiating temperature is assumed to be equal to the surrounding air temperature, allowing the convective and radiative heat transfer coefficients to be combined into a single proportionality coefficient relating dry heat loss from the skin to the temperature difference between the skin and the surrounding air. E_N denotes the local evaporative losses, given by the sum of basal evaporative losses occurring continuously at low levels, and additional losses occurring due to the evaporation of secreted sweat. In this model, sweat is assumed to evaporate as it is secreted, meaning that evaporative heat loss is set directly by the sweat rate of the body. A maximal sweat evaporation rate is determined at the skin surface of each body segment, however, to represent the reality that sweat evaporation cannot exceed the rate of water vapour mass transfer into the air that ambient conditions can support. This maximal rate is given by:

$$E_{MAX_N} = 2.2 * \left(P_{skin_N} - P_{\infty}\right) * HC_N * S_N$$

(2.29)

where P_{skin_N} is the vapour pressure at the skin, assumed to be equal to the saturation pressure of water at the local skin temperature, P_{∞} is the vapour pressure of the air which will depend on the ambient humidity, HC_N is the convective heat transfer coefficient, and 2.2 is the Lewis coefficient, which relates convective heat transfer to the analogous process of evaporative mass transfer. If the evaporative heat loss resulting from the body's uninhibited sweat response would exceed this maximal value, evaporative losses are truncated, and set equal to the maximal value itself.

The temporal derivatives of the local temperature values in equations 2.29 and 2.30, $\frac{dT_N}{dt}$, are then discretized using a linear approximation scheme. When these discretized equations are applied at all nodes, a governing system of equations is obtained relating temperature values across two successive timesteps. As is evident from Equations 2.29 and 2.30, these governing equations depend on parameters such as local blood flow and sweat rates. These parameters are determined by the controlling system, based on the sensed thermal state of the body. When an initial temperature distribution in the body is provided, these temperatures are compared to set point values to obtain error signals that describe the thermal stress within the body. These error signals are used to determine the levels of the thermoregulatory responses (sweat rates, skin blood flow rates, and

shivering rates), which are then used to populate the nodal heat balances and complete the governing system of equations. The equations are solved to determine the nodal temperature distribution at the following timestep, which is then fed back into the controlling system to obtain updated thermoregulatory responses. The governing system of equations are then reformulated with the updated parameters, allowing the nodal temperature distribution to be obtained an additional timestep into the future. This process is repeated iteratively across all timesteps to obtain the progression of body temperatures over the course of a desired simulation period.

Chapter 3
Experimental Assessment of Localized Forearm Cooling[1]

3.1 Motivation and Objectives

Heat stress during exercise can significantly reduce athletic performance, and can pose threats to athlete health. The highest levels of exertional heat injury are observed in endurance sports, such as cycling [200]. Consensus recommendations when thermally stressful conditions are unavoidable during athletic competition include the implementation of heat acclimation programs, ensuring sufficient hydration as well as the use of acute cooling techniques to fight the elevation of body temperature during competition [201]. Results outlined in Table 2.6 and Table 2.7 highlight the potential for acute cooling strategies to assist thermoregulation when exercising in the heat. While pre-cooling presents a useful option, its impacts can be lost during sustained endurance competitions such as cycling races [109], suggesting that the inclusion of per-cooling strategies could be even more helpful to fight the rise of core temperature. Accordingly, the development of effective and practical per-cooling techniques that could be applied during cycling in hot conditions could be especially valuable.

Water sprays have demonstrated potential benefits [151], though their application during outdoor cycling can be challenging. The ingestion of cold fluid has also demonstrated positive effects [146], and is straightforward to implement since fluid ingestion during cycling is already practised, though the extent to which it can have an impact is limited by the realistic amounts of fluid an individual can ingest, and additional cooling techniques are desired. The use of wearable garments

[1]Content from this chapter is published in 'Continuous forearm cooling attenuates gastrointestinal temperature increase during cycling' [1] in *The Journal of Sports Sciences*, studying the impacts of forearm cooling on cycling performance. This publication was co-authored by Eric T. Hedge, Kathryn A. Zuj, Alex Stothart, Erica Gavel, Sean D. Peterson, Len S. Goodman, and Andrew J. M. Buckrell. Kathryn A. Zuj. Len S. Goodman, Andrew J.M. Buckrell, and Sean D. Peterson contributed to the study conception and design. Material preparation and data collection were performed by Eric T. Hedge, Kathryn A. Zuj, Alexander G. Stothart, and Erica H. Gavel. Data analysis were performed by Eric T. Hedge, Kathryn A. Zuj, and Alexander G. Stothart. The first draft of the manuscript was written by Eric T. Hedge, and all authors commented on versions of the manuscript. All authors read and approved the final manuscript. Alexander G. Stothart specifically was responsible for the construction and operation of the cooling system apparatus, and collection and analysis of data related to heat energy absorbed by the cooling system. Alex assisted in experimental trial operation, and authored the first draft of publication sections relating to the employed forearm cooling system. The entirety of this chapter has been written by Alexander G. Stothart.

such as cooling vests, jackets, and collars is a plausible additional strategy that has demonstrated positive effects during stationary cycling in the heat [149] [145] [202], and such garments could theoretically be worn during true outdoor cycling competition. However, these garments add noticeable weight that must be accelerated and transported by the rider. Furthermore, while torso and head/neck movement during cycling is not extensive, these garments can be cumbersome and bulky compared to the garments cyclists typically wear, and their form factor could contribute additional aerodynamic resistance. Accordingly, torso and head/neck cooling garments do introduce clear downsides during cycling competition, which shifts focus to potential cooling strategies applied to peripheral body parts, such as the arms. This motivated the conception of a cooling approach employing a specially designed ice-water container mounted to the centre of a cyclist's aerobars that cools the forearms.

It is common during road cycling for riders to rest their arms on aerobars, allowing them to maintain an aerodynamic posture while propelling and controlling the bicycle. Figure 3.1 shows an aerobar setup on a bicycle – riders rest their forearms on the support pads while gripping the extended bars, allowing them to lean forward while riding, and minimizing frontal area contributing to drag. Water bottles are often positioned between the arms to enable the rider to drink water without disengaging from their aerodynamic position.

Figure 3.1: Typical cycling aerobars mounted on bicycle.

It is proposed to employ a specially designed container that houses a frozen mass of ice mounted to the centre of the aerobars. The rider rests their forearms against the cold surface of the ice container, allowing heat to be extracted from the riders' arms, flowing into the container, and melting the ice. The melted ice then serves as cold water that can be consumed as needed. This arrangement allows cooling to be applied to the rider in a way that does not require them to alter their positioning or wear cumbersome garments. Riders maintain their standard position with the added benefit that their forearms now rest against a cold surface. Since riders already carry water bottles with them when riding, this cooling strategy can be employed without the need to transport any additional mass.

While such a technique is practical to apply, it is only of value to riders if it effectively reduces body core temperatures. Because the goal of acute cooling strategies is generally to mitigate the rise of core temperature, the majority of research on the subject studies techniques that target the head and torso. Research on cooling of peripheral regions is minimal and inconclusive. Ruddock *et al.* [153] investigated the impact of cold water submersion of the arms during stationary cycling in the heat, and found it effective at reducing intestinal temperature rise. Hsu *et al.* [139] employed a specially designed commercial cooling device that held a cold heat sink against the palms of the hands while creating a negative pressure micro-environment to induce vasodilation, and observed a reduction in tympanic temperature rise during exercise in the heat. Another investigation employing the same device by Amorim *et al.* [203] during exercise in the heat did not observe significant benefits. Furthermore, Scheadler *et al.* [141] et al observed a harmful impact on performance and core temperature induced by the use of a palm cooling garment. Not only do these studies display inconclusive outcomes, but none of the cooling techniques employed are practical during cycling, as they occupy the cyclists hands, interfering with the ability to brake and steer. No research has been found investigating the potential for forearm cooling to reduce core temperature. Accordingly, the present work aimed to experimentally assess the impact of cooling applied to the medial forearms during cycling in hot and humid conditions. Because the proposed aerobar mounted system requires an iterative design process to fully develop and produce, its effects were simulated in the present study using a specially constructed system employing available laboratory equipment. This study therefore aims to serve as a proof of concept for the potential of localized forearm cooling to provide effective thermal relief. Specifically, the experimental study aims to answer the following questions:

- Can the use of localized forearm cooling significantly impact body core temperatures during cycling exercise in hot and humid conditions?
- Can the applied localized forearm cooling provide relief to other markers of thermal stress such as cardiovascular drift, sweat rate, thermal comfort, or perceived exercise exertion level?
- Can the heat extracted from the body be quantified to understand its impact on the body's total thermal balance?

3.2 Methods

3.2.1 Study Design

The study aimed to assess the impact of forearm cooling on body core temperature via a randomized repeated measures cross-over design. Participants acted as their own control subjects, completing one exercise trial with acute cooling applied to the forearms (COOL), and one trial without applied cooling (CON). Gastrointestinal temperature (T_{GI}) was used as a measure of core temperature, and was obtained using an ingestible radio capsule (VitalSense Core Temperature Capsule, Equivital Inc., New York, NY, USA) in both experimental conditions. The order of the trials was determined randomly via coin toss for initial participants, with the order for remaining participants selected to ensure an equal number completed the trials in each order among both men and women. Due to the nature of the applied cooling and the associated sensation, it was not possible to administer the intervention blindly.

3.2.2 Participants

The study featured a sample size of N = 11 participants (7 male, 4 female). Anticipated impact and variation of gastrointestinal temperature measurements based on previous hand cooling studies by Hsu [139] and Ruddock [153] were used for a sample size calculation, indicating that 10 participants would be necessary observe a change of 0.4°C (β=0.8, α = 0.05). 12 participants completed the protocol, though the results of one participant were discarded due to the ingestion of cold water impacting the gastrointestinal temperature reading, reducing the final sample size to 11. All participants were trained cyclists, and were healthy adults with no known musculoskeletal,

cardiovascular, or metabolic conditions. Subjects were screened with an activity readiness questionnaire (CSEP Get Active Questionnaire) and a health status form to ensure participation in the study was safe and that no exclusion criteria were met. Exclusion criteria were selected to minimize risk of completing vigorous exercise, and to ensure safe passage of the ingestible temperature capsule. Prior to participation, all participants were made fully aware of all study protocols and procedures, and were informed of their approval by the University of Waterloo Human Research Ethics Committee (ORE #22754) and the Defence Research and Development Canada Human Research Ethics Committee (DRDC HREC Protocol 2018–043). They were informed of their right to withdraw without prejudice, and signed a letter of informed consent prior to participation. Full details of the sample of participants is described in Table 3.1.

Table 3.1: Study participant characteristics.

Variable	Males	Females
N	7	4
Age [yrs]	37 ± 12 (28-62)	41 ± 15 (29-62)
Height [m]	1.77 ± 0.07 (1.68-1.84)	1.67 ± 0.05 (1.60-1.72)
Weight [kg]	72 ± 9 (56-82)	59 ± 6 (53-66)
Body surface area [m^2]	1.88 ± 0.15 (1.63-2.04)	1.66 ± 0.09 (1.55-1.75)
Self-reported FTP [W]	264 ± 45 (197-313)	198 ± 16 (182-220)
Self-reported training time [hrs/wk]	9 ± 4 (3.75-14)	6 ± 4 (2-10.5)

3.2.3 Testing Protocol

The study featured two experimental conditions, one with cooling directly applied to the forearms (COOL) and one without (CON). Trials for both COOL and CON conditions were otherwise identical, featuring the same exercise protocol and pre-exercise preparations. Trials were separated by roughly one week, but both were conducted at the same time of day, and participants were asked to adhere to the same diet and feeding schedule the night before and day of testing. Participants were asked to wear the same cycling gear and clothing for both trials, and the same exercise equipment was employed. The exercise protocol was completed on the participants' own bicycles, connected to an electromagnetically braked bicycle trainer (STAC Zero Halcyon Smart Trainer, New Hamburg, ON, Canada), allowing workload to be controlled and measured throughout the trial. The trainer employed

an “ergometer mode”, in which it modulates resistance based on the measured speed of the rider to assist in maintaining a set, constant work rate. The work rate of the sustained exercise bout for both trials was a self-reported value corresponding to 66% of the functional threshold power level of the participants, and the same workload was used for both COOL and CON trials. Functional threshold power (FTP) is a measure used in cycling to denote the highest workload a rider can sustain for an hour of continuous cycling. Trials were held in an environmental chamber (Constant Temperature Control Ltd., Weston, ON, Canada) located at Defense Research and Development Canada facility in Toronto, ON.

Participants were provided with the ingestible telemetry capsule ahead of their scheduled session, and were asked to ingest the capsule approximately 4 hours before the start of the trial. Upon arrival at the experimental facility, participants were asked to void their bladders, and led to the changing area where their pre-exercise nude weight was measured while standing behind a privacy curtain. They changed into their exercise clothing, before being outfitted with appropriate measurement equipment. Following this, participants were led into the environmental chamber where all testing and measurement equipment could be set up and connected. Participants completed five minutes of seated rest in the chamber prior to beginning the exercise protocol.

The exercise protocol began with a five-minute warmup consisting of 60s of sustained cycling at 40% of FTP, 70s at 50%, 70s at 60%, 70s at 66%, and 30s at 75% FTP. Following the warmup, cycling was paused while the cooling system was attached to the participants’ arms. Cycling was then resumed, with the work rate ramping up continuously from 0 to the 66% FTP intensity over the course of 1 minute, at which point the target intensity was sustained for 45 minutes. The cooling system was still attached the participants arms even during the CON trial, but was not turned on, meaning it would quickly equilibrate to the temperature of the wearers body, at which point it would not be able to extract any heat. This was done to ensure that any unintended additional hindrances to exercise imposed by the wearing of the cooling system, such as discomfort to the wearer and insulation from the cooling sleeves, did not interfere with the observation of the purely thermal impact.

Exercise was terminated before the completion of the sustained 45-minute bout if any of the following termination criteria were met: gastrointestinal temperature reaching 39.3°C, a participant showing any indication that they were feeling unwell or faint, or a participant voluntarily terminating

exercise. Following the termination of exercise, the cooling system was removed, thermal images of the participant's forearms were obtained, and participants were stripped of instrumentation and measurement equipment and lead out of the environmental chamber. They were then guided back to the changing area where the post-exercise nude weight was measured, and they were allowed to change out of their exercise clothing.

3.2.4 Physiological Measurements Performed

Gastrointestinal Temperature

Throughout the trials, gastrointestinal temperature, T_{GI}, was recorded using ingestible telemetry temperature measurement capsules (VitalSense Core Temperature Capsule, Equivital Inc., New York, NY, USA). Participants ingested the capsule roughly four hours (3h 55mins ± 39 mins) before the beginning of the trial. Readings from the capsule were transmitted remotely to a sensor electronics module (Equivital EQ02 LifeMonitor, Equivital Inc., New York, NY, USA). The T_{GI} reading was recorded every five minutes beginning at the start of the constant work rate exercise bout. To account for possible different starting temperatures before the cooling system was applied, the change in T_{GI} from the initial value at the start of the constant work rate bout, and the rate of change in °C/hr were determined from the T_{GI} data.

Heart Rate

Heart rate was continuously monitored using both a chest worn body activity monitoring system (Equivital EQ02 LifeMonitor, Equivital Inc., New York, NY, USA), and a heart rate monitor (Polar Electro PE3000, Oulu, Finland). Readings were transmitted to same sensor electronics module as the gastrointestinal capsule readings (Equivital EQ02 LifeMonitor, Equivital Inc., New York, NY, USA). Heart rate drift was determined from the recorded data as the difference between the 30s mean heart rate value observed at the 10^{th} minute of exercise, and the last 30s of exercise.

Sweat Rates

Whole body sweat loss was obtained from the difference between pre and post exercise nude body weight measurements. Participants were not permitted to consume fluids or void their bladder between pre and post weight measurements, and it was therefore assumed that any change in body

mass resulted from sweat loss. Sweat rates were normalized based on body surface area estimated according to the method of Dubois and Dubois [204].

Additionally, a local sweat rate measurement was obtained over the right scapula of all participants twice per exercise trial, once early in the trial, and once late. The early measurement was obtained 15 minutes into the constant work rate cycling bout for all participants, with the late measurement being taken 35 minutes into the bout for all participants but one. For this one participant, the late measurement was made 25 minutes into the bout in both the COOL and CON trials due to high T_{GI} values observed as the bout progressed, indicating that the T_{GI} termination criteria would likely be met before the sweat rate measurement could be obtained 35 minutes into the bout. In all cases, the technical absorbent method modified from Morris *et al.* [205] was employed. A dry absorbent patch measuring 6cm x 6cm (Technical Absorbents Ltd., Grimsby, U.K.) was placed on a towel-dried skin patch over the participants' right shoulders, and secured in place for 5 minutes, allowing it to absorb secreted sweat. The mass of the patch was measured before and after application using an analytical balance (Model AE163, Mettler- Toledo GmbH, Greifensee, Switzerland) to determine the mass of water absorbed. The change in mass was divided by the patch area and duration of application to obtain a sweat rate in mg/min/cm^2.

Forearm Skin Thickness

Forearm skin thickness was assessed in all participants due to the potential for it to provide insulation to deeper tissue and impact the effectiveness of the applied cooling. Prior to instrumentation and exercise tasks, b-mode ultrasound video clips were obtained of the volar forearm cross section at the midpoint of the arm in a supinated position (Mindray M5, Shenzhen Mindray Bio-Medical Electronic, Shenzhen, China). Imaging was performed using a 10MHz probe. Skin thickness was then estimated visually from the ultrasound frames from the straight-line distance between the skin surface and the transition point between dermis and subcutaneous tissue (ImageJ, National Institutes of Health, Bethesda, MD, USA).

Forearm thermal images

To obtain an estimation and visual representation of forearm skin temperature before and after all trials, thermal images of the volar forearm were obtained using an infrared camera (Model FLIR S65, FLIR Systems, Inc., Täby, Sweden). Images were obtained before warmup, and immediately after

cessation of exercise and removal of the cooling system for each trial. Participants were guided to the infrared camera setup immediately after stepping off of the bicycle and instructed to extend their arms with the palmar surface directed towards the camera lens.

Rating of Perceived Exertion and Thermal Comfort

Participants were asked to provide ratings of perceived exertion (RPE) and thermal comfort five minutes after entering the environmental chamber, and the end of the exercise warm-up, at every 10th minute during the exercise bout, and following the cessation of exercise. Ratings of perceived exertion were assessed according to the Borg RPE Scale [206], and thermal comfort assessed according to the McGinnis Thermal Scale [207].

Cadence

Cadence was monitored throughout exercise using a pedal mounted cadence meter (Garmin International, Inc., Olathe, KS, USA), with data remotely collected and logged by TrainerRoad software (TrainerRoad, Reno, NV, USA). Averages of cadence readings were taken over the first and last 5 minutes of steady state exercise during each trial to determine cadence drift and enable comparisons across conditions.

3.2.5 Forearm Cooling System and Heat Extraction Measurement

A custom cooling apparatus was constructed with the aim of providing the desired cooling to a small localized area of the participants' forearms, and to quantify the heat extracted from the wearer's body by this cooling. The system applied the cooling by circulating chilled water through two identical block-shaped aluminum flow-through heat exchangers with dimensions of 4.1 cm x 16.2 cm x 1.2 cm (Focalvalue Technology Co. Ltd, Shenzhen, China), shown in Figure 3.2.

Figure 3.2: Heat exchanger block employed by the cooling system. Attached tubing can be seen on the left hand side of the image, which supplies the heat exchanger block with cool water, and carries off water that has absorbed heat from the wearer.

One heat exchanger block was positioned against the medial side of each forearm, with the largest surface of the heat exchanger pressed flat against the skin of the arm. The perfusing coolant water allowed the heat exchangers to maintain a roughly constant, cold temperature against the skin of the participants. The temperature gradient between the surface or the arm and the cold surface of the heat exchangers drives heat flow from the arms, into the heat exchangers, where it is absorbed and carried away by the perfusing coolant water. Custom 3-D printed holsters were created to fit over the back of the exchangers and hold them in place during exercise. Armacell Armaflex Rubber pipe insulation covered the outside of the holsters to prevent heat from flowing into the exchangers from the ambient air through the sides not in contact with the skin. The combination of parts was held to each arm with a spandex sleeve (Under Armour, Inc., Baltimore MD, USA). This heat exchanger assembly was worn by the participants in both the COOL and CON trials. During the CON trial the heat exchangers were not supplied with cooled water, allowing for no sustained heat extraction from the arms. An image of the applied heat exchanger assembly is shown in Figure 3.3.

Figure 3.3: Arrangement of the cooling system when affixed to participants arms.

A constant temperature bath system (Model A81 Recirculating Chiller, Thermo Haake, Newington, NH, USA) was used to maintain a reservoir of coolant water at roughly 5°C, and to pump the water from the reservoir through a network of insulated flexible vinyl tubing, through the heat exchangers, and back to the reservoir to be cooled again. A schematic of the assembly is depicted in Figure 3.4.

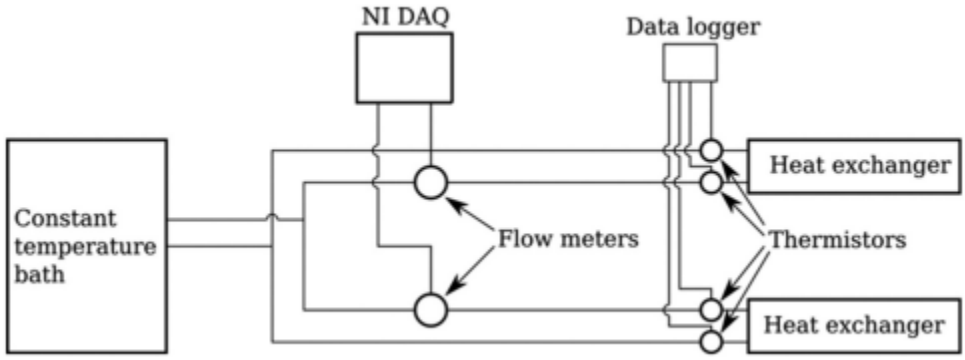

Figure 3.4: Schematic diagram of the flow network employed by the cooling system.

To quantify the heat extracted by the cooling system, the surfaces of the heat exchangers that were not in contact with the wearer's skin were well insulated to ensure that minimal heat was absorbed from the ambient air. Any warming of the perfusing coolant water was therefore attributed to heat absorbed from the body of the participant. Thermistors (Mallinckrodt Medical Inc., St. Louis, MO,

USA) were inserted in the vinyl tubing immediately upstream and downstream of each heat exchanger to measure the change in temperature of the water as it passed through the heat exchangers. Measurements were recorded and logged using a portable data logger (ACR SRP-001 TrendReader 3, Totronic Corp., Melrose, MA. USA). Flowmeters (FTB4605 Economical Long-life Pulse Output Water Meters OMEGA Engineering Canada, St-Eustache, QC, Canada) were connected to the flow network in series with each heat exchanger to measure rate at which water circulated, with data recorded using a National Instruments data acquisition module (card: NI-9205, National Instruments Corp., Austin, TX, USA; chassis: cDAQ-9174, National Instruments Corp., Austin, TX, USA) and LabVIEW software (LabVIEW, National Instruments Corp., Austin, TX, USA). The increase in water temperature as is passed from inlet to outlet was then be used to calculate the heat flow into the exchanger

$$\dot{Q}_{cool} = \dot{m} c_{p_w} (T_{out} - T_{in})$$

(3.1)

where $\dot{Q}_{cool}$ is the rate of heat flow, $\dot{m}$ is the mass flow rate of the cooling water, c_{p_w} is the specific heat capacity of the water, and T_{out} and T_{in} are the water temperatures at the outlet and inlet of the heat exchanger respectively. The heat extraction rates from the left arm and right arm were summed to obtain the total heat extraction rate. The extraction rate was integrated over the duration of the bout to give the total heat energy removed

$$Q_{cool} = \int_{t_{start}}^{t_{end}} \dot{Q}_{cool} dt$$

(3.2)

where t_{start} and t_{end} correspond to the starting and ending times of the exercise bout.

3.2.6 Statistical Analysis

Differences between CON and COOL conditions in T_{GI}, rate of rise in T_{GI}, heart rate drift, end-exercise heart rate, whole body sweat loss rate, whole-body sweat rate index, and ambient conditions were assessed using paired sample t-tests. Changes in thermal comfort and rating of perceived

exertion scores across conditions at the start and end of exercise were assessed using Wilcoxon signed-rank tests. Two-way repeated measures analysis of variance (ANOVA) was used to assess changes in T_{GI}, local sweat rate, and cadence, with main effects of condition and time. In the case of local sweat rate and cadence, two time points were used: first 5 minutes, and last five minutes for cadence, and minutes 15-20, and 35-40 for sweat rate. If Mauchly's test of sphericity was significant, the Greenhouse-Geisser correction was used. When significant main effects or interactions were observed, paired sample t-tests with Holm-Bonferroni corrections were conducted *post hoc*.

Statistical significance was set *a priori* at $p \leq 0.05$, with a trend towards significance at $0.05 < p \leq 0.1$. Results are presented as mean ± SD with paired p value and 95% confidence interval. Statistical analyses were conducted using SPSS version 25.0 (SPSS Inc., Chicago, IL., USA) and Microsoft Excel (Microsoft Corporation, Redmond, WA, USA).

3.3 Results

Six of the eleven participants completed the CON trial first, with the remaining five completing the COOL trial first. Environmental chamber temperature (CON: 29.95 ± 0.18, COOL: 29.99 ±0.24°C, $p = 0.453$) and relative humidity (CON: 72.03 ± 1.71, COOL: 72.21 ± 1.09%, $p = 0.599$) did not differ significantly across experimental conditions. While all participants were able to complete the entire 45-minute exercise bout during the COOL trial, the termination criterion of $T_{GI} \geq 39.3$°C was reached for five participants prior to completion of the CON trial exercise bout. Participants completed and average of 41.6 ± 5 minutes of the scheduled 45 minute bout during the CON trials. All participants were able to complete at least 30 minutes of all exercise bouts.

3.3.1 T_{GI} Rise

T_{GI} values were collected and compared over the first 30 minutes of exercise, as this was the latest time point attained by all participants under both experimental conditions. Recorded values are plotted in Figure 3.5.

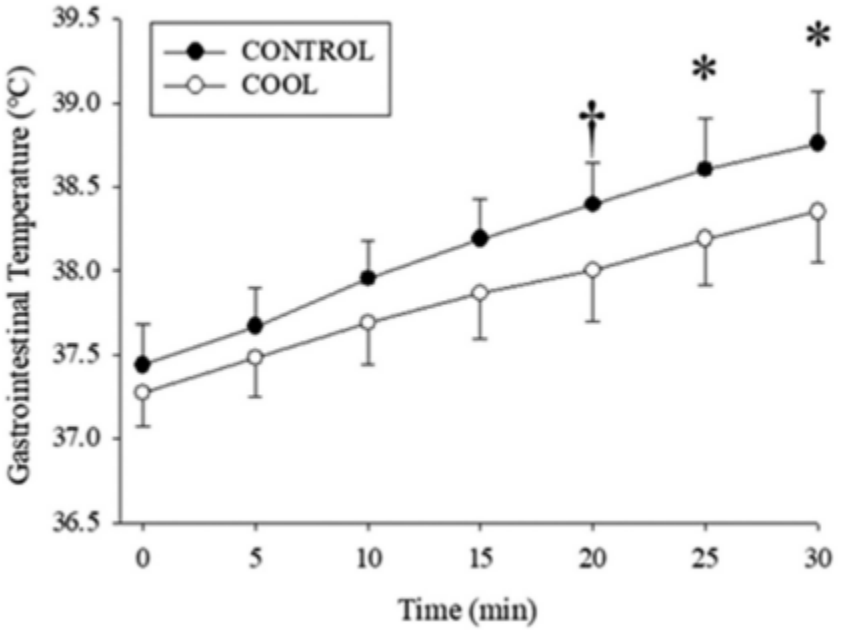

Figure 3.5: Average gastrointestinal temperature measured at 5-minute increments throughout exercise. * Denotes a significant difference ($p \leq 0.05$) between CON and COOL averages at a given time point. † Denotes a trend towards a significant difference ($0.05 \leq p \leq 0.1$) between CON and COOL averages at a given time point.

The rate of rise of gastrointestinal temperature ($\Delta\dot{T}_{GI}$) in °C/hr was compared between conditions, with a significantly lower rate observed in the COOL trial (CON: 2.46 ± 0.70, COOL: 2.03 ±0.63 °C/hr, p = 0.002, CI = 0.20-0.66°C/hr). Paired data for both experimental conditions are displayed in Figure 3.6.

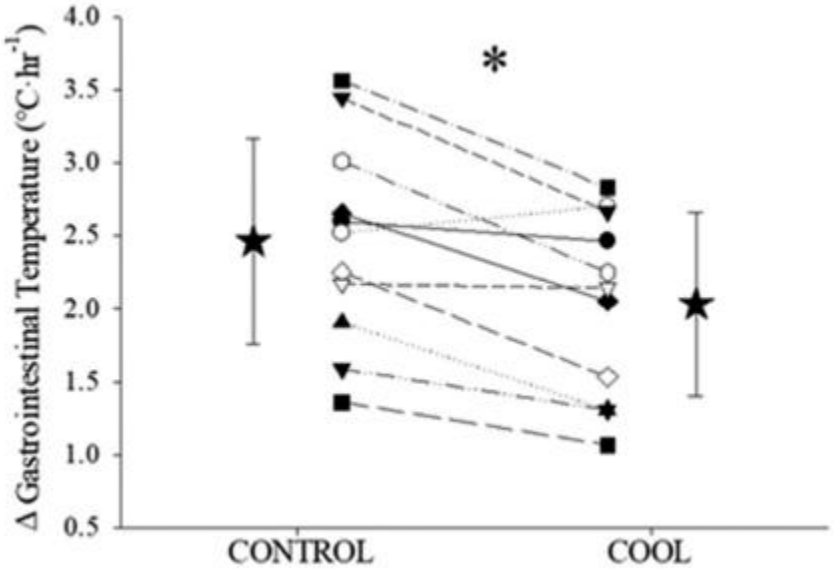

Figure 3.6: The rate of rise of gastrointestinal temperature observed for each participant during CON and COOL exercise bouts.

A significant interaction between experimental condition and time was observed for T_{GI} ($F(1.814,18.136) = 8.761$, $p = 0.003$, partial $\eta 2 = 0.467$; Figure 10). No differences were observed between conditions at the start of exercise, a trend towards a significant difference was observed after 20 minutes ($p = 0.063$), and statistically significant differences observed after 25 minutes ($p = 0.025$) and 30 minutes (0.009), with T_{GI} being lower in the COOL conditions.

3.3.2 Heart Rate and Cardiovascular Drift

Cardiovascular data for one participant was omitted due to sensor failure. Cardiovascular drift in beats/min was reduced significantly in the COOL conditions (CON: 20.46 ± 7.20, COOL: 17.15 ± 5.54 beats/min, $p = 0.05$, CI = 0-7 beats/min). The reduction in heart rate at the end of exercise trended towards significance (CON: 164 ± 13, COOL: 158 ± 18 beats/min, $p = 0.10$, CI = -1-12 beats/min). Paired data displaying heart rate drift is plotted in Figure 3.7.

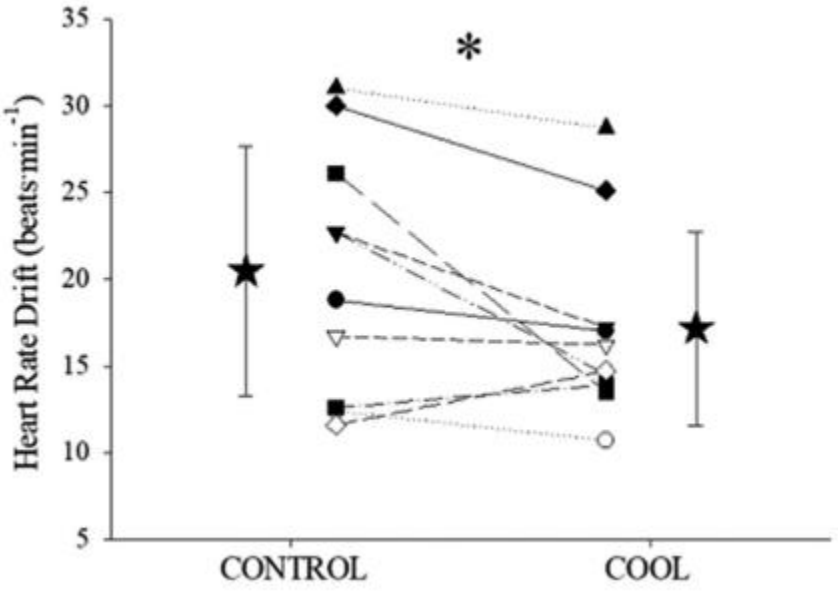

Figure 3.7: Cardiovascular drift observed for each participant during CON and COOL exercise bouts.

3.3.3 Sweat Rates

The difference in rate of body mass reduction from sweat loss trended towards significance (CON: 1.60 ± 0.53, COOL: 1.52 ± 0.50 kg/hr, p = 0.078, CI = -0.01-0.17 kg/hr). The whole body sweat loss index, which adjusts the rate of mass reduction for estimated skin surface area, also trended towards significance (CON: 0.88 ± 0.26, COOL: 0.84 ± 0.24 kg/m^2/hr, p = 0.065, CI = 0.00-0.09 kg/m^2/hr). Pre-exercise body mass did not differ significantly between conditions (CON: 67.4 ± 10.2, COOL: 67.7 ± 10.2 kg, p = 0.182). While a significant main effect of time was found on local sweat rate ($F(1,10)=7.782$, p = 0.019, partial $\eta 2 = 0.438$), a significant impact was not observed from the application of cooling ($F(1,10)=3.234$, p = 0.102).

3.3.4 Thermal Comfort and Rating of Perceived Exertion

Rating of perceived exertion did not differ at the start of exercise (CON: 7 ± 1, COOL, 7 ± 1, p = 1.000), though a reduction in RPE during the COOL trial that approached statistical significance was observed at the end of exercise (CON: 15 ± 2, COOL: 14 ± 2; p = 0.055). Thermal comfort was similarly identical at the start of each exercise trial (CON: 6 ± 0, COOL: 6 ± 0; p = 1.000) though

thermal comfort was significantly lower at the cessation of exercise in the COOL condition (CON: 10 ± 1, COOL: 9 ± 1; $p = 0.002$).

3.3.5 Cadence

Cadence data for one participant was omitted due to sensor failure. Main effects of both experimental condition ($F(1,9)=5.457$, $p = 0.044$; partial $\eta 2 = 0.377$) and exercise time ($F(1,9)=10.162$, $p = 0.011$, partial $\eta 2 = 0.530$) were observed, demonstrating that participants cycled at a slower cadence in the COOL trials, while also increasing their cadence as time elapsed during exercise bouts under both experimental conditions. Note that work rate was fixed in all cases, meaning a higher self-selected cadence would be compensated by less resistance faced while cycling.

3.3.5 Heat Extracted

Data collected for two participants was omitted from the analysis due to sensor failure, leaving nine remaining participants in the analysis. The cooling apparatus absorbed heat at an average rate of 30.3 ± 6.6 W across all participants. All participants were able to complete the entire 45-minute constant work rate exercise bout during COOL trials, resulting in an average of 81.7 ± 17.8 kJ absorbed over the course of the entire bout. No significant correlation was observed between heat extraction and forearm skin thickness ($r = 0.123$, $p = 0.771$). The average heat energy extracted over time throughout the exercise bout is displayed in Figure 3.8.

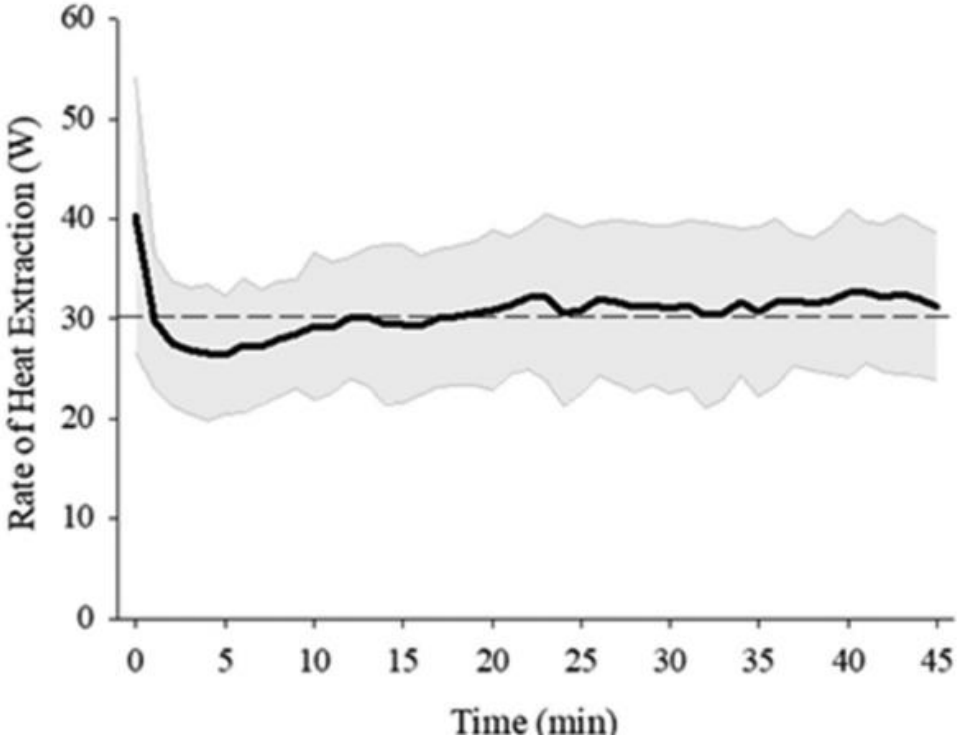

Figure 3.8: Average ± standard deviation of heat extraction rate for all participants throughout the 45-minute exercise bout. The dashed plotted line marks the average rate of extraction over the course of the bout of 30.3W.

3.4 Discussion

The goal of the study was to act as a proof of concept for the application of cooling to the inner forearms during sustained cycling exercise. It aimed to assess whether such a cooling modality could help mitigate the rise in core temperature during cycling in hot and humid conditions. Evidence indicating that such a cooling modality is effective would suggest that an aerobar mounted ice-water container cooling system represents a promising method for providing thermoregulatory assistance during actual cycling in thermally challenging environments.

The study did in fact observe evidence of the benefits of continuous cooling applied to the inner forearms during sustained cycling exercise. The rate of gastrointestinal temperature rise was significantly lower with the application of the cooling intervention, as was the observed heart rate drift. Self-reported thermal comfort was also improved, and a reduction of self-selected cadence was

observed. Trends towards statistical significance were observed for both a reduction in whole body sweat rate index, and self-reported rating of perceived exertion. Further discussion of these observations is presented in the following sections.

3.4.1 Rate of Gastrointestinal Temperature Rise, Heart Rate, and Heat Extraction

The strongest indication of the impact of the applied cooling is seen in the reduction of rate of gastrointestinal temperature rise. T_{GI} rose at a rate of 2.46 ± 0.70 °C/hr during the CON trial, but at only 2.03 ± 0.63 °C/hr during the COOL trial, displaying a paired reduction of 0.43 ± 0.34 °C/hr. Existing research on the effectiveness of peripheral cooling applied to the extremities of the arms is limited and inconclusive. The current results contrast findings of Sheadler *et al.* [141] and Amorim *et al.* [203], which did not observe any benefits of cooling applied to the hands, but are supported by results of Hsu *et al.* [139] and Ruddock *et al.* [153]. Hsu *et al.* provided hand cooling using a commercial device that employs a small negative pressure chamber to promote vasodilation while the palm rests against a metallic heat exchanger perfused with 22°C water. This cooling modality decreased tympanic temperature rise by 0.6°C over an hour of cycling exercise in a 32°C and 24% relative humidity environment. Ruddock *et al.* recorded intestinal temperatures during recumbent cycling exercise in 35°C and 50% relative humidity environment. In one trial, cooling was provided by submerging hands in 8°C water, and observed results were compared to a control trial where hands were immersed 34°C water. They observed a reduction in the rise of intestinal temperature of 1.00 ± 0.38°C over the course of one hour. Such methods are similar to those employed in the present investigation, applying cooling to peripheral upper body locations, and in fact resulted in greater reductions in core temperature rise than the current approach. However, both those methods are impractical to apply during cycling and many other forms of exercise. Not only is it impractical to transport a suction machine to maintain a negative pressure chamber, or cold water baths for immersion, but both methods require application directly to the hands. The ability to use the hands for steering, braking, or gear shifting is essential during cycling, and cooling modalities that occupy the hands are therefore not feasible during true cycling exercise that does not take place on a stationary ergometer.

In the present investigation, the total heat energy extracted over the entire duration of the bout was 81.7 ± 17.8 kJ. This heat energy would need to be stored in an external substance to in order for the cooling to be effectively implemented in true mobile applications. Employing the proposed

aerobar-mounted ice bottle technique will allow the heat to be stored by the melting ice. With a latent heat of fusion of water of 334J/g, less than 250g of frozen water would be sufficient to store the observed quantity of extracted heat, which is a very reasonable quantity to be transported in a cyclists mounted water bottle. Careful design of the bottle will still be required, however, to ensure the cooling is effectively applied to the arms as ice continually melts over time, while allowing the melted water to be consumed by the cyclist as needed.

Over the course of the experimental trials, the heat was extracted at an average rate of 30.3 ± 6.6W. With an average mass of all study participants of 67.3 kg, and an assumed average specific heat capacity of 3.47 kJ/kg/°C for human tissue [159], the average study participant can be assume to have an average total body heat capacity of 233 kJ/°C. If the body is simplified to a lumped thermal mass with this heat capacity, the rate of heat energy extracted would yield an expected reduction in the rise of body temperature of 0.47°C/hr. It can be seen that this agrees well with the true observed reduction in gastrointestinal temperature, but overestimates it slightly, which could be attributed to several factors. First, temperature will in fact vary within the body, and the representation of a lumped thermal mass is inaccurate. The extracted heat will not come from all parts of the body equally, and it is likely that it will disproportionately cool the tissue near the site at which cooling is applied. This can be seen in thermal images of the forearm skin following the exercise bouts shown in Figure 3.9, showing that the forearm tissue temperature is reduced far more than surrounding tissue.

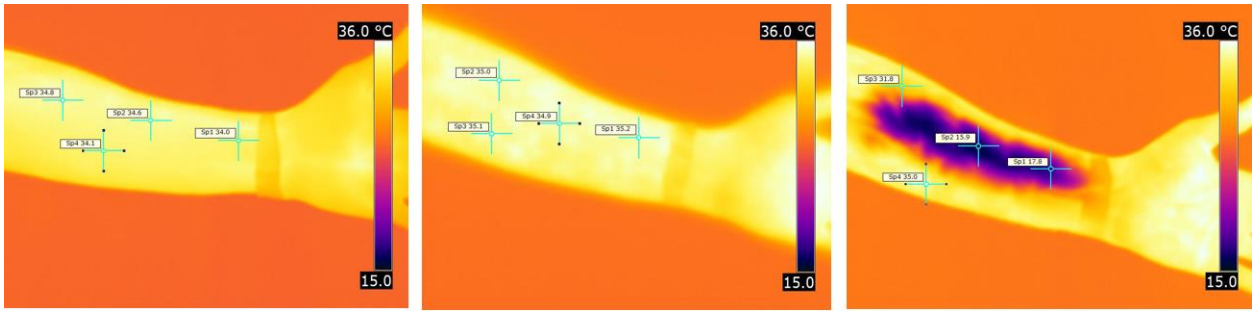

Figure 3.9: A representative thermal image of a participants left forearm before cycling (left), after cycling in the CON condition (centre), and after cycling in the COOL condition (right). The skin patch that was directly contacted by the applied cooling surface has dropped to a noticeably lower temperature over the course of the bout, with temperatures remaining relatively unchanged on the rest of the arm where cooling was not applied.

Furthermore, the reduction in body temperature resulting from the application of the cooling may lead to a reduced sensation of thermal stress by the body, and associated reduction in the drive of thermoregulatory mechanisms aiming to reduce body temperatures. This could result in less sweating and cutaneous vasodilation, resulting in less heat loss through traditional mechanisms during cooling trials, contributing to the overestimation of the reduction in body temperature rise.

A reduction in heart rate drift was observed in COOL conditions, which was used as an indicator of cardiovascular drift. Cardiovascular drift is a progressive decrease in stroke volume and compensatory increase in heart rate beginning roughly 10 minutes into sustained exercise. Heat stress during exercise exacerbates cardiac drift [4] by eliciting vasodilation in the cutaneous venous bed, resulting in diminished cardiac reserve and stroke volume (see Section XX for additional background information). Furthermore, fluid loss through sweating can reduce overall blood volume, exacerbating the reduction in cardiac reserve and ensuing cardiac drift. A trend towards reduced whole body sweat index under COOL conditions suggests that sweat loss differences may be contributing to the differences in observed heart rate drift, though changes in skin blood flow are likely to contribute as well. The increased cardiac drift observed during CON trials additionally resulted in an end-exercise heart rate increase that trended towards significance. The above observations are consistent with many other studies demonstrating the ability of various continuous cooling modalities to reduce heart rate and cardiovascular drift during exercise, including the work of Ruddock *et al.* [153], Hasegawa *et al.* [202], Ng *et al.* [208], and Wingo & Cureton [209]. Interestingly, attenuation of heart rate drift was prominent among male participants (CON: 23 ± 6 vs. COOL: 19 ± 6 bpm) in the current study, but a reduction was not observed among only the female participants (CON: 14 ± 3 vs. COOL: 14 ± 3 bpm), suggesting a possible sex-based difference in the body's response to the applied cooling modality. This study, however, was not sufficiently powered to analyze sex-based differences, as this was not the original intention, and may warrant further investigation in future work.

3.4.2 RPE, Thermal Comfort, and Cadence

Additionally, an improvement of end-exercise thermal comfort was observed, as well as a trend towards a significant reduction in end-exercise rating of perceived exertion. The improved thermal comfort likely results from the reduced core temperature observed at the end of the COOL trial exercise bout, though the local perception of the cooling surface and associated impact on skin temperature, as observed in the thermal images, may have additionally led to a psychophysiological

response [210]. Rating of perceived exertion is strongly associated with heart rate [211], and attenuation of heart rate drift may have contributed to the trend towards reduced end-exercise RPE. Furthermore, a significant reduction in self-selected cadence was observed in COOL trials. While end-exercise cadence remained lower in COOL trials, cadence drifted upwards over the course of the exercise bout in both experimental conditions, which generally agrees with expectation, as higher cadences require less force application to maintain a given work rate when cycling in ergometer mode, and reduce the impact of neuromuscular fatigue [212]. Pandolf and Noble [213], in fact, observed a negative relationship between pedal rate and RPE, supporting the notion that cadence would rise as exercise continues and fatigue accumulates. Despite this observation on the perceptual impact of cadence, lower cadences have in fact been observed to reduce the metabolic cost of maintaining a given power output [212] [214]. Accordingly, optimal cadence is not clearly understood, and it can be difficult to determine a causal relationship between cadence and perception of exercise difficulty, though it is possible that the positive impact of cooling on subjective sensation and perception allowed a lower, and potentially more efficient, cadence to be maintained by participants.

3.4.3 Potential Impacts on Performance and Health

Exercise in the heat exposes athletes to the risk of heat related injury [46]. The mitigation of various markers of heat stress observed in the current study suggest the proposed cooling modality may be capable of limiting some of these risks. The reduction of the rise in gastrointestinal temperature could contribute directly to delaying the onset of heat related illness. While several conditions can occur for moderate core temperatures, heat stroke generally tends to occur at core temperatures greater than 40°C, and represents the most dangerous risk of exercise in the heat. In a hypothetical exercise session where core temperatures, represented by T_{GI}, begin at 37°C and the rates of temperature rise observed in the present study are assumed to be sustained throughout exercise, a core temperature of 40°C would be attained over 15 minutes later with the application of forearm cooling. While it is unlikely in reality that temperature would continue to rise at a constant rate as it approaches dangerous levels, this illustrates the potential for the present cooling modality to fight the onset of heat related illness resulting from elevated core temperatures.

Furthermore, the observation of reduced heart rate drift suggests that the application of forearm cooling may assist in combatting other forms of heat related illness. During exercise in the

heat, the combination of enhanced skin blood flow and diminishing blood volume caused by dehydration lead to lower cardiac reserve volumes, and resulting impairment of cardiac filling [4]. This reduces stroke volume, requiring a compensatory rise of heart rate. The gradual onset of these phenomena over the course of an exercise bout results in heart rate drift. The reduction in heart rate drift observed in the present study suggests that the application of forearm cooling may have assisted in reducing one of, or both, of these mechanisms inducing heart rate drift. While a trend towards a reduction in whole body sweat rate index during COOL trials was observed, no direct measurements of hydration status or skin blood flow were performed in the current study. This makes it difficult to determine exactly what mechanisms contributing to heart rate drift were impacted by the application of forearm cooling, though it is likely that both dehydration due to sweating and skin blood flow were reduced to some extent. Reducing sweating and improving hydration status would mitigate the risk heat related illness such as heat cramps and heat rash, while limiting cutaneous vasodilation would mitigate the risk for heat edema and heat syncope.

While the present study did not include the direct measurement of a performance metric, and maintained a fixed work rate ensuring exercise performance was identical between trials, the effects of the applied cooling may be able to contribute to the mitigation of performance reductions owing to heat stress during exercise in competitive settings. As discussed previously, performance reductions generally result from the inhibition of central drive resulting from the body's sensation of thermal stress, the challenge of supplying blood to both working muscles and skin simultaneously, and the impacts of thermal perception on comfort, motivation, pacing etc. The inhibition of central drive due to heat stress is strongly related to core temperature, meaning the reduction of the rise of gastrointestinal temperature observed could mitigate such impacts on performance. Additionally, the observed heart rate drift suggests that the impacts of skin blood flow demand on general circulation are in fact being felt, meaning the ability of the applied cooling to limit heart rate drift could mitigate associated performance hindrances. Finally, thermal comfort was significantly improved with application of cooling, and as discussed, thermal perception alone can impact exercise performance [103], and the trend towards a reduction in rating of perceived exertion observed may allow for additional voluntary effort. While the impacts observed in the present study suggest that the proposed forearm cooling modality could have beneficial effects on performance, ultimately, a direct measurement of a performance metric would be necessary to determine the true impact. This presents a potentially valuable extension of the present work for future investigations.

3.5 Limitations and Concluding Remarks

Ultimately, the cooling intervention employed was observed to reduce the rise of core temperature during the 45-minute fixed-intensity exercise bout, under the described ambient conditions. It additionally led to a reduction in heart rate drift, and improved thermal comfort ratings, with trends towards significant improvements of whole-body sweat rate index and rating of perceived exertion. The combination of the above observations highlights the potential of the cooling technique, and suggests that further development and prototyping of the described aerobar-mounted cooling system may be warranted. It should be noted however, that the employed experimental approach featured several limitations that should be considered when interpreting the study observations.

The present work did not investigate the impact of the applied cooling on exercise performance, and comments on its potential impact are purely speculative. To draw definitive conclusions, on the performance change owing to cooling, a similar experiment would need to be conducted with a performance metric included. Additionally, while the study aimed to simulate road cycling exercise, it was conducted on a stationary cycle ergometer in an environmental chamber to facilitate data collection and provide controllable and repeatable ambient conditions. It neglected several relevant considerations, including the relative motion of the body through the air while performing true, mobile cycling will noticeably assist convective and evaporative cooling. Neglecting this consideration may have artificially increased participants' reliance on the applied cooling, and exaggerated its impact. Conversely, however, the indoor environmental chamber would have would have sheltered participants from incident sunlight, which would have had the opposite effect, as direct solar irradiation can be a significant source of heat gain in the body. Furthermore, the work rates maintained by participants throughout the sustained 45-minute experimental bouts were equal to roughly 2/3 of their respective FTP levels, which would be well below the levels typically maintained in an actual 45-minute cycling bout. While the exact core temperature response of participants could not be known ahead of time, it was suspected that exercising at higher intensities may have necessitated the premature cessation of exercise due to the core temperature termination threshold being attained. A relatively lower cycling intensity was therefore employed to increase the likelihood that riders could complete the planned exercise bouts. While hot conditions would probably result in some work rate reduction in true cycling competition or training, most riders would attempt to tolerate the high body temperatures and discomfort to maintain as high of a work rate as possible. Accordingly, they would attempt to ride at intensities approaching their own FTP. This would

contribute much more metabolic heat generation than was experienced at the experimental work rates, and lead to additional thermal stress that could alter the impact of the applied cooling on body temperatures. Further investigation of the impact of forearm cooling while accounting for realistic mobile cycling considerations is therefore warranted to provide additional valuable insights.

Chapter 4
Computational Modelling of Thermal Behaviour

4.1 Introduction

The experimental investigation of the impact of localized forearm cooling applied during cycling in hot and humid conditions demonstrates the potential impact of this cooling methodology. However, the discussed limitations to the experimental approach prevented it from being able to answer several questions of interest relating to the impact of cooling in a more realistic outdoor cycling setting. Specifically, these questions are:

- What impact would localized forearm cooling have on core temperature rise in true outdoor cycling, which features relative motion of air over skin, short wave radiative heat gain from sunlight, and higher work rates?
- How would this impact vary across a range of ambient outdoor conditions?

While experimental observation is often considered the gold standard when assessing human thermal behaviour, experimentation is expensive and time consuming, particularly when aiming to conduct parametric studies, such as varying ambient conditions, work rates, and testing durations. Alternatively, computational thermo-physiological modelling, once validated/calibrated against experimental data, can be used to predict trends over a range of conditions. While such models will necessarily feature simplifying assumptions based on empirical population data that will prevent them from providing exact results for a given individual, the ability to customize their configurations and inputs make these models suitable tools for parametric studies and preliminary conceptual design testing and development. Modelling additionally allows the thermal behaviour of the body to be simulated very quickly, enabling repeated simulations to be easily performed across a broad range of ambient conditions.

A thermo-physiological model based upon the work of Stolwijk [21] has been developed to address the identified questions of interest. While it is one the older models, with some newer examples including additional details and features, the model of Stolwijk was used as the base of the present work for several reasons. First, it's geometric representation of various body segments is comprehensive enough to allow cooling to be applied to peripheral body parts, which is a requirement

of the performed modelling. Furthermore, the model is still well regarded and used in modern applications, and in contrast to many newer models, it is well-documented in literature, allowing it to be recreated with confidence to provide an established and accepted foundation on top of which desired adjustments and extensions can be introduced.

The present work extended and adapted this original model of Stolwijk to capture additional aspects relevant to the current application. Comparison of model outputs with the experimental observations described in Chapter 3 was performed to validate and configure the model to accurately simulate the thermal behaviour resulting from the performance of cycling exercise in the heat, both with and without applied cooling. Once constructed and validated, the model was applied to various test cases to address the identified modelling goals. The base test case featured identical air temperature and relative humidity to the previously described experimental trials, but additionally included effects present in outdoor cycling, namely convective cooling and solar load, thus providing insight on the impact the applied cooling described in Chapter 3 may have in real applications. Additional repeated test case simulations were conducted, always featuring the same exercise protocol, but over a range air temperatures, solar irradiation levels, and relative humidity values, allowing the impact of ambient conditions on the simulated outcomes to be discussed.

4.2 Model Development

4.2.1 Construction

As discussed in Section 2.4.3, the original work of Stolwijk provides a nodal representation of the geometry of an average individual's body, with values provided for relevant thermal properties, and an initial thermoneutral internal temperature distribution. Additionally, it provides a comprehensive system of equations governing heat transfer between internal body nodes, heat exchange between surface nodes and surroundings, and human thermoregulatory responses to afferent temperature sensation. While this model serves as a foundation for the present work, it is not equipped to capture a variety of considerations relevant to the present application, and various adaptations and extensions were employed accordingly.

The original model is formulated to accept inputs describing the metabolic heat generation levels owing to exercise, surrounding air temperature, relative air speed, and relative humidity; however, only a single, constant numerical value is accepted for each of these inputs. Because the

thermal activity in the body during pre-exercise preparation and warmup will influence the thermal state of the body during the subsequent sustained bout, these periods were included in the performed simulations. Metabolic activity and ambient conditions do not remain constant during these periods, however, and the model therefore needed to be re-formulated to accept a vector describing the appropriate inputs at each time step of the simulation.

Additionally, the Stolwijk model does not account for the impact of clothing on heat flow and evaporation from the skin. To include these effects in the present model, the approach described by Roelofson & Vink [184] was employed, which introduces an additional series resistance to both heat loss and sweat evaporation from the skin. Rather than estimating evaporative resistances from the thermal insulation values of clothing garments as Roelofson & Vink did, however, values of both thermal and evaporative resistance of typical triathlon cycling garments obtained through direct measurement by Troynikov & Ashayeri [215] were used. For body regions that were only partially clothed, weighted average values were used based on skin areas reported by Yu *et al.* [216]. Reported values of the relevant properties of cycling shoes could not be found, so these properties were estimated based on the thermal and evaporative resistance of running shoes and sneakers reported by Yick *et al.* [217] and Nomoto *et al.* [218]. Final values used for all new and adjusted model parameters are tabulated in Table 4.1.

Additionally, heat gain through solar radiation was incorporated, as this contributes significantly to thermal stress when exercising outdoors in sunny conditions. Various approaches to quantifying heat gain from solar irradiation exist, and the approach employed was taken from the thermal model of Fiala *et al.* [28]. It computes an "operative temperature", T_{op}, for each body region according to Equation 4.1, that is then used in place of the ambient air temperature when calculating dry heat exchange between body surface and surroundings.

$$T_{op} = \frac{T_A\, h_{conv} + T_{mrt}\, h_{rad} + \alpha_{SW}\, F_s\, I}{h_{conv} + h_{rad}} \qquad \textbf{(4.1)}$$

where T_A is the surrounding air temperature, T_{mrt} is the mean radiating temperature of the enclosing long-wave radiating surfaces, h_{conv} is the convective heat transfer coefficient, h_{rad} is the long wave radiative heat transfer coefficient, α_{sw} is the short wave radiation absorptivity at the body surface, F_s is the solar area factor of the surface of interest, and I is the incident solar irradiation. Note that if I is

assigned a value of 0, indicating that there is no incident sunlight, Equation 4.1 reduces to the same radiative and convective heat exchange as the original formulation of the Stolwijk model.

The model was also adapted to capture the effects of the cooling surface applied to the skin of the forearms. Because the Stolwijk model featured only a single body region representing the arms, this region was split into two portions: one representing the cooled arm segment, and one representing the uncooled arm segment. Properties for these two segments were assigned by proportionately dividing the original single arm segment's properties according to the ratio of cooled and un-cooled arm surface area. The uncooled arm segment was then allowed to exchange heat with the surrounding environment like all other body segments, while the effects of the cooling surface were added to the cooled arm segment. It should be noted that this representation of the uncooled arm segment neglects the small amount of insulation offered by thin spandex material used to fasten the cooling surfaces to the forearms. The applied cooling was simulated as a surface at 6°C held against the skin of the cooled arm, with the thermal contact resistance between the surfaces estimated based on the experimentally measured heat flow into the cooling water, the known cooling surface temperature, and the arm surface temperature deduced from thermal images of the experimental participants' forearms.

The proportional division of the arm evidently makes for a simplified representation of the cooled arm segment, as it assumes that this segment will have the same radius, properties, and tissue layer breakdown as the rest of the arm, which is not the case in reality. The added insulation provided to deeper arm regions by the assumed thicknesses of the tissue layers limited the ability of the simulated cooling to extract heat when the cooled arm is represented this way. The goals of the present modelling revolve around extending the experimental observations to allow whole-body outcomes resulting from the experimentally applied cooling to be predicted in novel test cases. It was therefore important for the model to feature an accurate recreation the cooling-induced heat extraction observed in experiment, which required the properties of the cooled arm segment to be altered from those crudely assumed based on whole-arm properties. Detailed modelling of forearm tissue geometry and circulation is likely necessary to truly capture the full local behaviour, but falls beyond the scope of the current work. Accordingly, the present alterations were limited to increasing the thermal conductance values between deeper nodes and more superficial nodes in the cooled arm segment to reproduce the experimentally observed heat extraction resulting from the minimal insulation offered by the thin tissue layers. This involved first changing the conductance from the fat layer through the

skin layer based on the average skin thickness obtained from ultrasound measurements performed on the experimental participants. Very little else was known, however, regarding tissue layer properties in the forearms of the experimental participants, so in the present modelling, thermal conductance from the muscle layer into the fat layer was simply adjusted ad hoc to the level required to allow the model to produce the same average heat extraction rate as was observed in experiment under the same simulated conditions. Final updated properties of both cooled and uncooled arm segments, as well as all other body segments are included in Table 4.1.

Additionally, the base model of Stolwijk does not feature any maximal values for skin blood flow or sweat secretion. While this will not significantly impact results under minimal stress, it will impact the body's thermal behaviour under very stressful conditions, especially when exercising in hot environments. To capture this behaviour, maximal sweat production rate and skin blood flow rate from the thermal model of Fiala *et al.* [28] were adopted into the present model. Sweat production is limited to 1.8L/hr, and sweat secretion in each body region is therefore truncated proportionally when the total desired rate exceeds this maximum. Because skin will compete for blood supply with working muscles during exercise in the heat, the maximal rate of skin blood flow will be reduced when blood is required for muscular work. The following relationship from the work of Fiala *et al.* was employed governing maximal skin blood flow

$$BF_{skin_{max}} = 386.9 - 0.32\Delta BF \quad \textbf{(4.2)}$$

where ΔBF represents the current total blood flow in the body in excess of the basal value.

Finally, surface areas and masses of the simulated body segments were adjusted to reflect the average measured values of experimental participants reported in Chapter 3. Final values of all model parameters relevant to the discussed changes are reported in Table 4.1.

4.2.2 Numerical Solution Methodology

A forward difference temporal discretization scheme was employed, representing the rate of change of nodal temperatures according to equation 4.3:

$$\frac{dT_N}{dt} = \frac{(T_{N_{t+1}} - T_{N_t})}{DT} \quad \textbf{(4.3)}$$

where $T_{N_{t+1}}$ denotes the local temperature value a small timestep into the future, T_{N_t} denotes the current local temperature, and DT denotes the size of the timestep. Employing this representation in the governing nodal energy balance equations relates the current temperature at a given node to the temperature at that same node at the subsequent timestep. The initial nodal temperature distribution provided by the original Stolwijk model was assumed at the first timestep of the simulation period. The temporally discretized nodal energy balances were then used to explicitly project the temperatures at the second time step based on the initial distribution. These projected values were fed back into the controlling system to update the thermoregulatory responses, reformulate the nodal energy balances, and project temperatures an additional timestep into the future. This iterative process was repeated over the entire duration of all simulations with a selected time step of 0.0005 hours, or 1.8 seconds. A range of timestep values were tested to ensure time step independence of simulation results was achieved for the selected step size.

Table 4.1: Relevant properties of the thermal model. Any properties not included above were unchanged from their default value as reported in [14].

Head					
Property	**Dimensions**	**Value**	**Property**	**Dimensions**	**Value**
Core layer heat capacitance	kcal/K	2.00	Muscle layer heat capacitance	kcal/K	0.30
Fat layer heat capacitance	kcal/K	0.20	Skin layer heat capacitance	kcal/K	0.22
Core-to-muscle conductance	kcal/(hr.K)	1.38	Muscle-to-fat conductance	kcal/(hr.K)	11.4
Fat-to-skin conductance	kcal/(hr.K)	13.8	Skin surface area	m^2	0.126
Convective heat transfer coefficient	kcal/(hr.K.m^2)	3.79	Radiative heat transfer coefficient	kcal/(hr.K.m^2)	5.50
Clothing thermal resistance	Clo	0	Clothing evaporative resistance	hr.mmHg.m^2/kcal	0
Trunk					
Property	**Dimensions**	**Value**	**Property**	**Dimensions**	**Value**
Core layer heat capacitance	kcal/K	8.88	Muscle layer heat capacitance	kcal/K	14.60
Fat layer heat capacitance	kcal/K	3.84	Skin layer heat capacitance	kcal/K	1.09
Core-to-muscle conductance	kcal/(hr.K)	1.37	Muscle-to-fat conductance	kcal/(hr.K)	4.75
Fat-to-skin conductance	kcal/(hr.K)	19.8	Skin surface area	m^2	0.648
Clothing thermal resistance	Clo	0.083	Clothing evaporative resistance	hr.mmHg.m^2/kcal	0.0069
Arms					
Property	**Dimensions**	**Value**	**Property**	**Dimensions**	**Value**
Core layer heat capacitance	kcal/K	1.20	Muscle layer heat capacitance	kcal/K	2.60
Fat layer heat capacitance	kcal/K	0.50	Skin layer heat capacitance	kcal/K	0.37

Core-to-muscle conductance	kcal/(hr.K)	1.13	Muscle-to-fat conductance	kcal/(hr.K)	8.41
Fat-to-skin conductance	kcal/(hr.K)	24.76	Skin surface area	m^2	0.228
Clothing thermal resistance	Clo	0.04	Clothing evaporative resistance	hr.mmHg.m^2/kcal	0.0035
Cooled Arm Segment					
Property	**Dimensions**	**Value**	**Property**	**Dimensions**	**Value**
Core layer heat capacitance	kcal/K	0.07	Muscle layer heat capacitance	kcal/K	0.15
Fat layer heat capacitance	kcal/K	0.01	Skin layer heat capacitance	kcal/K	0.01
Core-to-muscle conductance	kcal/(hr.K)	0.07	Muscle-to-fat conductance	kcal/(hr.K)	3.50
Fat-to-skin conductance	kcal/(hr.K)	2.30	Skin surface area	m^2	0.013
Cooling surface contact conductance	kcal/(hr.K)	2.90			
Hands					
Property	**Dimensions**	**Value**	**Property**	**Dimensions**	**Value**
Core layer heat capacitance	kcal/K	0.13	Muscle layer heat capacitance	kcal/K	0.05
Fat layer heat capacitance	kcal/K	0.08	Skin layer heat capacitance	kcal/K	0.15
Core-to-muscle conductance	kcal/(hr.K)	5.50	Muscle-to-fat conductance	kcal/(hr.K)	9.65
Fat-to-skin conductance	kcal/(hr.K)	9.90	Skin surface area	m^2	0.090
Clothing thermal resistance	Clo	0	Clothing evaporative resistance	hr.mmHg.m^2/kcal	0
Legs					
Property	**Dimensions**	**Value**	**Property**	**Dimensions**	**Value**
Core layer heat capacitance	kcal/K	3.83	Muscle layer heat capacitance	kcal/K	8.29
Fat layer heat capacitance	kcal/K	1.29	Skin layer heat capacitance	kcal/K	0.98
Core-to-muscle conductance	kcal/(hr.K)	9.00	Muscle-to-fat conductance	kcal/(hr.K)	12.40
Fat-to-skin conductance	kcal/(hr.K)	64.00	Skin surface area	m^2	0.568
Clothing thermal resistance	Clo	0.05	Clothing evaporative resistance	hr.mmHg.m^2/kcal	0.0041
Feet					
Property	**Dimensions**	**Value**	**Property**	**Dimensions**	**Value**
Core layer heat capacitance	kcal/K	0.21	Muscle layer heat capacitance	kcal/K	0.05
Fat layer heat capacitance	kcal/K	0.12	Skin layer heat capacitance	kcal/K	0.20
Core-to-muscle conductance	kcal/(hr.K)	14.00	Muscle-to-fat conductance	kcal/(hr.K)	17.70
Fat-to-skin conductance	kcal/(hr.K)	14.10	Skin surface area	m^2	0.124
Clothing thermal resistance	Clo	1.15	Clothing evaporative resistance	hr.mmHg.m^2/kcal	0.15

4.3 Comparison with Experimental Measurement

The model was populated with appropriate inputs to simulate the experimental exercise bout described in Chapter 3, allowing its predicted outputs to be compared to the experimental measurements to validate its ability to effectively simulate the body's thermal response to cycling exercise in hot and humid conditions, both with and without applied cooling.

Input Population

The model required input describing the metabolic heat generation occurring in the muscles due to exercise in excess of basal activity. This input was supplied as a vector describing the metabolic activity over the entire experimental trial session beginning with participants' arrival at the indoor experimental facility. After arrival, participants remained in the facility, but outside of the environmental chamber for roughly 30 minutes while they changed into exercise clothing, and performed preparatory tasks and measurements. With no form of ergometry or calorimetry performed, metabolic activity during this period could only be estimated, and a heat generation value of 150W was assumed to represent light walking and movement. Following this, participants entered the environmental chamber, where they rested for five minutes, then completed a five-minute warmup protocol, followed by a brief pause where the cooling system was positioned and secured in place, and finally followed by the 45-minute sustained exercise bout. Because neither direct nor indirect calorimetry could be performed during the experiment, the excess heat generation rate while cycling could only be estimated based on the work rates measured by the ergometer, and an assumed value of the metabolic efficiency in cycling. The distribution of excess heat generation over time was therefore estimated from participants' average cycling work rates during the warmup and sustained exercise period, and a cycling efficiency of 21%, assumed based on a review conducted by Ettema & Loras [14]. This distribution is plotted in Figure 4.1.

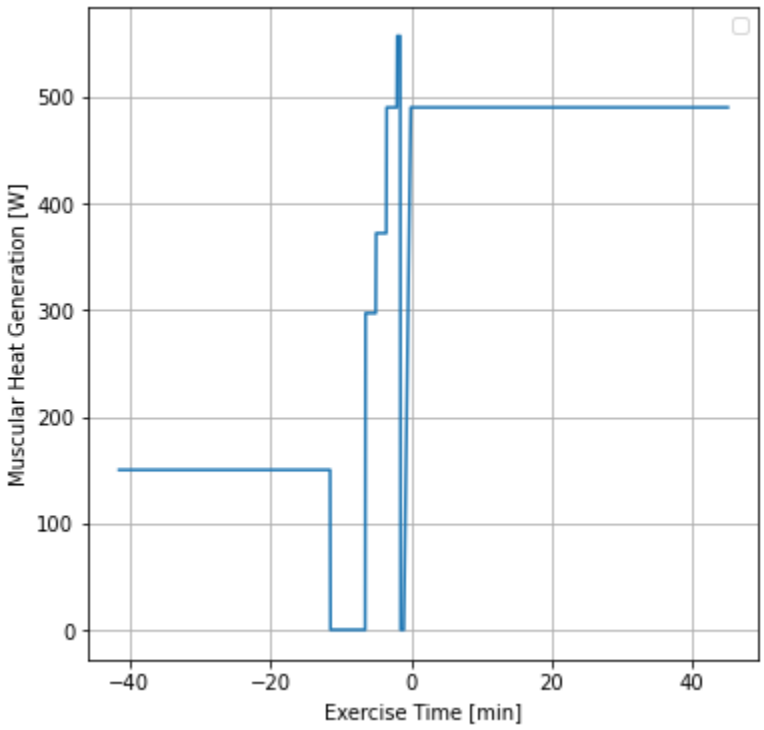

Figure 4.1: Muscular heat generation above basal levels due to metabolic inefficiency. The level of heat generation at any given time will result from the exercise intensity at that moment. The sustained low level of heat generation at the beginning of the plotted span corresponds with the light walking and movement occurring during pre-exercise preparation. This is followed by a five-minute period of rest, then the structured warmup, a brief pause in activity to affix the cooling system to the arms, followed by the sustained exercise bout of constant intensity. Time values were adjusted so that a time of 0 corresponded with the beginning of the constant-intensity sustained cycling bout.

The model additionally required population with appropriate values for the ambient temperature and relative humidity throughout the trial session. Because these properties differed between the environmental chamber and the locations within the experimental facility where pre-exercise preparation took place, these values were once again supplied as vectors describing the temperature and humidity values at all time steps. Air temperature and relative humidity in the environmental chamber were known to be roughly 30°C and 70% respectively. The ambient conditions in the experimental facility, but outside of the environmental chamber, were assumed to be typical indoor conditions of 25°C air temperature and 30% relative humidity. In all cases, it was

additionally assumed that the temperatures of indoor walls and other surfaces had equilibrated with surrounding air, and the enclosing mean long wave radiating temperature was set equal to local air temperature. The incident solar irradiation was set to zero throughout the session, as the experimental site featured no windows to the outdoors.

Additionally, values for relative airspeed at the surface of all body segments were required to capture the impact that the motion of cycling ergometry would have on local convective heat transfer coefficients. Convective heat transfer coefficient values around the body were measured directly by Nishi & Gagge during cycling ergometry exercise in [33]. Air velocity input values were adjusted for each body part so that the model's default relationship relating airspeed to convective transfer coefficients would produce the values reported by Nishi and Gagge. Accordingly, local relative airspeeds of 0.19, 0.16, 0.22, 0.15, 0.44, 1.00 m/s were used for the head, trunk, arms, hands, legs, and feet respectively during simulation periods where cycling ergometry occurred. The model's default free convection values for cases without bulk relative flow were used at all other simulation times.

Model Output

The described model formulation produces the trunk core temperature outputs shown in Figure 4.3. Plots of simulated results both with and without cooling applied are overlayed, alongside the average experimental measurements of gastrointestinal temperatures taken at five-minute intervals. Note, as indicated in Chapter 3, that the experimental averages are only plotted for the first 30 minutes of the exercise bout, as this was the last common time point attained by all before exercise was terminated for some participants due to high core temperatures.

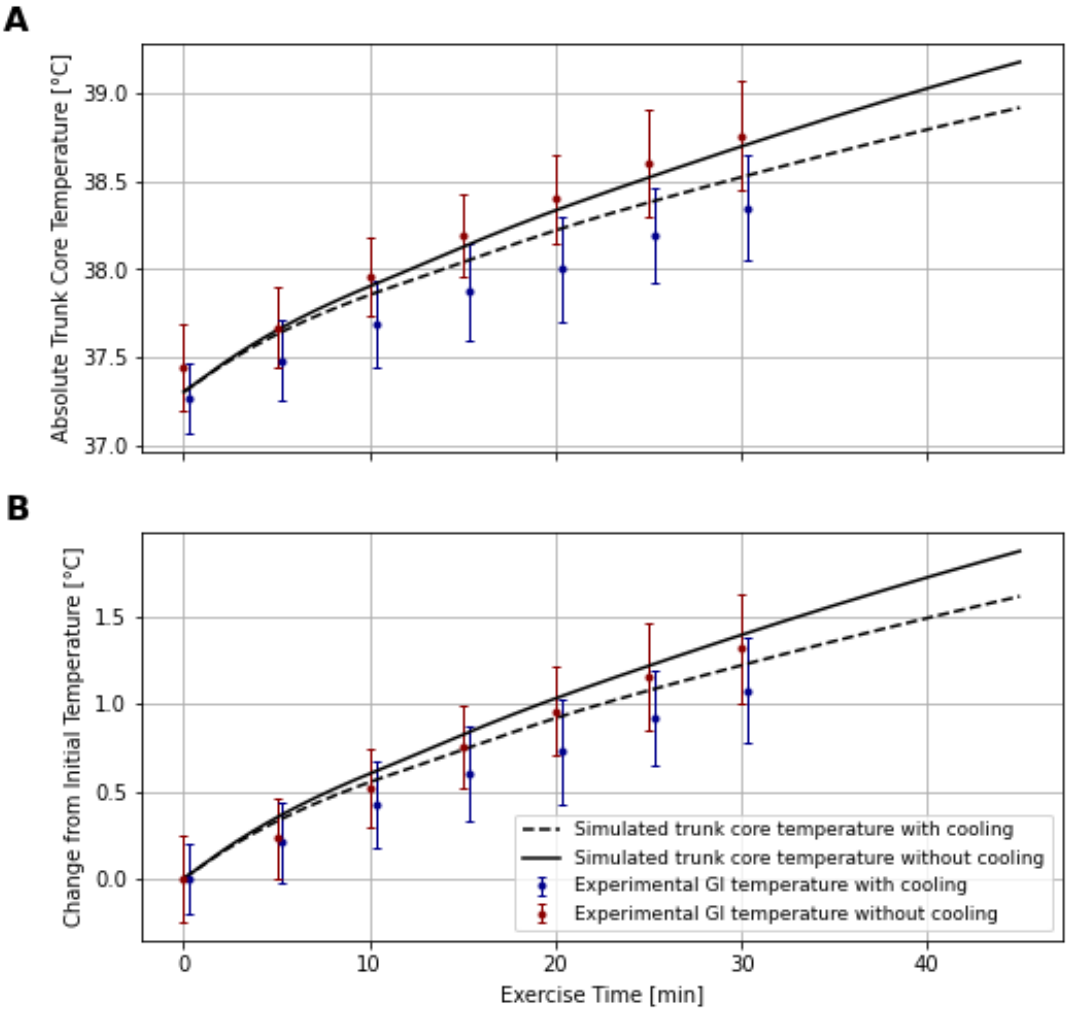

Figure 4.2: Simulated and experimentally recorded core temperature plotted over the course of the sustained 45-minute exercise bout. Model predictions are reasonably consistent with experimental observation, however, the model tends to slightly overpredict the absolute rise in core temperature over the course of the exercise bout, while slightly underpredicting the reduction in core temperature rise resulting from the applied cooling. Experimental temperature values obtained with cooling applied are offset in the plot for visual clarity, but were acquired at identical times to the values obtained without applied cooling. A) Absolute core temperatures. B) Change from the initial temperature value.

As can be seen in Figure 4.3, the predicted trends are similar to those observed in experiment; core temperatures begin between 37.25 and 37.5°C, and diverge over the course of the 45-minute

exercise bout. Core temperatures still rise over the course of the bout with applied cooling, though the cooling attenuates the rate of increase. The simulation predicts that core temperature will rise at a rate of 2.50°C/hr under control conditions, and at a rate of 2.16°C/hr with applied cooling, yielding a reduction in the rate of temperature rise of 0.35°C/hr. In experiment, a rate of rise of 2.43 ± 0.70°C/hr was observed under control conditions, and 2.03 ± 0.63°C/hr with applied cooling, yielding a paired reduction in the rate of rise of 0.43 ± 0.34°C/hr. Additionally, the simulation predicts a total sweat loss of 0.98kg without cooling, compared to 0.90kg with cooling applied. When adjusted for skin surface area and exercise duration, whole-body sweat rate indices of -0.73kg/m^2/hr and -0.66 kg/m^2/hr are obtained for the un-cooled and cooled simulated exercise respectively. For comparison, the experimental study observed whole-body sweat loss indices -0.88 ± 0.26 kg/m^2/hr in controls trials, and -0.84 ± 0.24 kg/m^2/hr with cooling applied.

Visual inspection of the plotted data, as well as comparison of the quantified temperature increase rates, make it clear that the model's predictions are reasonable, though they do underestimate the impact of the cooling on core temperature rise slightly. The underestimation is likely a result of inaccuracies in the representation of the body's thermoregulatory responses, such as skin blood flow and sweat secretion. Intuitively, the applied cooling attenuates the rise of core temperature in all cases by extracting heat from the body, leading to a lower level of net heat storage. Visually, this appears in Figure 4.3 as higher slopes in the plots of the uncooled core temperature curves, compared to the cooled equivalents at any given time. However, the quantified impact cooling has on the rate of core temperature rise is not determined solely by the rate of heat extraction, and will ultimately depend on a combination of physical and physiological behaviours. As non-cooled body temperature rises higher than the cooled equivalent, it produces two regulating effects that provide negative feedback to limit the rate at which the temperatures diverge any further. First, the warmer skin temperature found in the uncooled case produces a larger gradient between the body and surroundings, which naturally drives more convective and radiative heat loss. Additionally, the higher uncooled body temperature elicits a stronger thermoregulatory response than the cooled body temperature. This leads to more sweating and skin blood flow, both of which significantly elevate total convective, radiative, and evaporative heat losses, and oppose the additional rise of non-cooled core temperature. So while the heat extracted by the applied cooling allows the cooled body temperature to rise at a slower rate initially, the lower resulting temperatures lead to a more limited thermoregulatory response than would be seen if cooling were not present, and the ability of the cooling to reduce the rate of core temperature rise

diminishes as the cooled and uncooled body temperatures diverge. The quantified impact that the applied cooling will have on the rate of core temperature rise will therefore depend on the combination of the heat extraction rate, and the effectiveness of the additional thermoregulatory responses induced by the warmer, un-cooled body temperatures. Accordingly, if the assumed relationships relating body temperatures to thermoregulatory responses do not perfectly capture the true behaviour of the body, the quantified impact of applied cooling will differ. Comparison of the modelled and observed sweat rate indices suggest that relationships governing the modelled body's thermoregulatory responses may over-estimate the amount that sweat rate is increased in the non-cooled exercise. This would exaggerate the uncooled body's additional regulatory response to the hotter temperatures, and would therefore predict smaller differences between the rates of rise in cooling and non-cooling cases, as was observed.

The modelled heat extraction out of the forearm is compared to the experimental measurements in Figure 4.4. Note that the cooled arm segment was deliberately configured produce the same average heat extraction rate of 30.3W observed in experiment, but very similar trends can be noted in both simulated and measured extraction. Levels are initially high as the warm skin provides a large thermal gradient driving heat flow when it first comes in contact with the cooling surface. Skin temperature then drops, reducing the gradient, until it reaches a temperature sufficiently cool that conduction from deeper tissue and warm blood perfusing the region can supply enough heat to bring the skin to an approximate thermal balance. At this point, the skin temperature stabilizes, and provides a gradient that transfers heat to the cooling surface at a relatively consistent rate. Forearm skin temperature then continues to rise gradually throughout the bout as the rest of the exercising body progressively heats up, and increasingly warm blood perfuses the region.

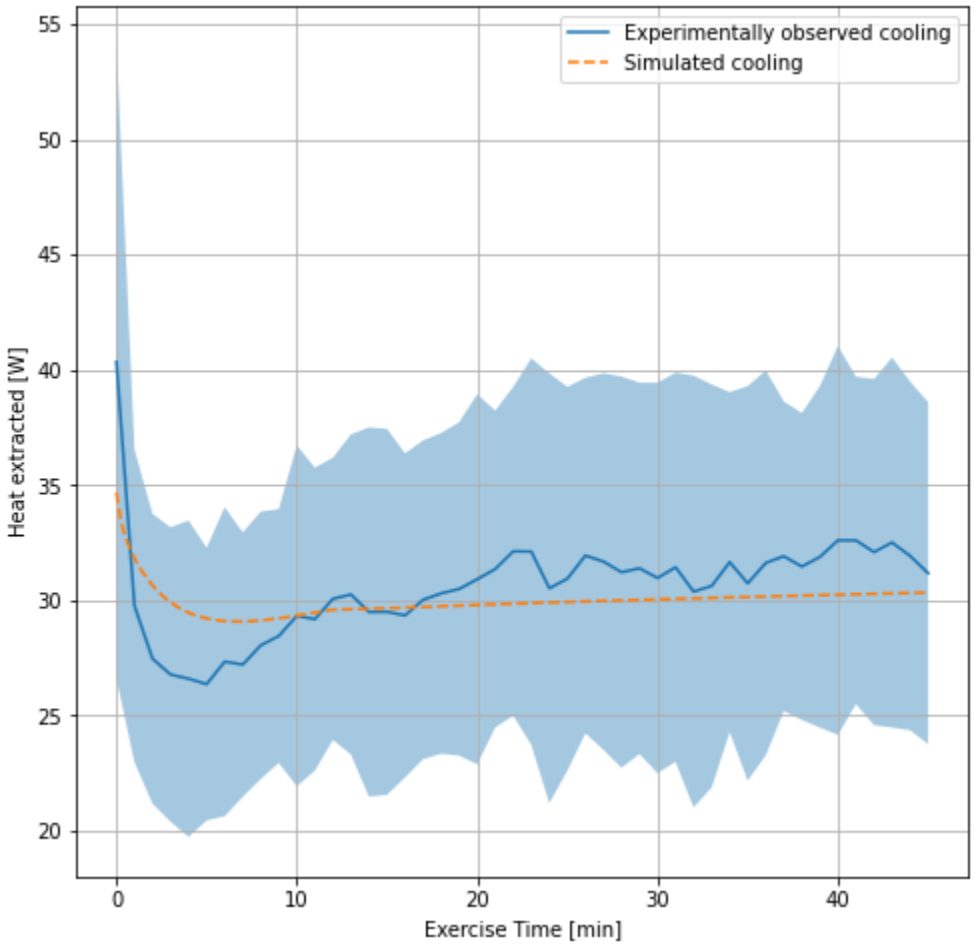

Figure 4.3: The rate of heat extraction over the duration of the exercise bout. Both simulated and measured extraction profiles display similar trends, beginning with high extraction rates. These rates quickly drop off to a minimum several minutes after the beginning of exercise. Following this, heat extraction rates remain relatively stable, though gradually rise over the remainder of the bout.

Ultimately, despite modest differences, the outcomes predicted by the model generally display similar values and trends to those observed in experiment. This suggests that the application of the current model to test cases studying the impact of cooling on core temperature rise during cycling in outdoor conditions can provide valuable insights on the expected behaviour.

4.4 Application of Model to Outdoor Cycling Test Cases

To address the identified questions regarding the impact of the proposed cooling in true cycling applications, the constructed model was configured to simulate a variety of outdoor test cases. The base test case featured identical ambient temperature and humidity inputs as the indoor experimental trials, but additionally included higher airspeeds over the body surface, heat gain from solar irradiation, and higher cycling work rates. This case aimed to provide insights on the impact that may have been observed in the conducted experimental trials if they had been able to account for these considerations. Additional test cases were conducted for a range of ambient temperatures, relative humidity values, and solar irradiation levels to observe the dependence of thermal outcomes and cooling impact on ambient conditions. The population of model inputs for each of these cases is outlined in the following sections, and predicted outcomes are presented and discussed.

Base Case: Outdoor Recreation of Experimental Trial

Input Population

As discussed, for the first studied test case, many of the model inputs remained the same as those described in Section 4.2.2. For ease of comparison, all inputs during pre-exercise preparation and warmup were left unchanged, allowing the body to begin the sustained exercise bouts in the same thermal state in all cases. Additionally, inputs describing ambient air temperature, effective long-wave radiating temperature, and relative humidity were kept identical to those described in Section 4.2.2 throughout the entire exercise bout. While the mean radiative temperature of surrounding long-wave radiating enclosure surfaces in the outdoors can, in general, differ from local air temperature depending on the nature of surrounding ground, structures, cloud cover, time of day, and other factors, it is assumed to remain equal to the local air temperature in the present modelling.

Other model inputs beyond the unchanged values highlighted above were adjusted, however, to reflect the inclusion of outdoor considerations. Relative airspeeds during the sustained cycling bout period were increased to reflect the movement of a bicycle and rider through the air. The airspeed inputs were set to 10m/s at the surface of all body segments to reflect a typical cycling ground speed for an experienced cyclist. Note that this assumes that the motion of various limbs relative to the translating body core of the rider contributes negligibly to the resultant local airspeed. It should also be noted that the default relationships included in the model that adjust convective coefficients based

on air motion were obtained for a human in a standing posture, not a cycling posture. No published information was found on the local convection coefficients for a body moving through air in a cycling posture, so the default relationships were kept. This may result in a slight overestimation of impact of air motion, since the orientation of the body during cycling resembles a crouching posture, which may partially obstruct airflow to all body segments. Additionally, the central axis of the torso is aligned with the free stream direction during competitive cycling for aerodynamic purposes. This orientation generally results in lower convective transfer coefficients for cylinders than an orientation where the axis is perpendicular to the free stream, which a standing posture resembles more closely. However, convective transfer coefficients measured for various postures were compared in Table 2.3, and relatively small differences were observed. Therefore, while coefficients determined specifically for cycling motion would be preferred, it is likely that they would not differ widely from those obtained for a standing posture. In future development of the model, computational fluid dynamics simulations represent a possible tool that could be employed to estimate convective transfer coefficients for specific cycling postures and speeds.

The level of incident solar irradiation during the sustained cycling bout also needed to be adjusted to reflect this element of outdoor thermal balance. Representative solar irradiation distributions over the course of a summer and winter day are shown in Figure 4.3. Solar irradiation can reach up to 1000 W/m^2 under direct peak sunlight [27]; accordingly, this value of incident solar irradiation was employed in the simulation to represent direct sunlight on a summer day. Published measurements of solar view factors for cyclists could not be found, so view factors employed in the modelling were estimated based on typical cycling posture when resting on aerobars. A value of 0.5 was assumed for the trunk and head due to their direct exposure to incident sunlight, 0.3 for the arms and hands due to their partial coverage by the rider's trunk and head, and a value of 0.1 for the legs and feet, which will be mostly shaded from overhead light, but will still be struck by scattered sunlight and light incident at an angle. A standard value of 0.7 was assumed for the short-wave absorptivity of the body surface and clothing [29].

Cycling work rates selected for the experimental trials were also well below the work rates that the participants would typically sustain for 45 minutes, and the heat generation rates in the present simulation needed to be adjusted to reflect these higher work rates expected in true cycling bouts. The simulation's excess muscular heat generation rate was therefore adjusted to 895W during

the sustained cycling period to reflect a typical functional threshold power output for amateur male cyclists of roughly 260W.

A final input adjusted in the outdoor cycling simulation was the addition of a thermal and evaporative resistance at the surface of the head to account for a helmet being worn. Experimental participants elected not to wear helmets during the stationary cycle ergometer trials, but would almost certainly wear one during true outdoor cycling. Values for the thermal and evaporative resistances were selected to be 0.006 Clo [2] and 0.010 hr.mmHg.m^2/kcal respectively, based on measurements performed by Mukunthan *et al.* [219].

Model Output

A plot of the temporal variation of trunk core temperature over the course of a 45-minute cycling bout with the described ambient conditions and work rate is shown in Figure 4.5.

[2] Clo is a unit of thermal resistance offered by clothing. 1 clo is equal to 0.155 K*m^2/W. This thermal resistance was selected as the reference value of 1 clo, as it corresponds to the average clothing resistance of an outfit that allows an individual to rest comfortably in a 21°C room, such as a business suit [225].

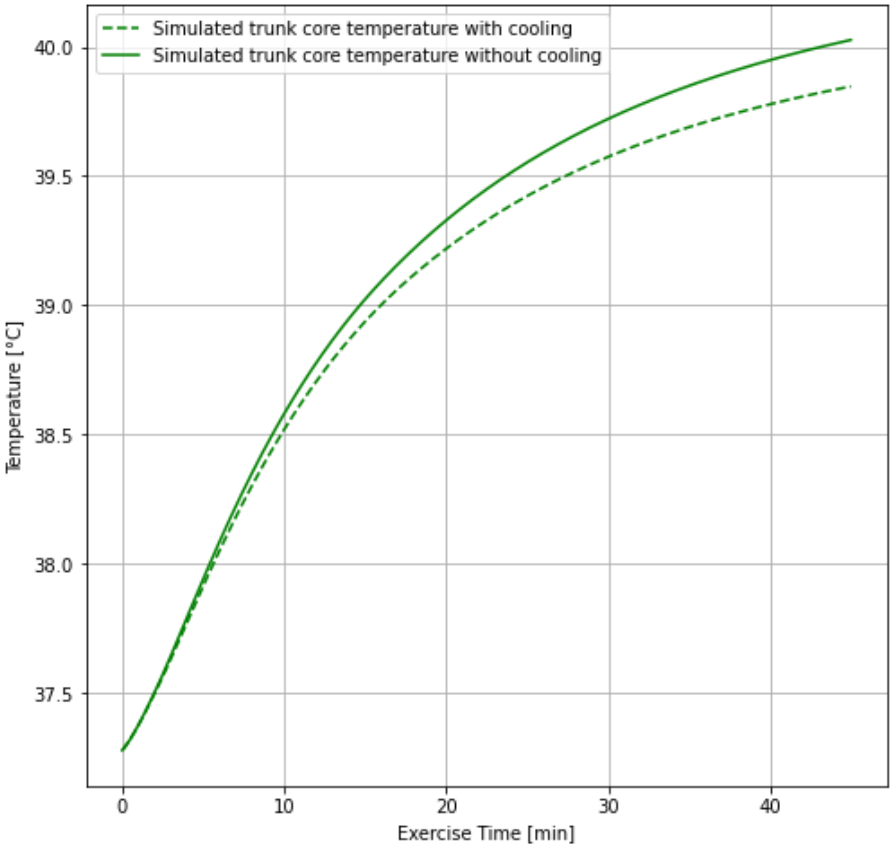

Figure 4.4: Trunk core temperature over the duration of the simulated 45-minute sustained exercise bout. Both cooled and uncooled body temperatures rise to levels higher than those predicted under experimental conditions, suggesting that the present conditions are more thermally stressful overall. The effectiveness of the applied cooling at limiting core temperature rise, which is represented visually by the gap between the cooled and un-cooled temperature curves, is smaller in the present case than it was in the case featuring stationary experimental input conditions.

As can be seen, the combination of ambient inputs results in higher absolute trunk core temperatures at the end of the exercise bout both with and without cooling than was predicted under indoor experimental conditions. While the inclusion of the effects of relative air motion assist in cooling the body, heat gained through solar irradiation, and the additional metabolic heat generated as a by-product of the higher work rate, result in higher body temperature overall. In this case, trunk core temperature rises at a rate of 3.52°C/hr without applied cooling, and a rate of 3.28°C/hr with

applied cooling, resulting in a change of 0.24°C/hr. An absolute fluid loss of 1.13kg without applied cooling, and 1.08kg with cooling are predicted by the model. This produces whole-body sweat rate index values of -0.84kg/m^2/min under control conditions, and -0.80kg/m^2/min with cooling applied.

While applied cooling clearly reduces the rate of trunk core temperature rise under both outdoor and stationary indoor conditions, the reduction is smaller in the outdoor case. This is likely a result of the augmented ability of sweat to evaporate when surrounded by fast moving air. As previously discussed, the hotter body temperatures achieved in simulations without applied cooling result in higher sweat rates. This allows the uncooled body to partially counteract the lack of applied cooling with additional evaporative heat loss, limiting the reduction of core temperature rise offered by the applied cooling. However, evaporative cooling will eventually be capped by maximal sweat evaporation rates at each body segment surface. If the body secretes sweat at a rate that is greater than the maximal evaporation rate, additional secreted sweat will not provide additional cooling to the body. Under these circumstances, the uncooled body's ability to respond to its hotter state with augmented evaporative losses is compromised. The effect of the applied cooling on the rate of core temperature rise will therefore be maximized under such circumstances. The low relative airspeed and high ambient humidity of the stationary experimental conditions caused the simulated rider's sweat secretion to exceed the maximal sweat evaporation rate at all body segment surfaces. This compromised the uncooled rider's ability to fight the faster rising temperatures, which made the applied cooling more impactful. In the outdoor case, the rapid air motion raises the maximum achievable sweat evaporation rates. As a result, sweat secretion does not exceed these maximum values at the majority of the body segment surfaces at any point in the exercise bout. This allows the body to maintain more ability to fight the faster uncooled temperature rise, and reduces the quantified impact of the cooling.

We also see in Figure 4.5 that trunk core temperature exceeds 40°C near the end of the 45-minute exercise bout under control conditions, with core temperature remaining slightly lower with forearm cooling applied. To observe how these trends would continue during longer cycling bouts, the simulation was extended, as shown in Figure 4.6. Note that a rider with a functional threshold power of exactly 260W would not be able to maintain this power level for much longer than an hour even under thermoneutral conditions. However, many fit cyclists would have sufficient functional threshold power levels to maintain this work rate for at least the plotted duration.

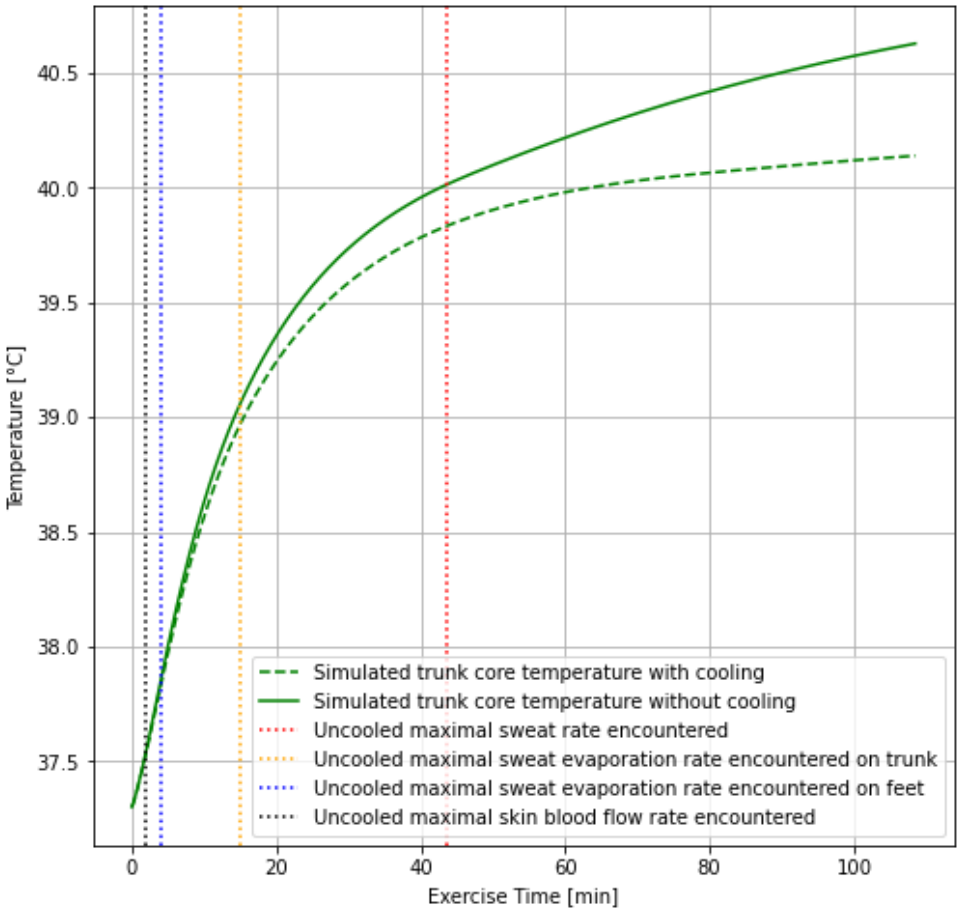

Figure 4.5: The simulated response of core temperature for an extended cycling exercise simulation lasting over 100 minutes. Vertical dotted lines represent the points at which limitations to thermoregulatory effectiveness begin to appear. Maximal skin blood flow is encountered less than 3 minutes into the exercise bout, maximal sweat evaporation is encountered at the surface of the feet after 4 minutes, maximal sweat evaporation at the surface of the trunk is encountered after 15 minutes, and maximal sweat secretion is encountered almost 44 minutes into the exercise bout.

Both curves display a similar overall trend, rising rapidly initially, and progressively flattening as exercise continues. This profile is common to any warming thermal mass with internally generated heat – if the simulation were run indefinitely, the curves would continue to rise, eventually approaching steady equilibrium temperatures where heat gains and losses are balanced. The ultimate

equilibrium temperatures, and the rates at which the temperature profiles rise towards them, will depend on the various properties governing heat loss from the body.

Core temperatures are initially equal in both cases, but begin diverging immediately due to the additional heat extracted by the applied cooling. The aforementioned regulating action taken by the uncooled body, namely faster elevation of sweat rate and skin blood flow in response to the faster rising body temperatures, limits the rate at which the curves diverge, however. Due to the high competing blood demand from working muscles, and the already elevated state of body temperatures resulting from the warmup, the uncooled body reaches its maximal skin blood flow rate less than 3 minutes into the bout, as indicated in Figure 4.6. This point represents the first hindrance of the body's thermoregulatory responses encountered, and the first restriction imposed on the uncooled body's ability to counteract the diverging core temperature values. The next limitations encountered are the maximal sweat evaporation rates for body segments fully covered by clothing. This occurs for the feet at after 4 minutes, and for the trunk after 15 minutes. After each of these thresholds marking thermoregulatory limitations are achieved, the core temperature curves in Figure 4.6 can be seen to diverge slightly more rapidly. Finally, after almost 44 minutes have elapsed, the maximal sweat secretion rate is encountered in the uncooled body. For the remainder of the exercise bout, the body no longer has any ability to further elevate thermoregulatory responses. Beyond this point, the effectiveness of the applied cooling is maximized, and the curves begin to diverge dramatically.

As can be seen in both cases however, trunk core temperature eventually exceeds 40°C. This would generally support the intuitive expectation that performing roughly an hour of cycling exercise at the highest sustainable intensity on a hot day, under direct sunlight, with very high ambient humidity would cause the body to reach dangerous temperatures. Without applied cooling however, trunk core temperature exceeds 40°C after only 43 minutes, whereas it is able to remain below this value for more than 62 minutes with forearm cooling applied. Because core temperatures exceeding 40°C expose an individual to risk of heat stroke, the ability of the applied cooling to allow a cyclist to complete a 60-minute ride without crossing this threshold could prevent the onset of such adverse health outcomes. The reduced core temperature at all equivalent time points observed in simulations with forearm cooling would additionally reduce the risk of experiencing other heat related illnesses or injuries at any point. The reduction in fluid loss from sweating due to applied cooling could also help prevent forms of heat related illness owing to dehydration, or to the conspiring effects of dehydration and hyperthermia.

In reality, however, it is unlikely that a cyclist with a core temperature rising up to and above 40°C would continue to ride uninterrupted. As discussed in Section 2.2, inhibition of central motor drive owing to thermal stress is likely to prevent the body from maintaining the constant work rate assumed in the simulations performed. A drastic reduction in the ability to perform work is often observed as core temperatures reach roughly 40°C. If it is assumed that a constant work rate can be maintained for all core temperature values below 40°C, and that exercise cannot continue at higher core temperatures, the applied cooling is therefore capable of extending the duration of the present exercise bout by almost 20 minutes. Similarly, the cooling would allow an athlete to maintain a higher pre-determined constant work rate over the course of an exercise bout of a fixed duration. Under the simulated outdoor conditions, a cyclist could perform 60 minutes of exercise at a work rate of 261W with the applied forearm cooling before their core temperature exceeds 40°C. Conversely, without applied cooling, they could only maintain a work rate of 255W for 60 minutes. While sharp declines in ability to perform exercise are commonly observed at a core temperature of 40°C, assuming that constant exercise intensity is maintained up until this temperature is achieved, and that exercise immediately ceases once it is exceeded is an over-simplification of the true behaviour. In reality, exercise performance is likely inhibited progressively for increasing body temperatures below 40°C as well. The ability of the applied cooling to reduce core temperature at all time points for a given work rate, however, is likely to limit performance reductions regardless of the nature of their onset.

Elevated core temperatures will also result in increased sensation of thermal stress and discomfort. The ability of the simulated cooling to limit temperature rises is therefore likely to improve thermal comfort as well. Subjective perception of thermal comfort itself can impact performance, as cyclists would be likely to terminate exercise prematurely, or voluntarily reduce work rate in response to the unpleasant sensation of thermal discomfort.

Additional Cases Investigating the Impact of Varied Ambient Conditions

Input Population

To gain a further understanding of the expected impact of the proposed cooling modality in true cycling applications, it is important to understand how the outcomes vary across a range of possible ambient conditions. The air temperature, relative humidity, and level of solar irradiation will all affect the thermal state of the simulated cyclist, and therefore the impact of the applied cooling.

Accordingly, additional simulations were performed to model the outcomes over a range of conditions. No further adjustments to the model construction itself were required in this case – the only changes adopted were to the ambient input conditions employed during the cycling bout. In order to have all simulated exercise bouts begin in an identical thermal state, all of the present simulations once again featured the same pre-exercise preparation activities and warmup as the simulated experimental trials. Ambient conditions were then adjusted and kept constant at their new values for the sustained exercise bouts. Simulations were conducted under 30 different combinations of ambient conditions. Solar irradiation was first set to a typical "low" constant value of 200 W/m^2, which would be representative of very cloudy conditions, or conditions at a time of day with lower levels of sunlight. Relative humidity was also set to a typical "low" constant value of 30%, and simulations were conducted for 5 different temperature values ranging from moderately warm (25°C) to very hot (35°C). Relative humidity was then adjusted to a typical "moderate" constant value of 50%, with solar irradiation unchanged, and simulations were conducted across the same span of air temperatures. Relative humidity was then adjusted to a "high" constant value of 70%, with solar irradiation kept constant, and air temperature swept again. Solar irradiation was then adjusted to a typical "high" value of 1000 W/m^2, and simulations were conducted once again for all combinations of the same three relative humidity levels and 5 temperatures. In each simulation, the trunk core temperature progression over the duration of the exercise bout was determined both with and without cooling.

Model Output

Trunk core temperature profiles obtained from simulations conducted over an array of ambient conditions are plotted in Figure 4.7, with metabolic heat generation being held at a constant level corresponding to a cycling work rate of 260W in each case.

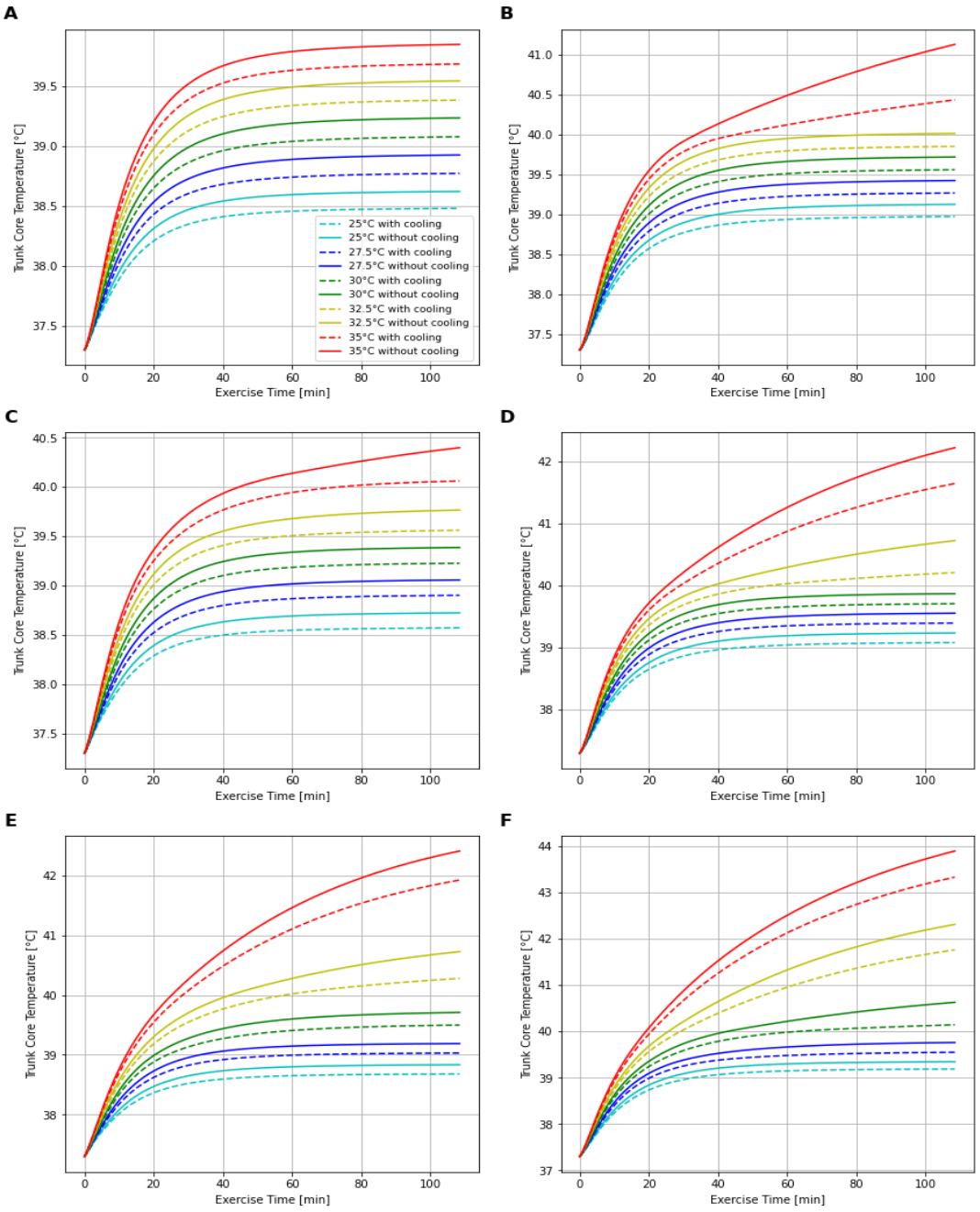

Figure 4.6: Core temperature responses plotted for an array of ambient condition combinations. In all cases, core temperature responses with applied cooling are plotted as dashed lines, while uncooled temperatures are plotted as solid lines. Each subplot represents different combination of solar irradiation level and relative humidity. A) Low sunlight and low relative humidity. B) High sunlight and low relative humidity. C) Low sunlight and moderate relative humidity. D)High sunlight and moderate ambient humidity. E) Low sunlight and high relative humidity. F) High sunlight and high humidity.

As one would expect, the combination of high temperature, humidity, and incident solar irradiation can cause the body to attain dangerously high core temperatures, with the several of the simulated conditions eliciting temperatures that could not practically be attained without first experiencing heat exhaustion or heat stroke. While hotter temperatures, higher levels of incident sunlight, and higher relative humidity levels will all contribute to elevated thermal stress, each of these ambient conditions will impact the exercising cyclist differently.

Increased humidity levels will impose a thermal challenge by opposing the ability of the body to cool itself via sweat evaporation. Maximal sweat evaporation rates depend on the vapour pressure gradient between the skin and the ambient air. With all other ambient conditions unchanged, a higher relative humidity reflects a higher ambient vapour pressure. This results in a smaller vapour pressure gradient between the skin and surrounding air, and a lower maximal sweat evaporation rate as a result. For low enough levels of thermal stress, where sweat rates around the body have not yet exceeded maximal evaporation rates, the impact of increasing relative humidity are minimal. Under more thermally stressful conditions, when body sweat rates are higher, the effect is more pronounced, as the maximal evaporation rates will limit evaporative losses despite the high sweat secretion rates. In the plotted simulations, the high relative air velocity assists sweat evaporation enough to ensure that areas of the body covered by relatively little clothing do not encounter their maximal sweat evaporation rates. However, areas that are more heavily clothed can experience maximal sweat evaporation. The higher simulated humidity levels cause more regions of the body to encounter their respective maximal evaporation rates, and cause the maximal rates to be encountered sooner. Accordingly, the body's ability to compensate for lack of applied cooling with additional sweat evaporation is compromised. Localized forearm cooling is therefore more effective at higher humidity levels. Visually, this leads to larger gaps between associated plots of cooled and uncooled core temperature in Figure 4.7 for increasing humidity levels at the same ambient temperature and solar irradiation level.

Increased levels of solar irradiation contribute additional heat gain to the body's thermal balance. Intuitively, this leads to higher core temperatures and more thermal stress overall. It does not, however, impact the evaporation of sweat, as ambient humidity does. Accordingly, as long as the sunlight does not heat the body sufficiently to encounter its maximal sweat secretion rate, additional solar irradiation does have a large impact on the quantified effect of forearm cooling on core temperature. This can be observed in Figure 4.7, by noting that in cases where overall thermal stress

is not very high, the gap between associated cooled and uncooled core temperature curves does not widen appreciably by additional solar irradiation for fixed ambient temperatures and humidity levels. If solar irradiation heats the body sufficiently to reach maximal sweat secretion rate, however, the impact of the cooling is increased, as the added sunlight compromises the uncooled body's ability to compensate for the rising temperatures.

Comparing to the overlayed curves corresponding to different air temperatures in all plots above, increasing ambient air temperature contributes significantly to the level of thermal stress experienced by the body. Furthermore, when combined with high humidity levels, the increasing ambient temperatures allow cooling to more effectively limit core temperature rise. This appears visually as widening gaps between associated cooled and uncooled core temperature curves for increasing ambient temperatures. Because relative humidity represents the ratio of the ambient vapour pressure to the saturation vapour pressure, and because the saturation vapour pressure increases with increasing air temperatures, hotter ambient air with the same relative humidity level will in fact have a higher absolute vapour pressure. Accordingly, hotter ambient air will lead to a smaller vapour pressure gradient from skin to surroundings for an equal relative humidity. For this reason, increasing air temperatures limit evaporative losses similarly to increasing relatively humidity levels, by reducing maximal sweat evaporation rates. Additionally, hotter air temperatures will decrease dry heat loss by reducing the temperature gradient from skin to surroundings, which will further increase body temperatures. This will cause hotter air to have an effect similar to the combination of both higher humidity and higher solar irradiation, by widening the gaps between associated core temperature curves, and by raising absolute core temperatures in all cases.

4.5 Concluding Remarks

The employed computational thermal modelling allowed the impact of the applied cooling to be assessed when accounting for thermal inputs that were not present in the experimentally studied conditions. This allowed the impact of cooling to be predicted when accounting for relative motion of air over a moving cyclist, solar irradiation incident on a cyclist's body, and additional heat generation resulting from higher cycling work rates. Ultimately, when accounting for these effects, the employed modelling predicts that the applied cooling will have a slightly smaller impact than it would under the studied experimental conditions. This is a result of the assistance provided by the relative air motion to the evaporation of sweat, allowing an uncooled body to more effectively compensate for the lack of

applied cooling through evaporative losses. Despite the reduced impact, the applied cooling is still expected to noticeably reduce the rate at which core temperature rises, which could reduce the risk of heat related illness in cyclists, and potentially help fight performance reductions associated with hyperthermia. Additionally, even when increased sweat evaporation is capable of offsetting the quantified impact of cooling on core temperature slightly, the applied cooling still provides the benefit of not necessitating sweat rate elevation, which could help prevent dehydration.

Ambient air temperature, relative humidity, and incident solar irradiation will all impact the thermal state of a cyclist predicted by the model. The quantified impact of the cooling on the rise of core temperature however, will be depend more strongly humidity and air temperature, rather than solar irradiation, as humidity and air temperature can interfere with the evaporation of sweat.

A potentially valuable use of the developed thermal model is the preliminary design of cooling garments and equipment, and in particular, the proposed forearm cooling device. The ability to rapidly simulate the effects of the cooling allow design parameters to be swept to iteratively assess and optimize design decisions. Parameters that could be studied include the skin surface area targeted by the applied cooling, temperature of the cooling surface applied, or the insulation level between skin and cooling surface. Without the ability to simulate the effects of the applied cooling with a theoretical model, iterative experimentation would be required gain insight on the impact of these parameters, which is a far more time consuming and costly alternative.

Chapter 5
Conclusion and Recommendations

5.1 Summary

Heat generation and loss are continually in competition in the body, with their balance ultimately determining the internal thermal state. When performing exercise in hot and humid conditions, elevated heat generation levels conspire with reduced heat loss to raise body temperatures, inducing potentially severe thermal stress. This stress exposes individuals to risk of heat related illness, and can hurt athletic performance, often prompting athletes to employ acute cooling strategies during activity. For some exercise modalities, peripheral body regions such as the arms are convenient locations to apply such cooling interventions. The present work has investigated one case of this in detail, namely, the application of cooling by holding a cold surface against the resting forearms of an individual during cycling exercise.

Experimental investigation of this modality observed that it is able to significantly improve whole body indicators of heat stress, including core body temperature rise, heart rate drift, and thermal comfort rating. This investigation, however, featured stationary cycle ergometer exercise, and was therefore unable to account for the effects of relative air motion and solar heat gain that would be experienced during true outdoor cycling. Furthermore, sustained work rates needed to be limited to levels below those that would typically be maintained by trained cyclists in realistic contexts. Questions therefore remained regarding the impact these considerations may have on the effectiveness of the forearm cooling in true cycling applications. Computational thermal modelling was employed to address these remaining questions. This modelling indicated that, while the assistance offered by true cycling motion to the evaporation of sweat does allow the body to compensate for a lack of applied cooling more effectively, the cooling would still reduce the rate of core temperature rise in these outdoor applications. It also suggested that the quantified impact cooling has on core temperature will generally be greater for warmer ambient temperatures and higher relative humidity levels.

5.2 Recommended Future Work

The insights provided by the present investigations are of note, but further iteration to extend the present work in a variety of ways is recommended.

While the lower core temperatures observed during cycling exercise with applied cooling are likely to enable improved exercise performance, the present experimental investigation focused solely on the impact of cooling on core temperature during a fixed cycling bout, and did not allow exercise intensity to differ between control and cooling conditions. The impact of the cooling on exercise performance was therefore not observed directly, and further experimental investigation is necessary to determine whether improvements would be observed. Many investigations into the impact of cooling feature cycling time trials to assess performance due to their resemblance to true cycling competition, however, the ability to cycle at different intensities in control and cooling trials means that comparison of core temperature progression across conditions is not meaningful. Conversely, time-to-exhaustion tests can also be employed to assess performance. Because time-to-exhaustion study participants will cycle at the same intensity in both control and cooling bouts, core temperature at equivalent time points can be compared across the experimental conditions to draw additional conclusions on the impact of the applied cooling. This form of assessment, however, will not be able to observe potential impacts of heat stress on self-selected pacing. Because the experimental work done to date already featured fixed intensity exercise and observed core temperature progression, a time trial test that studies self-paced performance would serve as a useful complement. If further core temperature study is of interest, however, a protocol featuring both fixed intensity cycling and a time trial test could be employed. Participants can be made to complete an abbreviated cycling bout of fixed intensity, immediately followed by a short time trial test, allowing core temperature and performance to be compared across control and cooling conditions.

Additionally, further iteration can be applied to the construction of the employed computational thermal model. While the model developed based on the work of Stolwijk allowed many of the desired effects to be captured, it could be altered to feature a more precise representation of the geometry of the various body regions, possibly by instead employing a more detailed modern model as a foundation. Perhaps the best candidate to serve as a foundation is the model of Fiala *et al.* [28] [174], as it is used in many noteworthy applications, and features detailed representation of body geometry and thermoregulatory controls. Detailed measurements of tissue geometry and circulatory behaviour at the forearm site could also be used to accurately model the region as heat is extracted by the applied cooling surface. The modelling could also be improved by better representing the studied population of cyclists. This would involve accounting for the sizes and proportions of body regions that may differ from the average population, such as the legs, as well as consideration of the impacts

of cycling training on blood flow and sweating behaviour. In fact, progression of the model to make it fully personalize-able by developing a measurement framework for body segment sizes, blood flow, metabolic rates etc. could allow the model to offer valuable predictions of thermal behaviour tailored to any individual.

Furthermore, a similar modelling approach to that presently employed could be applied to additional cases where cooling of peripheral body regions during exercise may be convenient. Examples of this include cooling the legs during paddle sports, wheelchair sports, or handcycling exercise, as the legs will often rest on supports and remain stationary during these exercise modalities. One consideration of note for such applications is that many athletes participating in these sports will have suffered spinal cord injuries (SCI), which can significantly alter thermoregulatory behaviour in the body. Individuals with SCI will possess a significantly different breakdown of body tissue in lower limbs due to muscular atrophy [220], and will also experience compromised afferent sensation, and sudomotor and vasomotor function below the level of injury, placing them at an increased risk of heat stress [221]. Adding these considerations to the presently constructed model by altering tissue type composition, blood flow and sweating behaviour in appropriate body regions, represents another potentially valuable extension of the present work. Altered models could then be applied to assess thermal responses and cooling effectiveness in athletes with SCI during sports such as wheelchair basketball, wheelchair rugby, wheelchair tennis, or handcycling.

Finally, due to the observed potential for forearm cooling to provide thermal benefits during cycling in the heat, further development and prototyping of the proposed aerobar-mounted ice bottle cooling device may be warranted. A variety of practical considerations must be addressed, including ensuring that ice in the bottle is held sufficiently close to the surface in contact with the arms to provide effective cooling, even as ice progressively melts. Additionally, the bottle must still be able to be used as a traditional water bottle once ice has melted to liquid water. The design must also be comfortable and practical to use, and should not contribute unwanted aerodynamic drag. Ultimately, a prototyped version of the proposed cooling device should be tested experimentally to observe its impact, in place of the present system constructed simply to mimic the effects.

References

[1] E. T. Hedge, K. A. Zuj, A. G. Stothart, E. Gavel, S. D. Peterson, L. S. Goodman and A. J. M. Buckrell, "Continuous forearm cooling attenuates gastrointestinal temperature increase during cycling," *The Journal of Sports Sciences,* 2020.

[2] E. V. Osilla, J. L. Marsidi and S. Sharma, "Physiology, Temperature Regulation," National Library of Medicine: National Center for Biotechnology Information, 2022. [Online]. Available: https://www.ncbi.nlm.nih.gov/books/NBK507838/. [Accessed 19 06 2022].

[3] C. L. Lim, "Fundamental Concepts of Human Thermoregulation and Adaption to Heat: A Review in the Contect of Global Warming," *International Journal of Environmental Research and Public Health,* vol. 17, no. 21, p. 7795, 2020.

[4] L. Nybo, P. Rasmussen and M. N. Sawka, "Performance in the Heat -- Physiological Factors of Importance for Hyperthermia-Induced Fatigue," *Comprehensive Physology,* vol. 4, pp. 657-689, 2014.

[5] G. J. Maw, S. H. Boutcher and N. A. S. Taylor, "Ratings of perceived exertion and effect in hot and cool environements," *European Journal of Applied Physiology,* vol. 67, pp. 174-179, 1993.

[6] C. C. W. G. Bongers, D. H. J. Thijssen, M. T. W. Veltmeijer and M. T. E. E. T. M. H. Hopman, "Precooling and percooling (cooling during exercise) both improve performance in the

heat: a meta-analytical review," *British Journal of Sports Medicine,* vol. 49, pp. 377-384, 2015.

[7] C. C. W. G. Bongers, M. T. E. Hopman and T. M. H. Eijsvogels, "Cooling interventions for athletes: An overview of effectiveness, physiological mechanisms, and practical considerations," *Temperature,* vol. 4, no. 1, pp. 60-78, 2017.

[8] E. H. Wissler, Human Temperature Control: A Quantitative Approach, Berlin, Germany: Springer Berlin Heidelberg, 2018.

[9] G. P. Kenny, L. E. Dorman, P. Webb, M. B. Ducharme, D. Gagnon, F. D. Reardon, S. G. Hardcastle and O. Jay, "Heat Balance and Cumulative Heat Storage during Intermittent Bouts of Exercise," *Medicine and Science in Sports and exercise,* vol. 41, no. 3, pp. 588-596, 2009.

[10] M. Steinach and H. Gunga, "Chaper 3 - Exercise Physiology, Section 3.3. Ergometry," in *Human Physiology in Extreme Environments (Second Edition)*, Academic Press, 2021.

[11] G. P. Kenny, S. R. Notley and D. Gagnon, "Direct Calorimetry: a brief historical review of its use in the study of human metabolism and thermoregulation," *European Journal of Applied Physiology,* vol. 117, pp. 1765-1785, 2017.

[12] C. B. Scott, "Contributions of anaerobic energy expenditure to whole body thermogenesis," *Nutrition and Metabolism,* vol. 2, no. 1, 2005.

[13] F. D. Reardon, K. E. Leppik, R. Wegmann, P. Webb, M. B. Ducharme and G. P. Kenny, "The Snellen human calorimeter revisited, re-engineered and upgraded: design and

performance characteristics," *Medical & Biological Engineering & Computing,* vol. 44, no. 8, pp. 721-728, 2006.

[14] G. Ettema and H. W. Loras, "Efficiency in cycling: a review," *European Journal of Applied Physiology,* vol. 106, pp. 1-14, 2009.

[15] A. Hedge, "Thermal Regulation," Cornell University, 2015. [Online]. Available: https://ergo.human.cornell.edu/studentdownloads/DEA3500notes/Thermal/thregnotes.html. [Accessed 15 June 2022].

[16] D. Quintela, A. Gaspar and C. Borges, "Analysis of sensible heat exchanges from a thermal manikin," *European Journal of Applied Physiology,* vol. 92, pp. 663-668, 2004.

[17] J. H. Lienhard IV and V. J. H. Lienhard, A Heat Transfer Textbook, Cambridge, MA: Phlogiston Press, 2020.

[18] D. Mitchell, C. H. Wyndham, A. J. Vermeulen, T. Hodgson, A. R. Atkins and H. S. Hofmeyr, "Radiant and convective heat transfer of nude men in dry air," *Journal of Applied Physiology,* vol. 26, pp. 111-118, 1969.

[19] ASHRAE, "Chapter 9. Thermal Comfort," in *ASHRAE Handbook - Fundamentals*, Atlanta, GA, 2009.

[20] D. N. Sorenson and L. K. Voigt, "Modelling flow and heat transfer around a seated human body by computational fluid dynamics," *Building and Environment,* vol. 38, pp. 753-762, 2003.

[21] J. A. J. Stolwijk, "A mathematical model of physiological temperature regulation in man," National Aeronautics and Space Administration, Yale University, New Haven, CT, 1971.

[22] M. Manabe, H. Yamazaki and K. Sakai, "Shape factor simulation for the thermal radiation environment of the human body and the VRML visualization," *Building and Environment,* vol. 39, no. 8, pp. 927-937, 2004.

[23] M. Ichihara, M. Saitou, S. Tanabe and M. Nishimura, "Measurement of convective heat transfer coefficient and radiative heat transfer coefficient of standing human body by using thermal manikin," *Proceedings of the Annual Meeting of the Architectural Institute of Japan,* pp. 379-380, 1995.

[24] R. J. de Dear, E. Arens, Z. Hui and M. Oguro, "Convective and radiative heat transfer coefficients for individual human body segments," *International Journal of Biometeorology,* vol. 40, pp. 141-153, 1997.

[25] D. R. Williams, "Sun Fact Sheet," NASA, 2018. [Online]. Available: https://nssdc.gsfc.nasa.gov/planetary/factsheet/sunfact.html. [Accessed 2022].

[26] O. Coddington, J. L. Lean, P. Pilewskie, M. Snow and D. Lindholm, "A Solar Irradiance Climate Data Record," *Bulletin of the American Meteorological Society,* vol. 97, no. 7, pp. 1265-1282, 2016.

[27] "Solar Irradiance," Alternative Energy Turotials, 2019. [Online]. Available: https://www.alternative-energy-tutorials.com/solar-power/solar-irradiance.html. [Accessed 07 08 2022].

[28] D. Fiala, K. J. Lomas and M. Stohrer, "A computer model of human thermoregulation for a wide range of environmental conditions: the passive system," *Journal of Applied Physiology,* vol. 87, no. 5, pp. 1957-1972, 1999.

[29] Y. Kurazumi, T. Sakoi and A. Nyilas, "The Influence of the Solar Radiation Absoptivity up on the Outdoor Thermal Environmental Evaluation Index and the Thermal Sensory Perceptions," *American Journal of Climate Change,* vol. 7, no. 2, pp. 204-217, 2018.

[30] M. Oguro, E. Arens, H. Zhang, K. Tsuzuki and T. Katayama, "Measurement of Projected Area Factors for Thermal Radiation Analysis on Each Part of the Human Body," *Journal of Architechture, Planning, and Environmental Engineering,* vol. 547, pp. 17-25, 2001.

[31] K. Kubaha, D. Fiala, J. Toftum and A. H. Taki, "Human projected area factors for detailed direct and diffuse solar radiation analysis," *International Journal of Biometeorology,* vol. 49, pp. 113-129, 2004.

[32] A. V. M. Oliviera, A. R. Gaspar, S. C. Francisco and D. A. Quintela, "Analysis of natural and forced convection heat losses from a thermal manikin: Comparative assessment of the static and dynamic postures," *Journal of Wind Engineering and Industrial Aerodynamics,* vol. 132, pp. 66-76, 2014.

[33] Y. Nishi and A. P. Gagge, "Direct evaluation of convective heat transfer coefficient by napthalene sublimation," *Journal of Applied Physiology,* vol. 29, no. 6, pp. 830-838, 1970.

[34] H. Ho and L. Jones, "Thermal Model for Hand-Object Interactions," in *14th Symposium on Haptic Interfaces for Virtual and Teleoperator Systems*, Alexandria, VA, 2006.

[35] M. Yovanovich, J. Culham and P. Teertstra, "Calculating interface resistance," 2004.

[36] M. Torii, "Maximal sweating rate in humans," *Journal of Human Ergology,* vol. 24, no. 2, pp. 137-152, 1995.

[37] J. W. McCutchen and C. L. Taylor, "Respiratory heat exchange with varying temperature and humidity of inspired air," *Journal of Applied Physiology,* vol. 4, pp. 121-135, 1951.

[38] P. O. Fanger, Thermal Comfort, Copenhagen: Danish Technical Press, 1970.

[39] P. Astrand and R. K, Textbook of work physiology, New York: McGraw-Hill, 1970.

[40] "Tissue Properties: Thermal Conductivity," ITIS Foundation, 2022. [Online]. Available: https://itis.swiss/virtual-population/tissue-properties/database/thermal-conductivity/. [Accessed 19 06 2022].

[41] University of Minnesota, "Altlas of Human Cardiac Anatomy: Blood Vessels," University of Minnesota, 2021. [Online]. Available: http://www.vhlab.umn.edu/atlas/physiology-tutorial/blood-vessels.shtml#:~:text=They%2C%20in%20turn%2C%20branch%20into,in%20the%20average%20human%20body).. [Accessed 18 06 2022].

[42] J. C. Chato, "Heat Transfer to Blood Vessels," *Journal of Biomedical Engineering,* vol. 102, no. 2, pp. 110-118, 1980.

[43] H. H. Pennes, "Analysis of Tissue and Arterial Blood Temperatures in the Resting Human Forearm," *Journal of Applied Physiology,* vol. 1, no. 2, pp. 93-122, 1948.

[44] Wissler, "Pennes 1948 Paper revisited," *Journal of Applied Physiology,* vol. 85, no. 1, pp. 35-41, 1998.

[45] M. N. Sawka, C. B. Wenger, A. J. Young and K. B. Pandolf, "Physiological Responses to Exercise in the Heat," in *Nutritional Needs in Hot Environments: Applications for Military Personnel in Field Operations*, Washington, DC, US Institute of Medicine Committee on MIlitary Nuttrition Research, 1993.

[46] A. S. Perrotta, N. J. Held and D. E. R. Warburton, "The Effect of Heat Stress of Health and Performance," *Health and Fitness Journal of Canada,* vol. 9, no. 4, pp. 3-17, 2016.

[47] Centers for Disease Control and Prevention, "Heat Stress -- Heat Related Illness," National Institute for Occupantional Safety and Health (NIOSH), 6 June 2018. [Online]. Available: https://www.cdc.gov/niosh/topics/heatstress/heatrelillness.html#:~:text=It%20occurs%20when%20the%20body,within%2010%20to%2015%20minutes. [Accessed 30 March 2022].

[48] S. A. Arngrimsson, D. J. Stewart, F. Borrani, K. A. Skinner and K. J. Cureton, "Relation of heart rate to percent VO2 peak during submaximal exercise in the heat," *Journal of Applied Physiology,* vol. 94, no. 3, pp. 1162-1168, 2003.

[49] J. Gonzalez-Alonso and J. A. L. Calbet, "Reductions in systemic and skeletal muscle blood flow and oxygen delivery limit maximal aerobic capacity in humans," *Circulation,* vol. 107, no. 6, pp. 824-830, 2003.

[50] K. Klausen, D. B. Dill, E. E. Phillips Jr. and D. McGregor, "Metabolic reaction to work in the desert," *Journal of Applied Physiology,* vol. 22, no. 2, pp. 292-296, 1967.

[51] A. J. Lafrenz, J. E. Wingo, M. S. Ganio and C. K. J, "Effect of ambient temperatyre on cardiovascular drift and maximal oxygen uptake," *Medicine and Science in Sports and Exercise,* vol. 40, no. 6, pp. 1065-1071, 2008.

[52] S. Lorenzo, J. R. Halliwill, M. N. Sawka and C. T. Minson, "Heat acclimation imprives exercise performance," *Journal of Applied Physiology,* vol. 109, no. 4, pp. 1140-1147, 2010.

[53] L. Nybo, T. Jensen, N. B and G.-A. J, "Effects of marked hyperthermia with and without dehydration on VO(2) kinetics during intense exercise," *Journal of Applied Physiology,* vol. 90, no. 3, pp. 1057-1064, 2001.

[54] F. Pirnay, R. Deroanne and J. M. Petit, "Maximal oxygen consumption in a hot environment," *Journal of Applied Physiology,* vol. 28, no. 5, pp. 642-645, 1970.

[55] L. B. Rowell, G. L. Brengelamann, J. A. Murray, K. K. Kraning II and K. F, "Human metabolic responses to hyperthermia during mild to maximal exercise," *Journal of Applied Physiology,* vol. 26, no. 4, pp. 395-402, 1969.

[56] M. N. Sawka, A. J. Young, B. S. Cadarette, L. L and K. B. Pandolf, "Influence of heat stress and acclimation on maximal aerobic power," *Erupean Journal of Applied Physiology and Occupational Physiology,* vol. 53, no. 4, pp. 294-298, 1985.

[57] C. G. Williams, G. A. G. Bredell, C. H. Wybndham, N. B. Strydom, J. F. Morrison, J. Peter, P. W. Fleming and J. S. Ward, "Circulatory and metabolic reactions to work in heat," *Journal of Applied Physiology,* vol. 17, no. 4, pp. 625-638, 1962.

[58] J. E. Wingo, A. J. Lafrenz, G. M. S, E. G. L and C. K. J, "Cardiovascular Drift is related to reduced maximal oxygen uptake during heat stress," *Medicine and Science in Sports and Exercise,* vol. 37, no. 2, pp. 248-255, 2005.

[59] N. Altareki, B. Drust, G. Atkinson, T. Cable and W. Gregson, "Effects of environemtnal heat stress (35 degrees C) with simulated air movements on the thermoregulatory responses during a 4-km cycling time trial," *International Journal of Sports Medicine,* vol. 30, no. 1, pp. 9-15, 2009.

[60] R. Bannister and C. J, "The effect of changes in environmental temperature upon body temperature and performance during strenuous exercise," *Journal of Physiology,* vol. 142, pp. 60-62, 1959.

[61] B. Dill, H. Edwards, P. Bauer and B. Levensen, "Physical Performance in relation to external temperature," *Arbeitsphysiology,* vol. 3, pp. 508-518, 1931.

[62] B. R. Ely, S. N. Cheuvront, R. W. Kenefick and M. N. Sawka, "Aerobic performance is degraded, despite modest hyperthermia, in hot environments," *Medical Science of Sports Exercise,* vol. 42, pp. 135-141, 2010.

[63] S. D. Galloway and R. J. Maughan, "Effects of ambient temprature on the capacity to perform prolonged cycle exercise in man," *Medicine and Science in Sports and Exercise,* vol. 29, no. 9, pp. 1240-1249, 1997.

[64] J. Gonzalez-Alonzo, C. Teller, S. L. Anderson, F. B. Jensen, T. Hyldig and B. Nielsen, "Influence of body temperature on the development of fatigue during prolonged exercise in the heat," *Journal of Applied Physiology,* vol. 86, pp. 1032-1039, 1999.

[65] J. D. MacDougall, W. G. Reddan, C. R. Layton and D. J. A, "Effects of metabolic hyperthermia on performance during heavy prolonged exercise," *Journal of Applied Physiology,* vol. 36, no. 5, pp. 538-544, 1974.

[66] J. D. Periard, M. N. Cramer, P. G. Chapman, C. Caillaud and M. W. Thompson, "Cardiovascular strain impairs prologued self-paced exercise in the heat," *Experimental Physiology,* vol. 96, pp. 134-144, 2011.

[67] B. Roelands, H. Hiroshi, P. Watson, M. F. Piacentini, L. Buyse, G. De Schutter and R. R. Meeusen, "The Effects of Acute Dopamine Reuptake Inhibition on Performance," *Medicine and Science in Sports and Exercise,* vol. 40, no. 5, pp. 879-885, 2008.

[68] A. J. Tatterson, A. G. Hahn, D. T. Martin and M. A. Febbraio, "Effects of heat stress on physiological responses and exercise performance in elite cyclists," *Journal of Science and Medicine in Sport,* vol. 3, no. 2, pp. 186-193, 2000.

[69] R. Tucker, L. Rauch, Y. X. R. Harley and T. D. Noakes, "Impaired exercise performance in the heat is associated with an anticipatory reduction in skeletal muscle recruitment," *Pflugers Archive,* vol. 448, no. 4, pp. 422-430, 2004.

[70] C. Tyler and C. Sunderland, "The effect of ambient temperature on the reliability of a preloaded treadmill time-trial," *International Journal of Sports Medicine,* vol. 29, no. 10, pp. 812-816, 2008.

[71] P. Watson, H. Hasegawa, B. Roelands, M. F. Piacentini, R. Looverie and R. Meeusen, "Acute dopamine/noradrenaline reuptake inhibition anhances human exercise performance in watm, but not temperate conditions," *Journal of Physiology,* vol. 565, no. 3, pp. 873-883, 2005.

[72] C. L. Benjamin, Y. Sekiguchi, L. A. Fry and D. J. Casa, "Perfromance Changes Following Heat Acclimation and the Factors That Influence These Changes: Meta-Analysis and Meta-Regression," *Frontiers in Physiology,* vol. 10, 2019.

[73] M. Waldron, R. Fowler, S. Heffernan, J. Tallent, L. Kilduff and O. Jeffries, "Effects of Heat Acclimation and Acclimatisation on Maximal Aerobic Capacity Compared to Exercise Alone in Both Thermoneutral and Hot Environemtns: A Meta-Analysis and Meta-Regression," *Sports Medicine,* vol. 51, pp. 1509-1525, 2021.

[74] S. Racinais, J. D. Périard, A. Karlsen and L. Nybo, "Effect of Heat and Heat Acclimatization on Cycling Time Trial Performance and Pacing," *Medicine and Science in Sports and Exercise,* pp. 601-606, 2014.

[75] M. R. Ely, S. N. Cheuvront, W. O. Roberts and S. J. Montain, "Impact of weather on marathon-running performance," *Medicine and Science in Sports and Exercise,* vol. 39, pp. 487-493, 2007.

[76] J. G. Guy, G. B. D. Deakin, A. M. Edwards, C. M. Miller and D. Pyne, "Adaptation to hot environmental conditions: an exploration of the perfromance basis, procedures and future direction to optimise opportunities for elite athletes," *Sports Medicine,* vol. 45, no. 3, pp. 303-311, 2015.

[77] K. T. Ozgunen, S. S. Kurdak, R. J. Maughan, C. Zeren, S. Korkmaz, Z. Yazici, G. Ersoz, S. M. Shirreffs, M. S. Binnet and J. Dvorak, "Effect of hot environmental conditions on physical activity patterns and temperature response of football players," *Scandiniavian Journal of Medicine & Science in Sports,* vol. 20, no. 3, pp. 140-147, 2010.

[78] M. Mohr, L. Nybo, J. Granthan and S. Racinais, "Physiological Resonses and Physical Performance During Football in the Heat," *PLoS Once,* vol. 7, no. 6, p. e39202, 2012.

[79] G. P. Nassis, J. Brito, J. Dvorak, H. Chalabi and S. Racinais, "The association of environmental heat stress with performance: analysis of the 2014 FIFA World Cup Brazil," *British Journal of Sports Medicine,* vol. 49, no. 9, pp. 609-613, 2015.

[80] R. J. Aughey, C. A. Goodman and M. J. Mckenna, "Greater chance of high core temperatures with modified pacing strategy during team sport in the heat," *Journal of Science and Medicine in Sport,* vol. 17, no. 1, pp. 113-118, 2014.

[81] Douglas College Biology Department, "Unit 7: Cellular Respiration and Energy Metabolism," in *Douglas College Human Anatomy & Physiology II (2nd ed.)*, Pressbooks, 2019.

[82] L. B. Rowell, "Regulation during physical stress," in *Human Circulation*, New York, Oxford University Press, 1986, pp. 363-406.

[83] L. B. Rowell, H. J. Marx, R. A. Bruce, R. D. Conn and F. Kusumi, "Reductions in cardiac output, central blood volume, and stroke volume with thermal stress in normal men during exercise," *Journal of Clinical Invesitation,* vol. 45, pp. 1801-1816, 1966.

[84] J. Gonzalez-Alonso, C. G. Crandall and J. M. Johnson, "The cardiovascular challenge of exercising in the heat," *Journal of Physiology,* vol. 586, pp. 45-53, 2008.

[85] E. J. Stohr, J. Gonzalez-Alonso, J. Pearson, D. A. Low, L. Ali, H. Barker and R. Shave, "Effects of graded heat stress on global left ventricular function and twist mechanics at rest and during exercise in healthy humans," *Experimental Physiology,* vol. 96, pp. 114-125, 2011.

[86] M. N. Sawka, R. P. Young, R. Francesconi, S. R. Muza and P. K. B, "Thermoregulatory and blood responses during exercise at graded hypohydration levels," *Journal of Applied Physiology,* vol. 59, pp. 1394-1401, 1985.

[87] J. Gonzalez-Alonso, J. A. Calbet and B. Nielsen, "Muscle blood flow is reduced with dehydration during proloned exercise in humans," *Journal of Physiology,* vol. 513, no. 3, pp. 895-905, 1998.

[88] J. Gonzalez-Alonso, R. Mora-Rodriguez, P. R. Below and E. F. Coyle, "Dehydration markedly impairs cardiovascular function in hyperthermic endurance athletes during exercise," *Journal of Applied Physiology,* vol. 82, pp. 1229-1236, 1997.

[89] B. Nielsen, J. R. Hales, S. Strange, N. J. Christensen, J. Warberg and B. Saltin, "Human circulatory and thermoregulatory adaptations with heat acclimation and exercise in a hot, dry environment," *Journal of Physiology,* vol. 460, no. 1, pp. 467-485, 1993.

[90] B. Nielsen, G. Savard, E. A. Richter, M. Hargreaves and B. Saltin, "Muscle blood flow and muscle metabolism during exercise and heat stress," *Journal of Applied Physiology,* vol. 69, no. 3, pp. 1040-1046, 1990.

[91] G. K. Savard, B. Nielsen, J. Laszczynska, B. E. Larsen and S. B., "Muscle blood flow is not reduced in humans during modrate exercise and heat stress," *Journal of Applied Physiology,* vol. 64, no. 2, pp. 649-657, 1988.

[92] F. Lee and E. Scott, "The action of temperature and humidity on the working power of muscles and on the sugar of the blood," *American Journal of Physiology,* vol. 40, pp. 486-501, 1916.

[93] L. Nybo and B. Nielsen, "Hyperthermia and central fatigue during prolongued exercise in humans," *Journal of Applied Physiology,* vol. 91, pp. 1055-1060, 2001.

[94] G. Todd, J. E. Butler, J. L. Taylor and S. C. Gandevia, "Hyperthermia: A failure of the motor cortex and the muscle," *Journal of Physiology,* vol. 563, pp. 621-631, 2005.

[95] S. Morrison, G. G. Sleivert and S. S. Cheung, "Passive Hyperthermia reduces voluntary activation and isometric force production," *European Journal of Applied Physiology,* vol. 91, pp. 729-736, 2004.

[96] M. M. Thomas, S. S. Cheung, G. C. Elder and G. G. Sleivert, "Voluntary muscle activation is impaired by core temperature rather than local muscle temperature," *Journal of Applied Physiology,* vol. 100, pp. 1361-1369, 2006.

[97] L. Nybo and N. H. Secher, "Cerebral perturbations provoked by prolonged exercise," *Progressive Neurobiology,* vol. 72, pp. 223-261, 2004.

[98] L. Nybo, "Hyperthermia and fatigue," *Journal of Applied Physiology,* vol. 104, pp. 871-878, 2008.

[99] L. E. Armstrong, R. W. Hubbard, B. H. Jones and J. T. Daniels, "Preparing Alberto Salazar for the heat of the 1984 Olympic Marathon," *Physiology & Spotrs Medicine,* vol. 14, pp. 73-81, 1986.

[100] B. R. Ely, M. R. Ely, S. N. Cheuvront, R. W. Kenefick, D. W. Degroot and M. S. J., "Evidence against a 40 degrees C core temperature threshold for fatigue in humans," *Journal of Applied Physiology,* vol. 107, pp. 1519-1525, 2009.

[101] M. Caputa, G. Feistkorn and C. Jessen, "Effect of brain and trunk temperatures on exercise performance in goats," *Pflugers Archive of Physiology,* vol. 406, pp. 184-189, 1986.

[102] M. D. White, "Components and mechanisms of thermal hyperpnea," *Journal of Apllied Physiology,* vol. 101, pp. 655-663, 2006.

[103] J. Van Cutsem, B. Roelands, K. De Pauw, R. Meeusen and S. Marcora, "Subjective thermal strain impairs endurance performance in a temperate environment," *Physiology and Behaviour,* vol. 202, pp. 36-44, 2019.

[104] G. A. Brooks, K. J. Hittelman, J. A. Faulkner and R. E. Beyer, "Temperature, skeletal muscle mitochondrial functions and oxygen debt," *American Journal of Physiology,* vol. 220, pp. 1053-1059, 1971.

[105] W. T. Willis and M. R. Jackman, "Mitochondrial function during heavy exercise," *Medicine and Science in Sport and Exercise,* vol. 26, pp. 1347-1354, 1994.

[106] A. J. Young, M. N. Sawka, L. Levine, B. S. Cadarette and K. B. Pandolf, "Skeletal muscle metabolism during exercise is influenced by heat acclimation," *Journal of Applied Physiology,* vol. 59, pp. 1926-1935, 1985.

[107] S. Lorenzo, J. R. Halliwill, M. N. Sawka and C. T. Minson, "Heat acclimation improves exercise performance," *Journal of Applied Physiology,* vol. 109, no. 4, pp. 1140-1147, 2010.

[108] O. R. Gibson, C. A. James, J. A. Mee, A. G. B. Willmott, G. Turner, M. Hayes and N. S. Maxwell, "Heat alleviation strategies for athletic performance: A review and practitioner guidelines," *Temperature,* vol. 7, no. 1, pp. 3-36, 2020.

[109] D. R. Bolster, S. W. Trappe, K. R. Short, M. Scheffield-Moore, A. C. Parcell, K. M. Schulze and D. L. Costill, "Effects of precooling on thermoregulation during subsequent exercise," *Medicine and Science in Sports and Exercise,* vol. 31, no. 2, pp. 251-257, 1999.

[110] G. Ferretti, "Cold and muscle performance," *International Journal of Sports Medicine,* vol. 13, no. S1, pp. 185-187, 1992.

[111] E. H. Wissler, Human Temperature Control: A Quantitative Approach, Berlin: Springer, 2018.

[112] B. K. Alba, J. W. Castellani and N. Charkoudian, "Cold-induced cutaneous vasoconstriction in humans: Function, dysfunction and the distinctly countrerproductive," *Experimental Physiology,* vol. 104, pp. 1202-1214, 2019.

[113] D. J. Casa, G. P. Kenny and N. A. Taylor, "Immersion Treatment for Exertional Hyperthermia: Cold or Temperate Water," *Medicine and Science in Sports and Exercise,* vol. 42, pp. 1246-1252, 2010.

[114] N. A. S. Taylor, J. N. Caldwell, A. M. J. Van den Huevel and M. J. Patterson, "To cool, but not too cool: that is the questino -- immersion cooling for hyperthermia," *Medicine and Science in Sports and Exercise,* vol. 40, no. 11, pp. 1962-1969, 2008.

[115] M. Bahrami, "Forced Convection Heat Transfer," in *Engineering Thermodynamics and Heat Transfer*, Victoria, Simon Fraser University, 2009.

[116] Engineering Toolbox, "Convective Heat Transfer," Engineering Toolbox, 2003. [Online]. Available: https://www.engineeringtoolbox.com/convective-heat-transfer-d_430.html. [Accessed 20 05 2022].

[117] Y. Nishi and A. P. Gagge, "Moisture Permeation of Clothing: A Factor Governing Thermal Equilibrium and Comfort," *ASHRAE Transactions,* vol. 76, no. 1, pp. 137-145, 1973.

[118] C. J. Stevens, B. Dascombe, A. Boyko, D. Sculley and R. Callister, "Ice slurry ingestion during cycling improves Olympic distance triathlon performance in the heat," *Journal of Sports Sciences,* vol. 31, no. 12, pp. 1271-1279, 2013.

[119] P. C. Castle, A. L. Macdonald, A. Philp, A. Webborn, P. W. Watt and N. S. Maxwell, "Precooling leg muscle improves intermittent sprint exercise performance in hot, humid conditions," *Journal of Applied Physiology,* vol. 100, no. 4, pp. 1377-1384, 2006.

[120] G. M. Minett, R. Duffield, F. E. Marino and M. Portus, "Volume-dependant response of precooling for intermittent-sprint exercise in the heat," *Medicine and Science in Sports and Exercise,* vol. 43, no. 9, pp. 1760-1769, 2011.

[121] S. A. Arngrimsson, D. S. Petitt, M. G. Stueck, D. K. Jorgensen and K. J. Cureton, "Cooling vest worn during active warm-up improves 5-km run performance in the heat," *Journal of Applied Physiology,* vol. 96, no. 5, pp. 1867-1874, 2004.

[122] R. Duffield, B. Dawson, D. Bishop, M. Fitzsimons and S. Lawrence, "Effect of wearing an ice cooling jacket on repeat sprint performance in warm/humid conditinos," *British Journal of Sports Medicine,* vol. 37, pp. 164-169, 2003.

[123] R. Duffield and F. E. Marino, "Effects of pre-cooling procedures on intermittent-sprint exercise performance in warm conditions," *European Journal of Applied Physiology,* vol. 100, no. 6, pp. 727-735, 2007.

[124] M. J. Quod, D. T. Martin, P. B. Laursen, A. S. Gardner, S. L. Halson, F. E. Marino, M. P. Tate, D. E. Mainwaring, C. J. Gore and A. G. Hahn, "Practical precooling: effect on cycling time

trial performance in warm conditions," *Journal of Sports Science,* vol. 26, no. 14, pp. 1477-1487, 2008.

[125] S. Uckert and W. Joch, "Effects of warm-up and precooling on endurance performance int he heat," *British Journal of Sports Medicine,* vol. 41, no. 6, pp. 380-384, 2007.

[126] C. A. Burdon, M. W. Hoon, N. A. Johnson, P. G. Chapman and H. T. O'Conner, "The effect of ice slushy ingestion and moutwash on thermoregulation and endurance performance in the heat," *International Journal of Sport Nutrition and Exercise Metabolism,* vol. 23, no. 5, pp. 458-469, 2013.

[127] C. Byrne, C. Owen, A. Cosnefroy and J. K. W. Lee, "Self-paced exercise performance in the heat after pre-exercise cold-fluid ingestion," *Journal of Athletic Training,* vol. 46, no. 6, pp. 592-599, 2011.

[128] M. Ihsan, G. Landers, M. Brearley and P. Peeling, "Beneficial Effects of Ice Ingestion as a Precooling Strategy on 40-km Cycling Time-Trial Performance," *Internation Journal of Sports Physiology and Performance,* vol. 5, no. 2, pp. 140-151, 2010.

[129] R. Siegel, J. Maté, G. Watson, K. Nosaka and P. B. Laursen, "Pre-cooling with ice slurry ingestion leads to similar run times to exhaustion in the heat as cold water immersion," *Journal of Sports Sciences,* vol. 30, no. 2, pp. 155-165, 2012.

[130] J. Stanley, M. Leveritt and J. M. Peake, "Thermoregulatory responses to ice-slush beverage ingestion and exercise in the heat," *European Journal of Applied Physiology,* vol. 110, no. 6, pp. 1163-1173, 2010.

[131] C. J. Stevens, B. Dascombe, A. Boyko, D. Sculley and R. Callister, "Ice slurry ingestion during cycling improves Olympic distance triathlon performance in the heat," *Journal of Sport Science,* vol. 31, no. 12, pp. 1271-1279, 2013.

[132] J. D. Cotter, G. G. Sleivert, W. S. Roberts and M. A. Febbraio, "Effect of pre-cooling, with and without thigh cooling, on strain and endurance exercise performance in the heat," *Comparative Biochemistru and Physiology Part A: Molecular & Integrative Physiology,* vol. 128, no. 4, pp. 667-677, 2001.

[133] R. Duffield, G. Steinbacher and T. J. Fairchild, "The use of mixed-method, part-body pre-cooling procedures for team-sport athletes training in the heat," *Journal of Strength and Conditioning Research,* vol. 23, no. 9, pp. 2524-2532, 2009.

[134] R. Duffield, A. J. Coutts, A. McCall and D. Burgess, "Pre-cooling for football training and competition in hot and humid conditions," *European Journal of Sports Science,* vol. 13, no. 1, pp. 1-10, 2011.

[135] G. M. Minett, R. Duffield, F. E. Marino and M. Portus, "Duration-dependant response of mixed-method pre-cooling for intermittent-sprint exercise in the heat," *European Journal of Applied Physiology,* vol. 112, no. 10, pp. 3655-3666, 2012.

[136] R. Duffield, R. Green, P. Castle and N. Maxwell, "Precooling can prevent the reduction of self-paced exercise intensity in the heat," *Medicine and Science in Sports and Exercise,* vol. 42, no. 3, pp. 577-584, 2010.

[137] D. Kay, D. R. Taaffe and F. E. Marino, "Whole-body pre-cooling and heat storage during self-paced cycling performance in warm humid conditions," *Journal of Sports Sciences,* vol. 17, no. 12, pp. 937-944, 1999.

[138] M. Skein, R. Duffield, J. Cannon and F. E. Marino, "Self-paced intermittent-sprint performance and pacing strategies following respective pre-cooling and heating," *European Journal of Applied Physiology,* vol. 112, no. 1, pp. 253-266, 2012.

[139] A. R. Hsu, T. A. Hagobian, K. A. Jacobs, K. A. Attallah and A. L. Friedlander, "Effects of heat removal through the hand on metabolism and performance during cycling exercise in the heat," *Canadian Journal of Applied Physiology,* vol. 30, no. 1, pp. 87-104, 2005.

[140] A. Minniti, C. J. Tyler and C. Sunderland, "Effects of a cooling collar on affect, ratings of perceived exertion, and running performance in the heat," *European Journal of Sports Sciences,* vol. 11, no. 6, pp. 419-429, 2011.

[141] C. M. Scheadler, N. W. Saunders, N. J. Hanson and S. T. Devor, "Palm cooling does not improve running performance," *International Journal of Sports Medicine,* vol. 34, no. 8, pp. 732-735, 2013.

[142] C. J. Tyler, P. Wild and C. Sunderland, "Practical neck cooling and time-trial running performance in a hot environment," *European Journal of Applied Physiology,* vol. 110, no. 5, pp. 1063-1074, 2010.

[143] C. J. Tyler and C. Sunderland, "Cooling the Neck Region During Exercise in the Heat," *Journal of Athletic Training,* vol. 46, no. 1, pp. 61-68, 2011.

[144] C. J. Tyler and C. Sunderland, "Neck cooling and running performance in the heat: single versus repeated application," *Medicine and Science in Sports and Exercise,* vol. 43, no. 12, pp. 2388-2395, 2011.

[145] M. J. Luomala, J. Oksa, J. A. Salmi, V. Linnamo, I. Holmer, J. Smolander and B. Dugue, "Adding a cooling vest during cycling improves performance in warm and humid conditions," *Journal of Thermal Biology,* vol. 37, no. 1, pp. 47-55, 2012.

[146] T. Mundel, J. King, E. Collacott and D. A. Jones, "Drink temperature influences fluid intake and endurance capacity in men during exercise in a hot, dry environment," *Experimental Physiology,* vol. 91, no. 5, pp. 925-933, 2006.

[147] L. Ansley, G. Marvin, A. Sharma, M. J. Kendall and D. A. Jones, "The effects of head cooling on endurance and neuroendocrine responses to exercise in warm conditions," *Physiological Research,* vol. 57, no. 6, pp. 863-872, 2008.

[148] M. V. De Carvalho, M. T. De Andrade, G. P. Ramos, A. Maia-Lima, E. R. Pereira, T. T. Mendes, J. C. Marins, F. T. Amorim and E. Silami-Garcia, "The temperature of water ingested ad libitum does not influence performance during a 40-km self-paced cycling trial," *Journal of Sports Medicine and Physical Fitness,* vol. 55, no. 12, pp. 1473-1479, 2015.

[149] S. A. Cuttell, V. Kiri and C. Tyler, "A Comparison of 2 Practical Cooling Methods on Cycling Capacity in the Heat," *Journal of Athletic Training,* vol. 51, no. 7, pp. 525-532, 2016.

[150] Z. J. Schlader, S. E. Simmons, S. R. Stannard and T. Mundel, "The independant roles of temperature and thermal perception int he control of human thermoregulatory behaviour," *Physiology & Behaviour,* vol. 103, no. 2, pp. 217-224, 2011.

[151] C. J. Stevens, A. Kittel, D. V. Sculley, R. Callister, L. Taylor and B. J. Dascombe, "Running performance in the heat is improved by similar magnitude with pre-exercise cold-water immersion and mid-exercise facial water spray," *Journal of Sports Sciences,* vol. 35, no. 8, pp. 798-805, 2017.

[152] L. P. J. Teunissen, A. de Haan, J. J. de Koning and H. A. M. Daanen, "Effects of wind applicatoni on thermal perception and self-paced performance," *European Journal of Applied Physiology,* vol. 113, pp. 1705-1717, 2013.

[153] A. D. Ruddock, G. A. Tew and A. J. Purvis, "Effect of hand cooling on body temperature, cardiovascular and perceptual responses during recumbent cycling in a hot environment," *Journal of Sports Sciences,* vol. 35, no. 14, pp. 1466-1474, 2017.

[154] G. A. Khomenok, A. Hadid, O. Preiss-Bloom, R. Yanovich, T. Erlich, O. Ron-Tal, A. Peled, Y. Epstein and D. S. Moran, "Hand immerion in cold water alleviating physiological strain and increasing tolerance to uncompensable heat stress," *European Journal of Applied Physiology,* vol. 104, no. 2, pp. 303-309, 2008.

[155] T. Yoshida, H. Shin-ya, S. Nakai, H. Ishii and H. Tsuneoka, "The effect of water-perfused suits and vests on body cooling during exercise in a hot environment," *Elsevier Ergonomics Book Series,* vol. 3, pp. 107-111, 2005.

[156] A. Sharma, V. V. Tyagi and D. Buddhi, "Review on thermal energy storage with phase change materials and applications," *Renewable and Sustainable Energy Reviews,* vol. 13, pp. 318-345, 2009.

[157] T. M. Eijsvogels, C. C. W. G. Bongers, M. T. W. Veltmeijer, M. H. Moen and M. Hopman, "Cooling during exercise in temperate conditions: impact on performance and thermoregulation," *International Journal of Sports Medicine,* vol. 35, no. 10, pp. 840-846, 2014.

[158] D. N. Pei, "What's inside an Ice Pack," National Capital Poison Center, 2020. [Online]. Available: https://www.poison.org/articles/whats-inside-ice-packs-201#:~:text=The%20gel%20beads%20in%20ice,are%20generally%20no%20longer%20available.. [Accessed 25 May 2022].

[159] G. P. Kenny and O. Jay, "Thermometry, calorimetry, and mean body temperature during heat stress," *Comprehensive Physiology,* vol. 3, no. 4, pp. 1689-1719, 2013.

[160] P. Flowers, K. Theopold, R. Langley and W. R. Robinson, Chemistry, Houston, Texas: OpenStax, 2019.

[161] "Latent Heat of Melting for some common Materials," Engineering Toolbox, 2003. [Online]. Available: https://www.engineeringtoolbox.com/latent-heat-melting-solids-d_96.html. [Accessed 28 May 2022].

[162] Mondal, "Phase change materials for smart textiles - An overview," *Applied Thermal Engineering,* vol. 28, pp. 1536-1550, 2008.

[163] S. L. Davey, B. J. Lee, M. Smith, M. Oldroyd and C. D. Thake, "Optimizing the Use of Phase CHnage Material Vests Worn During Explosives Ordnance Disposal Operations in Hot Conditions," *Frontiers in Physiology,* vol. 29, 2020.

[164] M. Trbovich, C. Ortega, J. Schroeder and M. Fredrickson, "Effect of a Cooling Vest on Core Temperature in Athletes With and Without Spinal Cord Injury," *Topics in Spinal Cord Injury Rehabilitation,* vol. 20, no. 1, pp. 70-80, 2014.

[165] "Water - Heat of Vaporization vs. Temperature," Engineering Toolbox, 2010. [Online]. Available: https://www.engineeringtoolbox.com/water-properties-d_1573.html. [Accessed 31 05 2022].

[166] A. Himmer, "Athletes to get spray-downs to beat searing Osaka heat," Reuters, 2007. [Online]. Available: https://www.reuters.com/article/us-athletics-world-heat-idUST27633720070824. [Accessed 30 May 2022].

[167] National Center for Biotechnology Information, "PubChem Compound Summary for CID 22985, Ammonium nitrate," PubChem, 2022. [Online]. Available: https://pubchem.ncbi.nlm.nih.gov/compound/Ammonium-nitrate. [Accessed 30 May 2022].

[168] Burton, "The Application of the Theory of Heat Flow to the Study of Energy Metabolism:," *Journal of Nutrition,* vol. 7, no. 5, pp. 497-533, 1934.

[169] H. Pennes, "Analysis of tissue and arterial blood temperatures in the resting human forearm," *Journal of Applied Physiology,* vol. 1, no. 2, pp. 93-122, 1948.

[170] E. H. Wissler, "Steady-State temperature distribution in man," *Journal of Applied Physiology,* vol. 16, pp. 734-740, 1961.

[171] P. O. Fanger, Thermal Comfort: Analysis and Applications in Environmental Engineering, vol. 92, Copenhagen: Danish Technical Press, 1970, p. 164.

[172] A. P. Gagge, J. A. J. Stolwijk and Y. Nishi, "An effective temperature scale based on a simple model of huma physiological regulatory response," *ASHRAE Transactions,* vol. 77, pp. 247-262, 1971.

[173] E. Wissler, "Mathematical Simulation of human thermal behaviour using whole body models," in *Heat transfer in medicine and biology*, New York, Plenum Press, 1985, pp. 325-373.

[174] D. Fiala, K. J. Lomas and M. Stohrer, "Computer predictin of human thermoregulatory and temperature responses to a wide range of environmental conditions," *International Journal of Biometeorology,* vol. 45, pp. 143-159, 2001.

[175] H. Zhang, C. Huizenga, E. Arens and T. Yu, "Considering Individual physiological differences in a human thermal model," *Journal of thermal biology,* vol. 26, pp. 401-408, 2001.

[176] C. Huizenga, H. Zhang and E. Arens, "A model of human physiology and comfort for assessing complex thermal environments," *Building Environment,* vol. 36, pp. 691-699, 2001.

[177] S. Tanabe, K. Kobayashi, J. Nakano and Y. Ozeki, "Evaluation of thermal comfort using combined multi-node thermoregulation (65MN) and radiation models and computational dynamics," *Energy Building,* vol. 34, pp. 637-646, 2002.

[178] B. R. M. Kingma, "Human thermoregulation: a synergy between physiology and mathematical modelling - PHD thesis," Maastricht University, 2012.

[179] B. Kingma, I. Schellen, J. H. Frijns and W. D. van Marken Lictenbelt, "Thermal Sensation: a mathematical model based on neurophysiology," *Indoor Air,* pp. 253-262, 2012.

[180] N. M. W. Severens, W. D. van Merken Lichtenbelt, A. J. H. Frijns, A. A. Van Steenhoven, B. A. J. M. de Mol and D. I. Sessler, "A model to predict patient temperature during cardiac surgery," *Physics in Medicine & Biology,* vol. 52, no. 17, pp. 5131-5145, 2007.

[181] D. Fiala, A. Psikuta, G. Jendriztky, S. Paulke, D. A. Nelson, W. D. van Marken Lichtenbelt and A. J. H. Frijns, "Physiological modeling for technical, clinical and research applications," *Frontiers in Bioscience ,* vol. 2, no. 3, pp. 939-968, 2010.

[182] D. Fiala and K. Lomas, "Application of a computer model predicting human thermal responses to the design of sports stadia," in *CIBSE National Conference Proceeding*, Harrogate, UK, 1999.

[183] P. Broede, G. Jendritzky, D. Fiala and G. Havenith, "The Universal Thermal Climaric Index UTCI in operational use," in *Windsor Conference on Thermal Comfort*, Windsor, UK, 2010.

[184] C. P. G. Roelofsen and V. P., "Improvement of the Stolwijk model with regard to clothing, thermal sensation and skin temperature," *Work,* vol. 54, pp. 1009-1024, 2016.

[185] M. Salloum, N. Ghaddar and K. Ghali, "A new transient bio-heat model of the human body," in *ASME Summer Heat Transfer Conference*, San Francisco, CA, 2005.

[186] M. Al-Othmani, N. Ghaddar and K. Ghali, "A multi-segmented human bioheat model for transient and asymmetric radiative environments," *International Journal of Heat and Mass Transfer,* vol. 51, pp. 5522-5533, 2008.

[187] A. P. Avilio, "Multi-brnached model of human arterial system," *Medical & Biological Engineering & Computing,* vol. 18, pp. 709-718, 1980.

[188] F. Mneimneh, N. Ghaddar, K. Ghali, I. Omeis and C. Moussalem, "An altered bioheat model for persons with cervical spinal cord injury," *Journal of Thermal BIology,* vol. 77, pp. 96-110, 2018.

[189] G. Havenith, "Individual model of human thermoregulation for the simulation of heat stress responses," *Journal of Applied Physiology,* vol. 90, pp. 1943-1954, 2001.

[190] L. W. D. Van Marken, A. J. H. Frijns, M. J. V. Ooijen, D. Fiala, A. M. Kester and A. A. V. Steenhoven, "Validation of an individualised model of human thermoregulation for predicting responses to cold air," *International Journal of Biometeorology,* vol. 51, pp. 169-179, 2006.

[191] S. Takada, T. Sakiyama and T. Matsushida, "Thermal model of human body fitted with individual characteristics of body temperature regulation," *Building Environment,* vol. 44, pp. 463-470, 2009.

[192] M. Yokota, L. G. Berglund and G. P. Bathalon, "Monte Carlo simulations of individual variability and their effects on simulated heat stress using thermoregulatory modeling," *Jounral of Thermal Biology,* vol. 35, pp. 154-159, 2010.

[193] M. S. Ferreira and J. I. Yanagihara, "A transient three-dimensional heat transfer model of the human body," *International Communications on Heat and Mass Transfer,* vol. 36, pp. 718-724, 2009.

[194] X. Sun, S. Eckels and Z. C. Zheng, "An improved thermal model of the human body," *HVAC&R Research,* vol. 18, no. 3, pp. 323-338, 2012.

[195] F. Li, Y. Wang and Y. Li, "A Transient 3-D Thermal Model for Clothed Human Body Considering More Real Geometry," *Journal of Computers,* vol. 8, no. 3, pp. 676-684, 2013.

[196] J. Werner and M. Buse, "Temperature profiles with respect to inhomogeneity and geometry of the human body," *Journal of Applied Physiology,* vol. 65, no. 3, pp. 1110-1118, 1988.

[197] Y. Tang, Y. He, H. Shao and C. Ji, "Assessment of comfortable clothing thermal resistance using a multi-scale human thermoregulatory model," *International Journal of Heat and Mass Transfer,* vol. 98, pp. 568-583, 2016.

[198] S. Mfolozi, A. Malan, T. Bello-Ochende and L. Martin, "Numeric Analysis of Temperature Distribution in Man using a 3D Human Model," 2018.

[199] M. P. Castellani, T. P. Rioux, J. W. Castellani, A. P. Potter and X. Xu, "A geomtrically accurate 3 dimensional model of human thermoregulation for transient cold and hot environments," *Computers in Biology and Medicine,* vol. 138, 2021.

[200] P. J. Gamage, L. V. Fortington and C. F. Finch, "Epidemiology of exertional heat illnesses in organised sports: A systematic review," *Journal of Science and Medicine in Sport,* vol. 23, no. 8, pp. 701-709, 2020.

[201] S. Racinais, J. M. Alonso, A. J. Coutts, A. D. Flouris, O. Girard, J. Gonzalez-Alonso, C. Hausswirth, O. Jay, J. K. Lee, N. Mitchell, G. P. Nassis, L. Nybo, B. M. R. B. Pluim, M. N. Sawka, J. Wingo and J. D. Periard, "Consensus recommendations on training and competing in the heat," *British Journal of Sports Medicine,* vol. 49, no. 18, pp. 1164-1173, 2015.

[202] H. Hasegawa, T. Takatori, T. Komura and M. Yamasaki, "Wearing a cooling jacket during exercise reduces thermal strain and improves endurance exercise performance in a warm environment," *Journal of Strength and Conditioning Research,* vol. 19, no. 1, pp. 122-128, 2005.

[203] F. T. Amorim, P. M. Yamada, R. A. Robergs and S. M. Schneider, "Palm cooling does not educe heat strain during exercise in a hot, dry environment," *Applied Physiology, Nutrition, and Metabolism,* vol. 35, pp. 480-489, 2010.

[204] D. DuBois and E. F. DuBois, "A formula to estimate the approximate surface area if height and weight be known," *Archives of Internal Medicine,* vol. 17, no. 6_2, pp. 863-871, 1916.

[205] N. B. Morris, M. N. Cramer, S. G. Hodder, G. Havenith and O. Jay, "A comparison between the technical absorbent and ventilated capsule methods for measureing local sweat rate," *Journal of Applied Physiology,* vol. 114, no. 6, pp. 816-823, 2013.

[206] Borg, "Psychophysical bases of perceived exertion," *Medicine and Science in Sports and Exercise,* vol. 14, pp. 377-381, 1982.

[207] N. R. S. Hollies, A. G. Custer, C. J. Morin and M. E. Howard, "A human perception analysis approach to clothing comfort," *Textile Research Journal,* vol. 49, no. 10, pp. 557-564, 1979.

[208] J. Ng, W. C. Dobbs and J. E. Wingo, "Effect of ice slurry ingestion on cardiovascular drift and VO2max during heat stress," *Medicine and Science in Sports and Exercise,* vol. 51, no. 3, pp. 582-589, 2019.

[209] J. E. Wingo and K. J. Cureton, "Body cooling attenuates the decrease in maximal oxygen uptake associated with cardiovascular drift during heat stress," *European Journal of Applied Physiology,* vol. 98, no. 1, pp. 97-104, 2006.

[210] Z. J. Schlader, S. E. Simmons, S. R. Stannard and T. Mundel, "Independent roles of temperature and thermal perception in the control of human thermoregulatory behaviour," *Physiology & Behaviour,* vol. 103, no. 2, pp. 217-224, 2011.

[211] J. Scherr, B. Wolfarth, J. W. Christle, A. Pressler, S. Wagenpfiel and M. Halle, "Associations between Borg's rating of percieved exertion and physiological measures of exercise intensity," *European Journal of Applied Physiology,* vol. 113, no. 1, pp. 147-155, 2013.

[212] C. R. Abbiss, J. J. Peiffer and P. B. Laursen, "Optimal cadence selection during cycling," *International SportMed Journal,* vol. 10, no. 1, pp. 1-15, 2009.

[213] K. B. Pandolf and B. J. Noble, "The effect of pedalling speed and resistance changes on percieved exertion for equivalent power outputs on the bicycle ergometer," *Medicine and Science in Sports and Exercise,* vol. 5, no. 2, pp. 132-136, 1973.

[214] R. A. Ferguson, D. Ball, P. Krustup, P. Aagaard, M. Kjaer, A. J. Sargeant, Y. Hellston and J. Bangsbo, "Muscle oxygen uptake and energy turnover during dynamic exercise at different contraction frequencies in humans," *The Journal of Physiology,* vol. 536, no. 1, pp. 261-271, 2001.

[215] O. Troynikov and E. Ashayeri, "Thermoregulatory evaluation of triathlon suits in regards to their physiological comfort properties," *Procedia Engineering,* vol. 13, pp. 357-362, 2011.

[216] C. Yu, C. Lin and Y. Yang, "Human body surface area database and estimation formula," *Burns,* vol. 36, no. 5, pp. 616-629, 2010.

[217] K. Yick, K. M. Tang, P. Li, A. Yu, J. Yip and S. Ng, "Instruental Evaluation of Dry Heat Loss of Footwear under different Activity Levels," *IEEE Access,* vol. 7, pp. 65319-65331, 2019.

[218] A. Nomoto, Y. Takahashi, S. Yoda, M. Ogata, S. Tanabe, S. Ito, Y. Aono, Y. Yamamoto and K. Mizutani, "Measurement of local evaporative resistance of a typical clothing ensemble using a sweating thermal manikin," *Japan Architechtural Review,* vol. 3, no. 1, pp. 113-120, 2020.

[219] S. Mukunthan, J. Vleugels, T. Huysmans, K. Kuklane, T. S. Mayor and G. De Bruyne, "Thermal-Performance Evaluation of Bicycle Helmets for Convective and Evaporative Heat Loss at Low and Moderate Cycling Speeds," *Applied Sciences,* vol. 9, no. 3672, 2019.

[220] L. Giangregorio and N. McCartney, "Bone Loss and Muscle Atrophy in Spinal Cord Injury: Epidemiology, Fracture Prediction, and Rehabilitation Strategies," *Journal of Spinal Cord Medicine,* vol. 29, no. 5, pp. 489-500, 2006.

[221] M. J. Price, "Thermoregulation during Exercise in Individuals with Spinal Cord Injuries," *Journal of Sports Medicine,* vol. 36, no. 10, pp. 863-879, 2006.

[222] K. Katic, R. Li and W. Zeiler, "Thermophysiological mdoels and their applications: A review," *Building and Environment,* vol. 106, pp. 286-300, 2016.

[223] D. Rainmaker, "Redshift Sports Aero System In-Depth Review," 17 July 2014. [Online]. Available: https://www.dcrainmaker.com/2014/07/redshift-aero-system-review.html. [Accessed 23 08 2022].

[224] P. Storchle, W. Muller, M. Sengeis, S. Lackner, S. Holasek and Furhapter-Rieger, "Measurement of mean subcutaneous fat thickness: eight standardized ultrasound sites compared to 216 randommly selected sites," *Scientific Reports,* vol. 8, no. 16268, 2018.

[225] "clo unit," Oxford Reference, 2022. [Online]. Available: https://www.oxfordreference.com/view/10.1093/oi/authority.20110803095619345. [Accessed 2022].